Evolution of the amphibian head and neck: fate and patterning of cranial mesoderm in the axolotl (*Ambystoma mexicanum*)

A dissertation presented

by

Elizabeth Marie Sefton

to

The Department of Organismic and Evolutionary Biology

in partial fulfillment of the requirements

for the degree of

Doctor of Philosophy

in the subject of

Biology

Harvard University

Cambridge, Massachusetts

December 2015

Dissertation Advisor: James Hanken Elizabeth Marie Sefton

Evolution of the amphibian head and neck: fate and patterning of cranial mesoderm in the axolotl (*Ambystoma mexicanum*)

Abstract

The vertebrate head is a complex structure derived from all three embryonic germ layers. Cranial mesoderm forms most of the neurocranium, cardiovascular tissues and voluntary muscles required for intake of food and oxygenated fluid. Despite its essential role in shaping cranial and neck anatomy, long-term fate maps of cranial mesoderm are known only from the mouse and chicken, as effective labeling techniques for use in other species have been developed only recently. Data from additional species are needed to determine the embryonic origin of features absent in amniotes but present in other vertebrates and to evaluate the extent of conservation in the development of homologous structures. This dissertation examines the role of cranial mesoderm as well as its interactions with neural crest in shaping the tetrapod craniofacial and neck region, focusing on the skull and head muscles in the axolotl, *Ambystoma mexicanum*. I demonstrate a dual embryonic origin of the pharyngeal skeleton, including derivation of basibranchial 2 from mesoderm closely associated with the second heart field. Additionally, heterotopic transplantation experiments reveal lineage restriction of mesodermal cells that contribute to pharyngeal cartilage. The entire parietal bone is derived from mesoderm. Several structures arise from both mesoderm and cranial neural crest, including the squamosal, parasphenoid and stapes. The mesodermal contribution to the dorsal portion of the squamosal bone supports the homology of the corresponding dorsal ossification center, which fuses to the ventral center early in development, to the supratemporal, a bone lost repeatedly in tetrapods. I locate the posterior limit of myogenic

cranial mesoderm, extending the head-trunk boundary to the axial level of the third somite. Using fate mapping, gene expression and comparative anatomy, I provide evidence that the cucullaris muscle, a homologue of the mammalian trapezius, is a cranial muscle allied with the gill levators of anamniotes. Finally, I generate two novel transgenic lines of *Xenopus tropicalis* that will be used to fate map neural crest and mesoderm. Taken together, these results add to our understanding of cranial homologies and point to a larger role for cranial mesoderm in the evolution of a mobile neck.

Table Of Contents

List of Figures

Dedicated to the women who brought me up

Mary Jean Sefton, Juanita Fisher, Marie Sefton and Francis Erwin

What luck, to be surrounded by such love and love of learning

Acknowledgements

I am most grateful to my advisor, James Hanken, for giving me the opportunity to join his lab and providing so much support and guidance over the years. His feedback improved my writing and speaking skills, which allowed me to grow as a student and scientist. I received wonderful advice and support from my current and former committee members, including Cassandra Extavour, Arkhat Abzhanov, Farish Jenkins, and Cliff Tabin. I had the great pleasure of teaching with Farish Jenkins for two years, who showed the great elation that can come from research and teaching. I am indebted to Arkhat for all his thoughtful suggestions and encouragement throughout my time as a graduate student.

I thank all members of the Hanken lab for their invaluable support, feedback, advice and friendship. I am especially grateful to Nadine Piekarski for teaching me to work with axolotls and perform grafting experiments. I thank Zachary Lewis, Hillary Maddin, Yunke Wu, Brent Hawkins, Breda Zimkus and Mara Laslo for their kindness and conviviality. I am grateful to Anne Everly, Melissa Aja, Caroline DeVane and Matthew Gage for outstanding animal care. I thank Victoria Lellis for her assistance cryosectioning and Zahra Mohaddes, a talented post-baccalaureate intern, for her help and skillful in situ hybridizations. I thank Anjan Bhullar for contributing numerous micro-CT scans, imparting his enthusiasm for comparative anatomy and spending far too much time playing Spaceteam.

I am very grateful to Mustafa Khokha at Yale University for his generosity and encouragement in generating transgenic frog lines. I thank Ryan Kerney, John Griffin and Sarah Kubek for their assistance with constructs, performing injections, breeding and screening frogs. Chapter 5, quite simply, could not have happened without them.

I am grateful to the staff at the Ernst Mayr Library for their always-gracious help in locating material, especially Ronnie Broadfoot and Mary Sears. I thank Chris Preheim in OEB Administration for providing helpful advice on numerous occasions during graduate school. I thank Timothy Cox for his assstance with optical projection tomography.

I am thankful for the support I received from the National Science Foundation Graduate Research Fellowship, a Graduate Women in Science Vessa Notchev Fellowship, and a Goelet Award from the Museum of Comparative Zoology. I am very grateful for the companionship of my friends and family who have given their love and support for many years. My cohort of OEB students are such a talented, friendly and inspiring group of people. Zack Lewis and Shane Campbell-Staton have been fabulous herpetology buddies from the very beginning and I will miss pop tart runs and keeping the change. Laura Lagomarsino, Didem Sarikaya, Dipti Nayak and Heather Olins are brilliant, hilarious and incredibly energizing friends who have made my time in graduate school immeasurably brighter. Amanda Brown has been my partner-in-crime (Laura Summers, anyone?) since middle school and I've been lucky to have her friendship. Connor Shaughnessy has traveled, laughed and subjected himself to dangerous glass table-wrecking for me. I am grateful to Michelle Tomasik, Andrew Cheng, Nicole Burgoyne, Glenna Clifton, and Kara Fellich for their advice and friendship.

My husband's family has given me so much encouragement, especially Aparajita Shubhra, Avinash Sahay, Ananya Sahay, Apoorva Sahay, Ashesh Prasann and Pranay Sinha. I love and am ever grateful to my parents, Mary Jean Sefton and John Sefton, for their boundless care and support. I thank my dad for sharing his enormous curiosity about the world and taking me on my earliest herping trips in the swamps of Florida. My stepmother, Ellen Sefton, has been a thoughtful and fun confidante for nearly 15 years. My brother, John Christopher Sefton, sister and her husband. Lauren and Seth Cottrell, have always been wonderful role models for me. Lauren has taught me how laugh and live fully in the face of just about anything. Lastly, I thank my husband, Apratim Sahay; his LateX skills very tangibly put this thesis together. I am so grateful to share my life with Apratim, whose love, insightful perspective, linguistics happy hours and beautiful, sponge-like way of seeing the world has filled my life with joy.

Chapter 1

Introduction

There are concepts of such centrality, that their origin, change and disintigration, in short, their history captures the development of the science they are part of. Homology is such a concept for comparative anatomy. - Hans Spemann, 1915

The capacity to move the head independently of the body is a landmark anatomical adaptation associated with the evolution of tetrapods (Daeschler et al. 2006; Shubin et al. 2015). This innovation required the elaboration of the cucullaris muscle to stabilize the head while enabling turning and the loss of dermal elements attaching the head to the pectoral girdle. Loss of dermal elements in the skull is a recurring trend in tetrapod lineages (Janvier 1996), although the developmental basis of these losses is relatively unexplored. In the following dissertation, lineage tracing, gene expression analysis and comparative morphology will be used to investigate development and homology of cranial features in the axolotl.

1.1 The role of embryology as a guide for homology

Traits are considered homologous when their similarity in different species results from common ancestry. According to Etienne Geoffroy Saint-Hilaire, homologous features are identified based on a shared relationship to surrounding anatomical structures (Geoffroy Saint-Hilaire 1818). The first clear definition of a homologue was formulated by Richard Owen prior to Darwinian evolution and did not depend on community of descent: "the same organ in different animals under every variety of form and function" (Owen 1843). Following the publication of *On the Origin of Species* (Darwin 1859), the definition of homology was revised to focus on the importance of common ancestry, to the extent that homology cannot be independent of a phylogenetic hypothesis (Patterson 1982; Wake 1999).

While homology is recognized as a "central concept for *all* of biology" (Wake 1994), the nature of correspondence (or 'sameness') has been frought with challenges, especially in relating cell-type homologies to organs (Wagner 2014). Various criteria have been proposed to identify homologous structures. Adolf Remane suggested homology should be based on positional identity, a shared distinct morphological feature, and continuity in transitional forms, either through developmental stages or presence in closely related species (Remane 1952). Van Valen emphasized the 'continuity of information' as the cause of resemblance in homology (Van Valen 1982). The type of information is not restricted to genetic sources and might extend to culture, for example.

Developmental processes can provide insights on homologus traits. Gunter Wagner proposes that homology is tied to gene regulatory networks, termed Character Identity Networks (Wagner 2007; Wagner 2014). Character Identity Networks allow for differential gene expression and translate positional information into the activation of a trait-specific developmental program (Wagner 2014). Individual genes can be co-opted for divergent, non-homologous traits, such as the gene *Distal-less* and its ortholog (*Dlx*) in butterfly eyespots (Carroll et al. 1994) as well as vertebrate and arthropod appendage development (Panganiban et al. 1997; Cohen et al. 1989). The co-option of an entire network is less probable. However, Shubin et al. suggest that a gene regulatory network might have been established

in the common ancestor of vertebrates and arthropods that was independently deployed in novel appendages (Shubin et al. 1997). Genetic evidence also suggests pre-existing regulatory networks involved in limb outgrowth were co-opted in the evolution of beetle horns (Emlen et al. 2007). Thus, at least partial gene regulatory networks may be deployed in novel structures.

What role does embryonic derivation play in determining homology? For Carl Gegenbaur, homology was "the relationship between two organs that share common origin (ancestry) and therefore were derived from the same anlagen" (Gegenbaur 1870; quote translated by Hall 2003). Homologous characters generally derive from homologous embryonic sources. This has given rise to the germ layer theory where each structure is derived from the same typical cell layer in the embryo (Hall 1999). Although embryonic origin is often conserved between homologous structures, developmental processes evolve. A classic example involves the regeneration of the lens. When the lens is surgically removed in the axolotl *Ambystoma mexicanum*, it regenerates from cells in the iris (Wolff 1895). While the process of lens regneration is also present in the frogs *Xenopus laevis* and *X. tropicalis*, the regenerating cells are derived from a different source: the cornea (Freeman 1963; Henry and Elkins 2001). E.B. Wilson forcefully argued embryological methods should not be the predominant evidence in the field of morphology (Wilson 1894). There are numerous cases where homologous features have divergent developmental underpinnings (Spemann 1915; de Beer 1971; Northcutt 1990; Striedter and Northcutt 1991; Hall 1995; Bolker 1992; Hall 1994; Minsuk and Keller 1996; Hall 2003; Piekarski et al. 2014).

Developmental timing may be a significant factor in these differences. Willi Hennig introduced the concept of a semaphoront, where the individual organism bears the characters in a particular time-span of its life (Hennig 1966). During this potentially very small period of time, the organism itself does not change. The semaphoront can be used to describe similarity at earlier stages in ontogeny as well as subsequent divergent development giving rise to non-homologous structures (Havstad et al. 2015). It is complementary to von Baer's Laws of development, wherein more general features of embryos appear prior to specialized characters (von Baer 1828), although these laws have been revised to reflect differences

divergence in bilaterian embryos prior to mid-gastrulation (Abzhanov 2013).

Laubichler argues that no developmental process can have a set *a priori* relationship to homology (Laubichler 2000). Rather, evolution and development are reference processes required to interpret homology (Laubichler 2013). The appropriate level of description must ultimately be determined empirically (Wagner and Laubichler 2000). In this dissertation, I empirically evaluate the extent to which the embryonic origin of the skull and cranial musculature is conserved in the axolotl *Ambystoma mexicanum*. How flexible are the fates of embryonic tissues in development and evolution of the head and neck? How reliably can embryonic origin be used in assessing homologous relationships in the skull? To address these questions, it is essential to first establish which cells in the embryo directly contribute to adult structures in a range of extant vertebrate groups. Fate-maps address this aim by illustrating the long-term derivatives of embryonic tissues. Comparing fate-maps across species may offer insight into how species-specific morphologies are derived from the same embryonic tissues (Rudel and Sommer 2003). A detailed fate map will also play a vital role in understanding the genetic and morphological interactions needed to form complex structures (Clarke and Tickle 1999).

1.2 Mesoderm in Cranial Development and Evolution

Changes in cranial and neck anatomy have accompanied major adaptive transitions in vertebrate evolution (Hanken 1993). Two mesenchymal populations, the paraxial and lateral plate mesoderm, generate all volunatary muscles in the head, heart and portions of the skull (Gans and Northcutt 1983). Studies in the chicken and mouse have revealed differences in the contribution of mesoderm and neural crest to the bony skull, including derivation of the skull vault (Noden 1983a; Couly et al. 1993; Jiang et al. 2002; McBratney-Owen et al. 2008). Further examination of cranial mesoderm is required to determine the extent of these differences across tetrapods. The dermal skull of early tetrapods was comprised of numerous elements, but the number of bones has been significantly reduced in extant lineages (Janvier 1996). Developmental and paleontological evidence indicates that remaining elements

have conserved their position and growth trajectory through evolutionary transformations (Schoch 2006; Koyabu et al. 2012). Documenting how these bones were lost or fused remains an ongoing question in tetrapod evolution.

Decades of molecular and fate mapping studies have determined the patterning and derivatives of the overtly segmented paraxial mesoderm. In the trunk, paraxial mesoderm cyclically forms a series of epithelial somites on either side of the neural tube. Somite formation is characterized by opposing anterior to posterior gradients of fibroblast growth factors (FGFs)/Wnts and retinoic acid (RA) to determine the wavefront (reviewed by Dequéant and Pourquié 2008). Additionally, the segmentation clock utilizes periodic expression of Notch and Wnt pathway genes; the timing of these oscillations correspond to the time required to form one somite, which follows a clock-and-wave-front model of segmentation (Cooke and Zeeman 1976). By contrast, cranial mesoderm remains mesenchymal. However, cranial mesoderm undergoes two distinct pulses of cyclical gene expression, leading to the hypothesis that two regionalized domains exist (Jouve et al. 2002).

The topic of head segmentation is highly contentious (Neal 1918; Romer 1949; Olsson et al. 2005). Early models of head segmentation proposed that cranial mesoderm forms metameric units, similar to the brain. These units align with a segmental series of motor nerves that emerge starting at the midbrain and continue caudally (Romer 1949). The morphological presence of segments in cranial mesoderm was suggested based on scanning electron microscopy (SEM) of the superficial surface. Filopodial and lamellipodial processes were aligned in concentric arrays around a central position, which corresponded to a single "somitomere" (Meier 1979). Somitomeres have been described in numerous species (Meier and Tam 1982; Jacobson and Meier 1984; Meier and Packard 1984; Martindale et al. 1987); however, recent attempts have been unable to confirm the presence of somitomeres (Freund et al. 1996). Furthermore, lineage tracing using fluorescent dies in the mouse found no lineage restriction within somitomeres, as is present in somites (Trainor et al. 1994).

Fate-mapping studies in the chicken, mouse and zebrafish have determined the migratory pathways used by cranial mesoderm cells to populate the myogenic core of the branchial arches (Noden 1983a; Couly et al. 1993; Schilling and Kimmel 1994; Trainor et al. 1994;

Hacker and Guthrie 1998). The head muscle precursors leave their initial locations in cranial mesoderm and move into branchial and periocular locations surrounded by connective tissue-forming neural crest. Cranial mesoderm and somites generate the same cell types, although the timing and proportion of cell types vary. Cranial mesoderm forms smooth and skeletal muscle cells, loose and dense connective tissues, angioblasts and hemangioblasts. The locations where skeletal muscles, cartilages and bone originate in the chicken and mouse are illustrated in Figure 1.

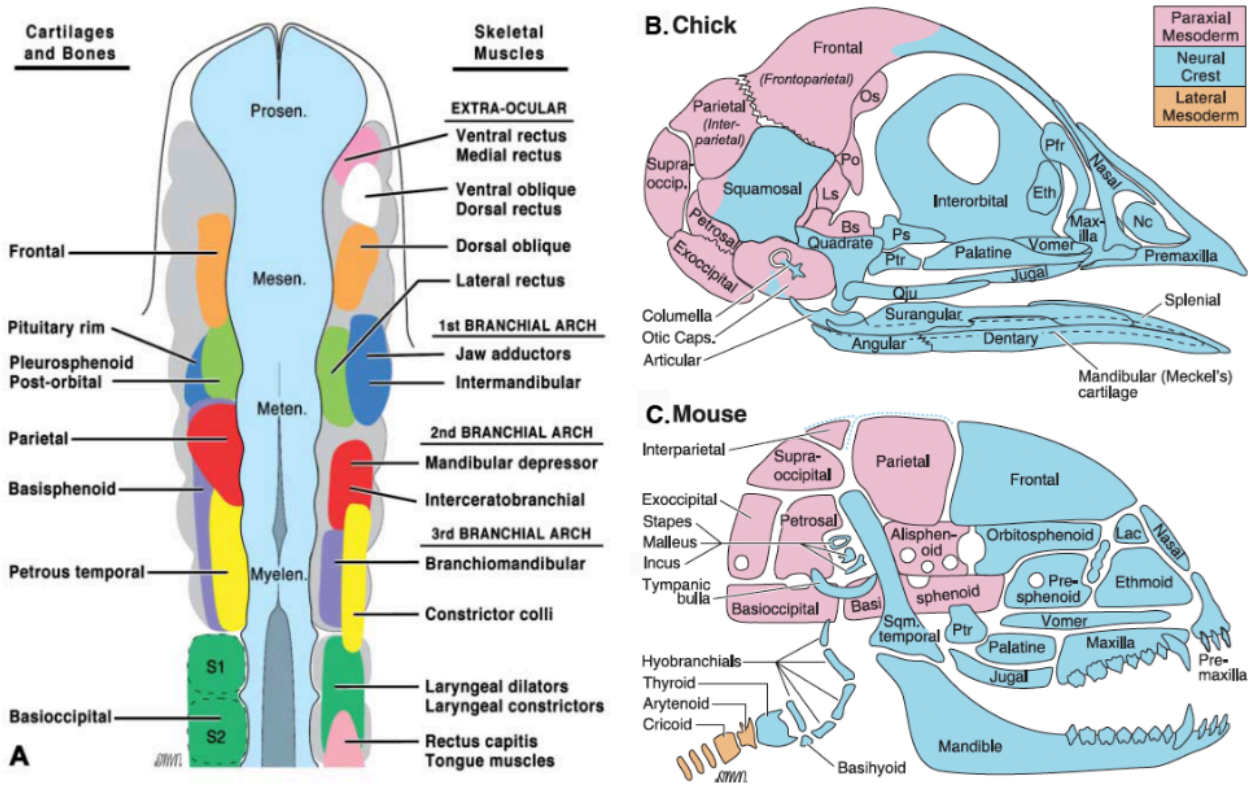

Figure 1.1 | Meosdermal derivation of the skull and cranial muscles in the chicken.. (A) Summary fate map in the chicken embryo illustrating sites of skeletal muscle origin (right side) and bone/cartilage elements (left side). Schematic chicken (B) and mouse (C) skulls indicating the contributions of neural crest, paraxial mesoderm and lateral mesoderm. One study has indicated an entirely neural crest origin to the frontal bones in chicken (Couly, 1993). (Schematics from Noden and Trainor 2005). Abbreviations: Bs, basisphenoid; Eth, ethmoid; Lac, lacrimal; Ls, laterosphenoid; Nc, nasal capsule; Os, orbitosphenoid; Pfr, prefrontal; Po, postorbital; Ps, presphenoid; Ptr, pterygoid; Qju, quadratojugal; Sqm, squamosal.

Cranial mesoderm forms voluntary muscles in the head (Noden 1983a; Couly et al. 1992). Craniofacial skeletal muscles are distinct from body musculature both in function and development. They participate in feeding, breathing and facial expression, but are not required for locomotion (Kelly 2010). Craniofacial muscles can be broadly divided into three groups: 1) six extraocular muscles (EOM), which move and rotate the eye; 2) muscles involved in moving the neck and forming the tongue, which are derived from the trunk (somites); 3)

muscles controlling the jaw, facial expression, pharyngeal and laryngeal function (Romer, 1949; Grifone and Kelly, 2007). Prechordal mesoderm as well as cranial paraxial mesoderm contribute to the EOMs (Evans and Noden, 2006; Lescroart et al., 2010). Mesoderm from the first arch forms the adductor musculature; second arch muscle forms the mandibular depressor, facial expression muscles in mammals and hyobranchial muscles (Noden, 1983a; Couly et al., 1993). Striated muscles of the esophagus, which are not present in amphibians, are also derived from cranial mesoderm in mice (Gopalakrishnan et al. 2015).

Cranial mesoderm later forms cartilaginous and bony elements of the neurocranium. In the mouse, the frontal is derived from neural crest and the parietal from mesoderm (Figure 1; Jiang et al., 2000). In the chicken, conflicting results from different groups have been reported for the neural crest-mesoderm boundary in the skull vault. In one case, the frontal and parietal have been reported to derive exclusively neural crest (Couly et al. 1993). Contrasting results indicate that the frontal has a dual origin from mesoderm and neural crest and an exclusively mesodermal origin of the parietal (Noden, 1983a; Evans and Noden, 2006). In either case, differing embryonic populations give rise to the same calvarial bone in chickens as compared to mice. In frogs, cranial neural crest streams contribute to the entire length of the fronto-parietal, although a contribution from cranial mesoderm cannot be excluded (Gross and Hanken 2005; Piekarski et al. 2014). Fate-mapping of cranial mesoderm into the bony skull has not been performed in an amphibian, nor any vertebrate other than the mouse and chicken, due in part to technical challenges associated with embryonic tranplantation of cranial mesoderm and the dearth of transgenic tools available, until recently, for non-murine vertebrate models.

In the axolotl, neural crest is not required for the start of muscle differentiation at the site of origin, but neural crest is necessary for head muscle morphogenesis and extension toward their insertions (Ericsson et al. 2004). Neural crest plays a key role in patterning the head muscles during embryogenesis (Olsson et al. 2001; Ericsson et al. 2004; von Scheven et al. 2006). Neural crest cells can reorganize skeletal and muscle patterns when grafted to different anteroposterior levels (Horstadius 1946); Noden, 1983b). Additionally, interspecific neural crest transplantations between quail and duck show muscle-patterning characteristic of the

donor; this is correlated with spatiotemporal changes in gene expression in the skeletal and muscular connective tissue (Tokita and Schneider 2009). Cranial mesoderm is also capable of patterning neural crest; when small numbers of neural crest cells are transplanted to ectopic regions of the hindbrain, cranial mesoderm is the source of permissive signals needed to maintain *Hox* expression patterns (Trainor and Krumlauf 2000).

The flexibility of patterning between several different tissue types has been examined by transplanting cells into a new location in the embryo, termed heterotopic transplantation. Somitic mesoderm transplanted to regions of cranial mesoderm is able to migrate into core of the pharyngeal arches and downregulate *Pax3* expression; conversely, cranial mesoderm can incorporate into somites and upregulate *Pax3* expression upon transplantation (Hacker and Guthrie, 1998). Segmental plate mesoderm does not have the capacity to migrate into developing branchial arches (Hacker and Guthrie 1998). Neural crest is able to form head mesoderm structures when expanded by transplantation into regions of cranial mesoderm, including the lateral wall of the braincase (Schneider 1999). The entire length of the cranial mesoderm has equivalent myogenic potential, as revealed by heterotopic transplantation studies in the chicken (von Scheven et al. 2006).

Long-term lineage tracing of cranial mesoderm has been performed in the mouse and chicken (Noden 1988; Couly et al. 1993; Evans and Noden 2006; McBratney-Owen et al. 2008; Yoshida et al. 2008); as the lineage tracing in the mouse was performed by genetic labeling of mesoderm, it does not distinguish between somitic mesoderm and regions of the cranial mesoderm. Although extirpation studies of cranial mesoderm have been performed in *A. mexicanum* (Piatt 1938), long-term labeling of cranial mesoderm in an anamniote will provide valuable information about the evolution of this important tissue, especially in regards to the bony skull and cranial muscles.

1.3 Genetic regulation of cranial mesoderm

While relatively little is known about the molecular organization of cranial mesoderm as compared to somites, several studies have described gene expression patterns and function

within cranial mesoderm, primarily in the chicken. These have shown distinct patterning mechanisms between somites and cranial mesoderm (Hacker and Guthrie 1998; Mootoosamy and Dietrich 2002; Bothe and Dietrich 2006; reviewed by Noden and Francis-West 2006). In particular, the head mesoderm has been considered a zone with reduced retinoic acid (RA) signaling as compared to the trunk, as RA initiates the Hox system to confer trunk identities (Burke 2000; Kmita and Duboule 2003). The expression of a RA degrading enzyme *Cyp26c1* has been recorded in cranial mesoderm (Bothe and Dietrich 2006).

No evidence for molecular segmentation of cranial mesoderm has been found, although markers indicate regionalization of cranial mesoderm. Two somitic markers, *Paraxis* and *Pax3* are not expressed segmentally in cranial mesoderm and taper from the somitic region into the posterior cranial mesoderm (Bothe and Dietrich 2006; Mootoosamy and Dietrich 2002; Hacker and Guthrie 1998). *Paraxis* is also expressed in lateral rectus precursors (Borue and Noden 2004; Mootoosamy and Dietrich 2002). *Hoxb-1* is briefly expressed in cranial mesoderm up to the level where rhombomeres 2 and 3 will later develop (Frohman et al. 1990). Expression analysis demonstrates two regions of molecular patterning: Pitx2, *Alx4* and *MyoR* label cranial mesoderm from the diencephalon to the metancephalon; *Tbx1* and *Twist* mark cranial mesoderm at the level of the hindbrain, with region overlap adjacent to the metencephalon (Bothe and Dietrich 2006).

Myogenic regulatory factors of the MyoD family are required for all skeletal muscle formation; loss of MRFs results in cells adopting different identities (Buckingham 2006). The genetic hierarchies that converge on MRF expression differ in somites and cranial mesoderm (Summerbell et al. 2000; Hacker and Guthrie 1998; Mootoosamy and Dietrich 2002). The neural tube secretes canonical Wnt signaling molecules and bone morphogenetic protein (BMP) to repress skeletal muscle formation. In the trunk, by contrast, Wnt ligands stimulate myogenesis. Cranial neural crest cells secrete Wnt inhibitors such as Frzb and BMP inhibitors including Noggin and Gremlin, which in vitro promote myogenesis of cranial mesoderm (Tzahor et al. 2003).

In *Pax3Myf5* double mutant embryos, trunk muscle development fails, while head muscle development is unaffected. Pax3 is required for Myf5 to independently activate MyoD in

muscles derived from somites (Figure 1.2; Tajbakhsh et al. 1997). In branchiomeric musculature Myf5 and MyoD are together required for myogenesis within core arch mesoderm, while Mrf4 can rescue trunk muscle development in the absence of Myf5 and MyoD (Kassar-Duchossoy et al. 2004). Multiple discrete enhancers dispersed over a large regulatory region drive Myf5 expression; Myf5 enhancers operate in specific arches and muscle precursors (Summerbell et al. 2000; Carvajal et al. 2001; Miller et al. 2004). In the anterior cranial mesoderm, FGF8 promotes branchiomeric muscle over extraocular fates in the chicken and zebrafish (von Scheven et al. 2006; Knight et al. 2008).

Genetic experiments in mice have revealed craniofacial muscle identity is controlled by at least four transcription factors that are distinct from somitic muscle. Instead of the Pax3 driven activation of Myf5 present in somites, Capsulin (Tcf21) and MyoR, bHLH transcriptional repressors, are required to drive expression of Myf5 in the mandibular arch; adductor musculature does not form in their absence (Lu et al. 2002). The homeobox transcription factor Pitx2 is necessary for extraocular muscle idntity in prechordal mesoderm as well as the differentiation and survival of myogenic precursors in the mandibular arch (Shih et al. 2007; Dong et al. 2006; Zacharias et al. 2011). Tbx1 regulates the activation of *Myf5* and *MyoD* in all branchiomeric muscles, including laryngeal muscles and the cervical portion of the trapezius muscle (Kelly et al. 2004; Grifone et al. 2008; Dastjerdi et al. 2007). The LIM domain-containing Lhx2 is down stream of Tbx1 and required for myogenic specification through the early activation of *Myf5* in the pharyngeal arches (Harel et al. 2012).

Fate mapping of splanchinic mesoderm cells in the chicken has revealed contributions to the distal core of the mandibular arch, while cranial paraxial mesoderm contributes to the proximal core (Nathan et al. 2008). Proximal myoblasts of the first branchial arch then give rise to the mandibular adductors and the splanchnic mesoderm-derived arch myoblasts give rise to more ventral muscles, such as the intermandibular (Marcucio and Noden 1999; Noden et al. 1999; Nathan et al. 2008). Lineage tracing in the chicken and mouse has demonstrated Isl1-positive splanchnic mesoderm cells contribute to a set of branchiomeric muscles in both the first and second branchial arches, though not the extraocular muscles (Nathan et al.

2008). *Isl1* is expressed in both cardiac and head muscle progenitors (Bothe and Dietrich 2006; Nathan et al. 2008; Tirosh-Finkel et al. 2006).

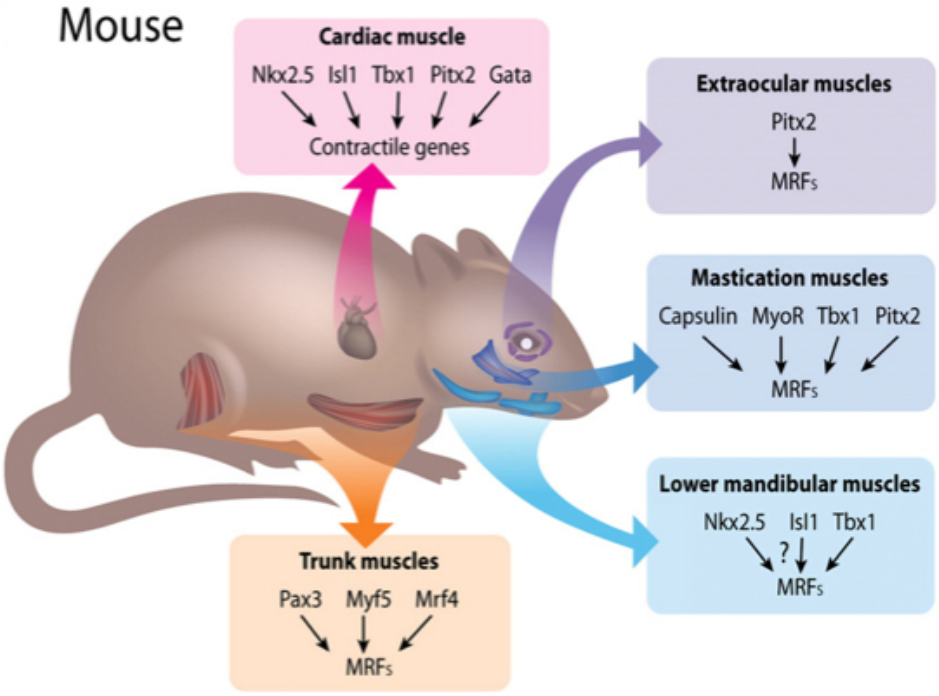

Figure 1.2 | Genetic lineage analysis and knockdown in mice indicates cranial muscle development varies between muscle groups.. Unlike the trunk, cranial muscle development is not dependent on Pax3. There are cellular and genetic links between cranial and cardiac muscle development. From Tzahor (2009).

Clonal analysis in the mouse has indicated that a single progenitor cell gives rise to both heart and head muscles (Lescroart et al. 2010). Two distinct lineages of branchiomeric muscles segregate: the anterior contributes to the adductor complex, extraocular muscles and the myocardium of the right ventricle; the posterior contributes to the second arch derived muscles and the outflow tract of the heart (Lescroart et al. 2010). The progenitor cells of the branchiomeric musculature share the same genetic signature as an adjacent group of pharyngeal mesodermal cells that form part of the myocardium at the extremities of the heart tube during cardiac looping (Figure 1.2; Grifone and Kelly 2007; Tzahor 2009). The overlapping fates have demonstrated a cardiocraniofacial field that is the source for head and heart development (Hutson and Kirby 2007; Diogo et al. 2015). In the tunicate *Ciona*, heart precursors also form the atrial siphon muscles, expressing *Islet* and *Tbx1*

(Stolfi et al. 2010). This suggests the presence of a cardiopharyngeal field in the last common ancestor of tunicates and vertebrates. Gene expression patterns of cranial mesoderm markers in amphioxus suggests vertebrate embryos have reorganized head mesoderm into a novel structure with antero-posterior polarity (Onai et al. 2015).

1.4 Connecting the Head and Shoulder

The vertebrate neck spans the region of cucullaris and hyobranchial muscle attachments to the pectoral girdle (Kuratani 1997; Kuratani 2008a). The cucullaris is a gnathostome muscle that is homologous to the mammalian sternocleidomastoid and trapezius muscles; the cucullaris split into two parts during the evolution of amniotes (Lubosch 1938). The expansion of the neck in amniotes involved infolding of the body wall to separate the shoulder musculature from the diaphragm (Hirasawa et al. in press).The cucullaris binds the neurocranium, pharynx and pectoral girdle (Kuratani 2008b). Fate-mapping experiments in the chicken indicate that it is derived from rostral somites (Noden 1983a). The connective tissue of the neck region in chickens is reported from cephalic neural crest cells (Le Lièvre and Le Douarin 1975). Neural crest-derived connective tissue is characteristic of extraocular and pharyngeal arch muscles derived from cranial mesoderm. Additionally, neural crest cells are involved in patterning the cucullaris and hyobranchial musculature (Noden 1983b; Evans and Noden 2006; Ericsson et al. 2004). The cucullaris, with its muscle fibers derived from the most anterior somites and its connective tissue from neural crest, has been proposed as the interface between the head and the trunk (Kuratani 1997; Kuratani 2008a; Ericsson et al. 2013).

Muscles of the fin/limb as well as hypobranchial and cucullaris muscles share molecular markers of migrating myoblasts. They require *Pax3* expression to upregulate Lbx1, which permits continued migration (Dietrich 1999; Gross et al. 2000; Birchmeier and Brohmann 2000). This implies a developmental and evolutionary link between the acquisition of fins and the cucullaris (Kuratani 2008a). In the agnathan lamprey, topographical position and the expression of *Pax3* and *Lbx* suggest the infraoptic muscle, a circumpharyngeal muscle

derived from anterior somites, represents the homologue of the cucullaris (Kusakabe et al. 2011).

With the exception of the shoulder girdle, the axial skeleton is derived from somites and the appendicular skeleton from lateral plate mesoderm. Detailed lineage-tracing studies utilizing transplantation and/or vital-dye labeling have revealed a somitic contribution to the scapula and cucullaris/trapezius muscles in chicken, mouse and axolotl (Chevallier 1977; Noden 1983a; Huang et al. 2000a; Huang et al. 2000b; Valasek et al. 2010; Piekarski and Olsson 2011). Lateral plate mesoderm gives rise to the anterior head and neck of the scapula blade in the chicken (Huang et al., 2000). Piekarski and Olsson have proposed a model in which the embryonic contribution of somitic vs. lateral plate mesoderm to the scapula is dependent upon its position in the developing embryo relative to these tissues (2011). An understanding of the genetic basis of neck and shoulder development is in an early phase. Studies primarily focus on the scapula in the chicken and mouse (Timmons et al. 1994; Pellegrini et al. 2001; Prols et al. 2004; Kuijper et al. 2005; Huang et al. 2006; Capellini et al. 2010).

Genetic lineage tracing in the mouse has revealed that part of the scapular spine is derived from neural crest (Matsuoka et al. 2005). This neural crest-derived population is interpreted as the "ghost" of the cleithrum, wherein the embryonic origin of muscle connective tissue and its skeletal attachment region form a highly conserved skeletomuscular connectivity code (Matsuoka et al. 2005; Köntges and Lumsden 1996). This hypothesis received significant criticism, however, as it does not take into account the fossil record showing the gradual reduction and loss of the cleithrum in synapsids (Sanchez-Villagra and Maier 2006) and the neomorphic rise of the scapular spine in therian mammals, given its absence in cynodonts and stem-group mammals (Jenkins 1979). Neural crest does not contribute to the axolotl shoulder girdle, providing evidence against the connectivity code (Epperlein et al. 2012).

The cleithrum forms a major component of the shoulder girdle in early tetrapods such as *Acanthostega* and *Tulerpeton*. It was eventually lost independently in amphibian and amniote lineages, as the endochondral elements proceeded to form the bulk of the shoulder girdle (reviewed by McGonnell 2001).

1.5 An unexpected source of neck musculature?

Until five years ago, lateral plate mesoderm was not known to make structural contributions, other than cardiovascular tissues, anterior to the laryngeal region. Theis et al. (2010) have proposed the chicken cucullaris is derived primarily from lateral plate mesoderm, which was interpreted as a novel embryonic source of neck musculature. Previous work has demonstrated a somitic contribution to the trapezius/cucullaris (Huang, 2000; Piekarski and Olsson, 2007) via transplantation experiments. Theis et al. repeated somite transplantation in the chicken, but used Dispase to remove any lateral plate cells that might "contaminate" the somite. Using this method, the trapezius was shown to have a dual origin from somites and lateral plate mesoderm.

Additional support comes from molecular profiling of the trapezius in mice, which indicates greater similarity with the head molecular program than with the trunk myogenesis, including the expression of *Islet1*. In mice, the trapezius is still present following knockdown of Pax3, while all somite-derived trunk muscles are affected. Intriguing similarities in gene expression have been reported in occipital lateral plate mesoderm and head mesoderm, such as *MyoR*, *Capsulin* and *Tbx1* (Pu et al. 2015). In mice, non-somitic neck musculature and the heart myocardium are clonally related (Lescroart et al. 2015). The lateral plate mesoderm adjacent to anterior somites sets a trajectory for the migration of tongue muscle progenitors (Lours-Calet et al. 2014). It is unclear, however, if the myogenic capacity of lateral plate mesoderm arose from a posterior expansion of the molecular boundary that patterns muscle or if instead it represents true cranial mesoderm.

1.6 Thesis summary and outline

While branchial skeletal features are available in fossil data, the record for most structures derived from cranial mesoderm is incomplete. Lineage-tracing studies are required to identify the embryonic and possibly phylogenetic precursors (Noden and Trainor 2005). The addition of long-term fate maps of cranial mesoderm in a broader phylogenetic framework

will determine if patterns of mesodermal contribution to the muscles and bones of the skull are conserved across vertebrates or more labile.

Lissamphibians occupy a phylogenetically important position between aquatic vertebrates (including fishes) and amniotes (including reptiles and mammals). They may shed light on the ancestral pattern of cranial development of early tetrapods as well as the evolution of derived patterns seen in amniotes. In particular, they possess external gills and their associated musculature, features likely present in larval Paleozoic amphibians (Schoch and Witzmann 2011). Growing understanding of the molecular underpinnings of cranial muscle development makes this an opportune time to examine head mesoderm development and evolution in amphibians.

In this thesis, I construct a fate map of cranial mesoderm in the axolotl *Amybstoma mexicanum*. I demonstrate contributions of cranial mesoderm to the pharyngeal skeleton, skull and cranial musculature. Mesodermal contribution to the otherwise neural-crest derived squamosal sheds light on potential homology with bones in the temporal series lost in tetrapod evolution. Moreoever, I define the posterior limit of myogenic unsegmented mesoderm, which pushes back the posterior boundary of cranial mesoderm to the axial level of somite 3. In my final chapter, I generate two transgenic lines of *Xenopus tropicalis* that can aid in determining the neural crest-mesoderm boundary in the dermal shoulder girdle of amphibians.

These three projects investigate musculoskeletal evolution in the head and neck of amphibians and will add to our knowledge of how different embryonic tissue layers interact to generate complex structures.

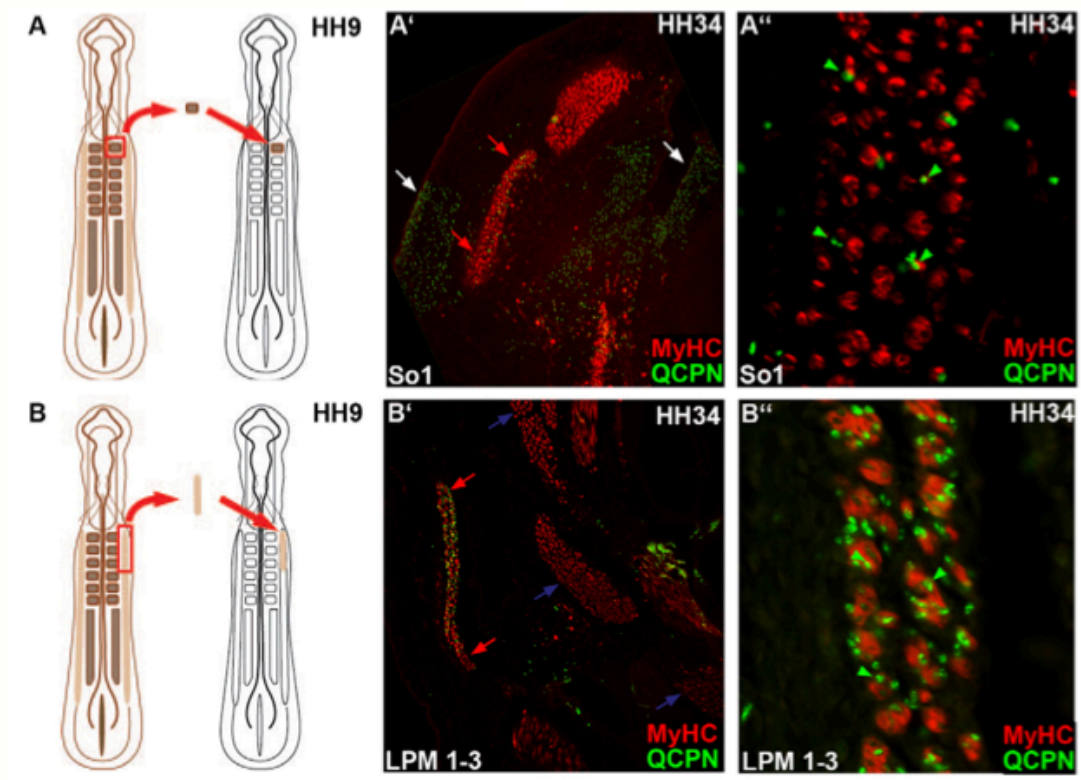

Figure 1.3 | Relative contribution of lateral plate mesoderm vs. somitic mesoderm to the chicken cucullaris.. (A) Schematic of somite transplantation at HH 9. (A', A") Transplantation of quail somite 1 into a chick host in transverse section at HH 34. (A, A") Low-magnification image with quail cells primarily in the skin and skull cartilage. White arrows are QCPN+ cells and red arrows indicate the cucullaris muscle. (A") Higher magnification of the cucullaris muscle following transplantation of somite 1. The cucullaris muscle is sparsely labeled (green arrowheads). (B) Schematic of lateral plate mesoderm transplantation at HH9. (B') Low magnification of cucullaris muscle showing a large number of QCPN+ cells in the cucullaris muscle (red arrows), but not present in axial muscles (blue arrows). (B") High-magnification image with extensive labeling of the cucullaris muscle following lateral plate mesoderm transplantation (green arrows). From Theis et al. (2010).

Chapter 2

Dual embryonic origin and patterning of the pharyngeal skeleton in the axolotl (*Ambystoma mexicanum*)

Elizabeth M. Sefton, Nadine Piekarski, James Hanken

Abstract

The impressive morphological diversification of vertebrates was achieved in part by innovation and modification of the pharyngeal skeleton. Extensive fate mapping in amniote models has revealed a primarily cranial neural crest derivation of the pharyngeal skeleton. Although comparable fate maps of amphibians produced over several decades have failed to document a neural crest derivation of ventromedial elements in these vertebrates, a recent report provides evidence of a mesodermal origin of one of these elements, basibranchial 2, in the axolotl. We used a transgenic labeling protocol and grafts of labeled cells between GFP+ and white embryos to derive a fate map that describes contributions of both cranial

This chapter has been adapted from the following manuscript: Sefton, E. M., Piekarski, N. and Hanken, J. Dual embryonic origin and patterning of the pharyngeal skeleton in the axolotl (*Ambystoma mexicanum*). *Evol Dev* 17: 175–184

neural crest and mesoderm to the axolotl pharyngeal skeleton, and we conducted additional experiments that probe the mechanisms that underlie mesodermal patterning. Our map confirms a dual embryonic origin of the pharyngeal skeleton in urodeles, including derivation of basibranchial 2 from mesoderm closely associated with the second heart field. Additionally, heterotopic transplantation experiments reveal lineage restriction of mesodermal cells that contribute to pharyngeal cartilage. The mesoderm-derived component of the pharyngeal skeleton appears to be particularly sensitive to retinoic acid (RA): administration of exogenous RA leads to loss of the second basibranchial, but not the first. Neural crest was undoubtedly critical in the evolution of the vertebrate pharyngeal skeleton, but mesoderm may have played a central role in forming ventromedial elements, in particular. When and how many times during vertebrate phylogeny a mesodermal contribution to the pharyngeal skeleton evolved remain to be resolved.

2.1 Introduction

The pharyngeal skeleton, an autapomorphy of gnathostomes, has undergone dramatic morphological change across the vertebrate clade (Lauder 1982; Mallatt 1996). In extant fishes and larval amphibians it supports the gills, tongue and muscles of the pharynx, whereas in adult tetrapods it surrounds the larynx and trachea and contributes to the middle ear. Despite its morphological diversity in gnathostomes, the pharyngeal skeleton is believed to have a highly conserved embryonic origin from cranial neural crest (Creuzet et al. 2005; Knight and Schilling 2006). Indeed, the extensive contribution of neural crest to the pharyngeal skeleton and other cranial tissues (Platt 1893; Le Lièvre and Le Douarin 1975; Tan and Morriss-Kay 1986; Langille and Hall 1987; Couly et al. 1993; Köntges and Lumsden 1996; Mongera et al. 2013) is a primary feature of the "New Head" hypothesis, wherein neural crest functions in the head, similar to mesoderm in the trunk, to generate novel structures associated with a predatory lifestyle (Gans and Northcutt 1983). Moreover, neural crest is a source of interspecific variation in craniofacial morphology, capable of carrying out autonomous developmental programs (Schneider and Helms 2003).

Fate-mapping studies of amphibians, however, have failed to document a neural crest origin of some midline pharyngeal cartilages. In neural crest extirpation experiments in the spotted salamander, Ambystoma maculatum, basibranchial 2, a ventromedial element, formed in the absence of neural crest cells (Stone 1926; Supplemental Figure 1). In frogs, neural crest does not contribute to either the basihyal or basibranchial 2, two ventromedial cartilages in tadpoles (Stone 1929; Sadaghiani and Thiébaud 1987; Olsson and Hanken 1996). It is unknown whether the absence of a neural crest contribution to midline cartilages represents a derived trait within amphibians or instead represents a character that is more widely distributed among gnathostomes.

Much less is known regarding the long-term lineage of cranial mesoderm in comparison to cranial neural crest, although fate maps of cranial mesoderm have been produced for mouse and chicken (Noden 1988; Couly et al. 1992, 1993; Evans and Noden 2006; McBratney-Owen 2008; Yoshida et al. 2008). Mammals, however, have a highly modified pharyngeal skeleton and lack basibranchials, whereas in the chicken, the basihyal and single basibranchial are derived exclusively from neural crest (Le Lièvre 1978). This begs the question of the embryonic origin of homologous elements in species, such as salamanders, that retain an evolutionarily more ancestral condition of the pharyngeal skeleton. Such information may provide important insight into the plesiomorphic pattern of development in tetrapods, or even bony fishes. Previous mesodermal fate-mapping studies of the salamander head have described the skeletal and muscular derivatives of individual somites (Piekarski and Olsson 2007), and a recent study reported a mesodermal origin of basibranchial 2 in the axolotl, *Ambystoma mexicanum* (Davidian and Malashichev 2013).

Here, we examine mechanisms that mediate pharyngeal skeletal patterning in the axolotl, with particular focus on mesodermal derivatives. To fate map contributions of neural crest and cranial mesoderm to the pharyngeal skeleton, cells are grafted orthotopically from GFP+ transgenic donor embryos into white mutant (dd) hosts (Sobkow et al. 2006). In addition, we evaluate the cell potency of cranial mesoderm through heterotopic transplantations. Finally, we evaluate the role of retinoic acid in regulating development of the pharyngeal skeleton during embryogenesis. We discuss our results in a broader context of

the evolution of the pharyngeal skeleton.

2.2 Materials and Methods

Ambystoma mexicanum embryos

White mutant (dd), GFP+ white mutant and albino (aa) embryos of the Mexican axolotl (*Ambystoma mexicanum*) were obtained from the Ambystoma Genetic Stock Center at the University of Kentucky and from our laboratory breeding colony. Before grafting, embryos were decapsulated manually by using watchmaker forceps. They were staged according to Bordzilovskaya et al. (1989).

Grafting procedure

In all transplantation experiments, labeled cells were grafted from GFP+ white mutant donor embryos into white mutant (dd) hosts. The donor embryos ubiquitously express GFP under the control of the CAGGS promoter (Sobkow et al. 2006). After dejellying, embryos were transferred into agar-coated dishes (2% agar in 20% Holtfreter solution) containing sterile 100% Holtfreter solution. Operations were carried out with tungsten needles on the left side of the embryo. Explants of individual cranial neural crest streams (stages 15—17) or cranial mesoderm (stages 19—23) from donor embryos were grafted unilaterally into stage-matched hosts whose comparable regions had been extirpated. Donors and hosts were of equivalent size and form. Explants were kept in place with a glass coverslip for the first several minutes to promote healing. Cranial mesoderm has no obvious morphological segments or boundaries; we differentiated graft regions based on the morphology of the overlying neural tube. There is undoubtedly a small amount of overlap between adjacent sections, whose borders are approximate. To avoid contamination with neural crest, cranial mesoderm transplants were carried out before migrating neural crest cells had reached the level of paraxial mesoderm (Piekarski 2009).

Cranial mesoderm cells were grafted heterotopically from GFP+ white mutant donor embryos into stage-matched white mutant (dd) hosts. Transplantations were performed between stages 19 and 22. Host embryos were prepared through a cut into the overlying

ectoderm with tungsten needles. Cranial mesoderm cells from region 1 and 4 of hosts were extirpated. After removal of overlying donor ectoderm, GFP+ cranial mesoderm cells from regions 5 and 6 were transplanted into regions 1 and 4 of the host.

Immunohistochemistry

Chimeric embryos were anaesthetized in tricaine methane-sulfonate (MS-222; Sigma, St. Louis, MO) and fixed in 4% paraformaldehyde in phosphate-buffered saline (PFA/PBS) overnight at 4℃ . After washing in PBS, specimens were transferred to 15% sucrose for several hours, followed by 30% sucrose overnight. Specimens were soaked in a 1:1 solution of 30% sucrose and Tissue Tek OCT Embedding Compound (Electron Microscopy Sciences, Hatfield, PA) for several hours. Specimens were embedded in OCT and sectioned at 12—16 μM thickness. Sections were incubated with rabbit polyclonal anti-GFP ab290 (1:2000; Abcam, Cambridge, MA), followed by AlexaFluor-488 goat anti-rabbit (1:500; Life Technologies, Carlsbad, CA). Sections were also stained with DAPI (0.1—1 μg/ml in PBS) to label cell nuclei. Some sections were stained with the skeletal muscle marker 12/101 monoclonal antibody (1:100; Developmental Studies Hybridoma Bank, Iowa City, IA).

Retinoic acid treatments

Stock solutions (10 mM) of all-trans retinoic acid (RA; Sigma R2625) were prepared in dimethyl sulfoxide (DMSO). White (dd) axolotls were incubated in the dark with final concentrations of 0.01-0.1 μM RA at indicated stages. Control embryos were incubated in 0.1% DMSO. Whole-mount clearing and staining followed the standard protocol by Klymkowsky and Hanken (1991).

RNA in situ hybridization

Albino (aa) embryos were used for in situ hybridization. Antisense riboprobes were synthesized from the cloned fragment (DIG RNA labeling kit; Roche Diagnostics, Indianapolis, IN). In situ hybridization was performed as previously described (Henrique et al. 1995), with the addition of an MAB-T wash overnight at 4℃ (100 mM maleic acid, 150 mM NaCl, pH 7.5, 0.1% Tween 20). Hybridization was performed at 65℃ . The *cyp26b1* forward primer sequence is 5'-CATTCACCGCAACAAGAGAA-3'; the reverse

primer is 5'-TTGAGCTCTTGCATGGTCAG-3'. Forward and reverse primers for *islet1* are 5'-CACACCCAACAGCATGGTAG-3' and 5'-TGCTACAGGAGACCCAGCTT-3', respectively.

2.3 Results

2.3.1 Embryonic derivation of the pharyngeal skeleton

To determine the contributions of both cranial mesoderm and cranial neural crest to the pharyngeal skeleton, we used transgenic axolotls that ubiquitously express GFP under the control of the CAGGS promoter (Sobkow et al. 2006). Fate-mapping individual cranial neural crest streams revealed contributions to all cartilage elements except basibranchial 2 (Figure 2.1A—C, L). The mandibular stream forms Meckel's cartilage of the lower jaw (as well as the palatoquadrate cartilage and the anterior portion of the trabecula cranii). The hyoid stream forms elements of the hyoid arch, including the ceratohyal and the anterior portion of basibranchial 1. The branchial streams contribute to the posterior half of basibranchial 1 and to the cerato- and hypobranchials.

We performed orthotopic transplantations of six different regions of cranial mesoderm between GFP+ and white (dd) embryos (Figure 2.1K). Cells from regions 5 and 6 contribute to basibranchial 2 (n = 17; Figure 2.1F —H), corroborating recent fate-mapping results in the axolotl, which show that lateral plate mesoderm gives rise to basibranchial 2 and the heart (Davidian and Malashichev 2013). Cells from regions 5 and 6 overlap with those forming ventral craniofacial muscle in most explants (n = 11/17). Regions 5 and 6 likely include lateral splanchnic mesoderm (SpM), a population of cells that, in mouse and chicken, is adjacent to cranial paraxial mesoderm (CPM) and includes precursors of both head musculature and the second heart field (Nathan et al. 2008). The boundary between CPM and SpM is defined by gene expression, including *Nkx2.5*, *Isl1* and *Fgf10* in SpM, and *Cyp26c1* in CPM (Bothe and Dietrich 2006; Nathan et al. 2008). In the chicken, the boundary between CPM and SpM mesoderm cannot be identified morphologically, as CPM is continuous and indistinguishable from SpM mesoderm (Noden and Francis-West 2006).

Similarly, hyoid and branchial arch paraxial mesoderm is continuous with lateral plate mesoderm in the axolotl. In the chicken, SpM contributes to the distal myogenic core of the first branchial arch, which forms the ventral intermandibular muscle (Marcucio and Noden 1999; Noden et al. 1999; Nathan et al. 2008). Formation of the intermandibularis muscle in region 5 and 6 transplants in the axolotl is consistent with labeling of SpM that contributes to the distal cores of the branchial arches. The labeling of basibranchial 2 without labeling of cranial muscle indicates that at least a portion of basibranchial 2 progenitors is distinct from intermandibularis muscle progenitors.

Our results suggest a link between pharyngeal skeleton and second heart field development: in every specimen in which basibranchial 2 is labeled, the heart is also labeled. In most cases ($n = 15/17$), heart labeling is present in the outflow tract, which is formed by the second heart field (Figure 2.1H; Lee and Saint-Jeannet 2011). In the mouse, cells from the second heart field form the outflow tract myocardium and contribute to the right ventricle and the venous pole of the heart (Cai et al. 2003), and clonal analysis indicates common lineage relationships between cranial muscles and second heart field derivatives (Lescroart et al. 2010). The second heart field also contributes to the growth of the cardiac tube (Buckingham et al. 2005). In the chicken, neural crest contributes to the septation of the outflow tract (Kuratani and Kirby 1991).

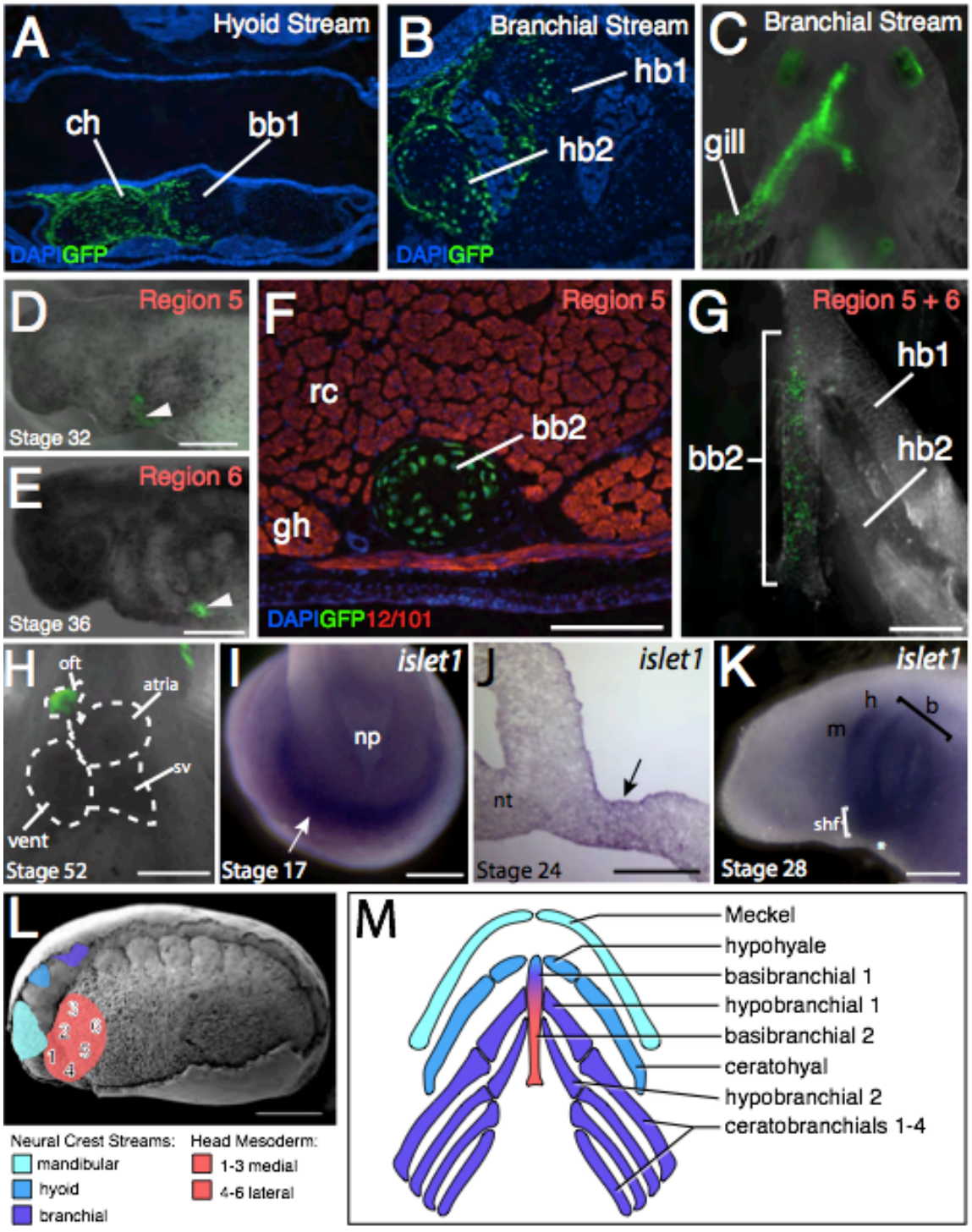

Figure 2.1 | Fate of cranial neural crest and contribution of cranial mesoderm to the pharyngeal skeleton and heart. (A—B) Transverse sections following hyoid and branchial neural crest stream transplantations. (A) Basibranchial 1 (bb1) and the ceratohyal (ch) are labeled following a hyoid stream transplant. (B) Hypobranchials 1 and 2 (hb1, hb2) are labeled following a branchial stream transplant. (C) Ventral view of a branchial stream transplant; anterior is at the top. Labeling is present in the hypobranchial region and the gills. (D) Region 5 mesoderm graft (arrowhead) in a stage-32 embryo after transplantation at stage 19. (E) Region 6 mesoderm graft (arrowhead) in a stage-36 embryo.

Figure 2.1 | Continued. (F) Transverse section of a region 5-labeled specimen at stage 55. GFP-labeled cells are present in basibranchial 2 (bb2). Muscle (red) is labeled with the 12/101 antibody; nuclei (blue) are stained with DAPI. (G) Dissected pharyngeal skeleton of a stage-46 larva shows labeling of basibranchial 2. Ventral view, anterior is at the top; lateral cartilages have been removed from the right side. (H) Regions 5 and 6 graft in a stage-52 larva. Labeling is visible in the outflow tract (oft) of the heart. Additional heart regions: sv, sinus venosus; vent, ventricle. Ventral view, anterior is at the top. (I—K) *islet1* expression. At stage 17, *islet1* is expressed in the anteriormost region of the embryo, including the cardiac crescent (arrow in I). Anterior view, dorsal is at the top. At stage 24, a parasagittal section shows expression in ventral cranial mesendoderm (arrow in J). Anterior is to the left, dorsal to the top. At stage 28, *islet1* is expressed in the hyoid (h) and branchial (b) arches, with additional strong expression ventral to the arches in the proposed second heart field (shf) region. Asterisk indicates the ventral region of the embryo where *islet1* expression is minimal. Lateral view, anterior is to the left. (L) Scanning electron micrograph of a stage-21 embryo. Overlying ectoderm has been removed from the left side, revealing the mandibular (light blue), hyoid (blue) and branchial (purple) cranial neural crest migratory streams and mesoderm (red). (M) Derivation of the pharyngeal skeleton; ventral view, anterior is at the top. Additional abbreviations: gh, geniohyoideus muscle; m, mandibular arch; nt, neural tube; rc, rectus cervicis muscle. Scale bar: 500 μM.

The LIM-homeodomain transcription factor *islet1* is expressed in the second heart field in amphibians as well as amniotes (Brade et al. 2007; Cai et al. 2003). In Xenopus, *nkx2.5* is expressed in a broad domain, including both first and second heart fields, whereas *islet1* is restricted to an anterior and more dorsal region in the heart field beginning at stage 28 (Brade et al. 2007; Gessert and Kühl 2009). To determine the location of the second heart field in the axolotl, we examined expression of *islet1* (Figure 2.1I, J). *islet1* is expressed at stage 17 in the anterior region of the embryo, which includes the heart field. At stage 28, *islet1* is strongly expressed in the ventral hyoid and branchial arches in addition to the more dorsal branchial arches. Based on our fate-mapping data, ventral expression of *islet1* appears to closely overlap the region expected to form both basibranchial 2 and the outflow tract. Pharyngeal mesoderm cells give rise to both cranial muscle and cardiac progenitors (Tirosh-Finkel et al. 2006). The axolotl mesodermal cardiocraniofacial field thus encompasses a portion of the pharyngeal skeleton in addition to the heart and branchiomeric muscles.

2.3.2 Heterotopic transplantation of basibranchial 2-forming cells

We performed heterotopic transplantations to evaluate the degree of lineage restriction of cranial mesoderm at early tailbud stages. Cells that contribute to basibranchial 2 (including the posterior portion of region 5 and the anterior part of region 6) were moved anteriorly into regions 1 and 4, which normally do not contribute to the pharyngeal arch skeleton but typically form mandibular arch musculature (Figure 2.2A).

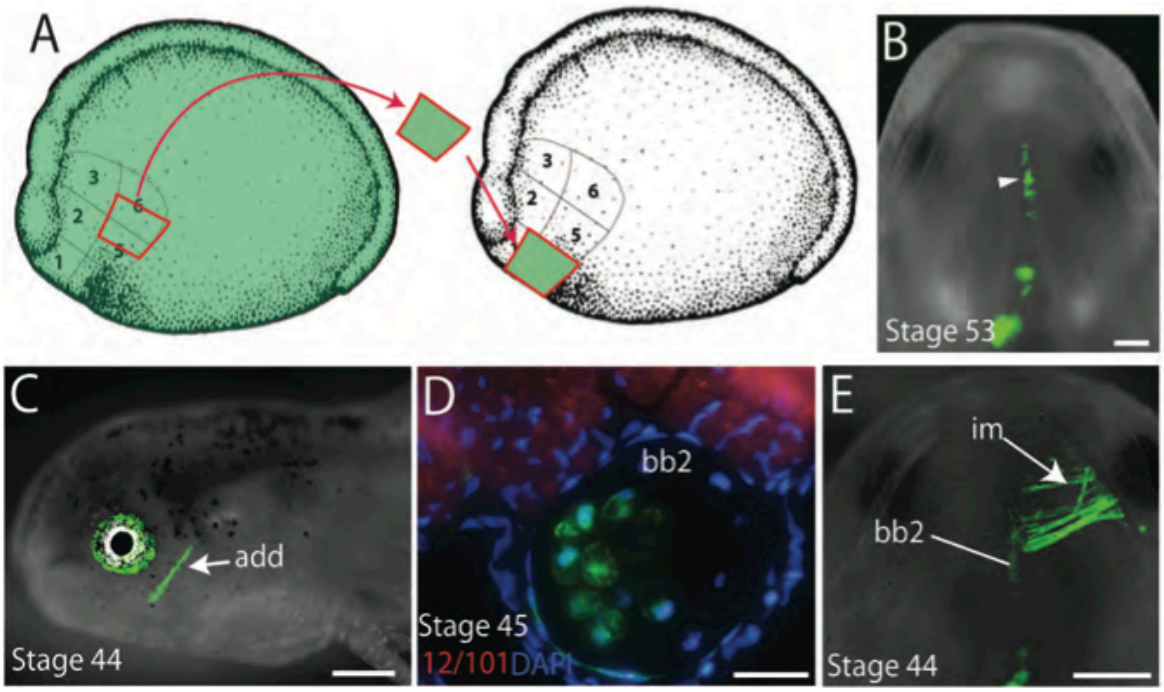

Figure 2.2 | Heterotopic grafting of cranial mesoderm. (A) Drawing of stage-19 embryos illustrating the grafting protocol. Regions 1 and 4 were extirpated from white (dd) hosts and replaced with regions 5 and/or 6 from GFP+ donors. (B) Region 6 graft at stage 53 shows labeling of basibranchial 2 (arrowhead). Ventral view, anterior is at the top. (C) Regions 5 and 6 graft at stage 44 shows labeling of the mandibular levator adductor muscle (add). Lateral view, anterior is to the left. (D) Transverse section of a regions 5 and 6 graft at stage 45 shows labeling of basibranchial 2. Muscle (red) is labeled with the 12/101 antibody; nuclei (blue) are stained with DAPI. (E) Regions 5 and 6 graft at stage 44 shows labeling of basibranchial 2 and the intermandibularis muscle (im). Scale bars: B, C and E–500 μM; D–100 μM.

Heterotopically transplanted cells form anterior musculature, including jaw adductors and the intermandibularis muscle (Figure 2.2C, E). Muscles form in most cases (n = 9/12), but transplanted cells also form basibranchial 2 as well as the heart in its normal location

(Figure 2.2B, D—E; n = 8/12). No heterotopically transplanted cells contribute to anterior pharyngeal arch structures, such as Meckel's cartilage, which suggests cranial mesoderm cannot replace neural crest as a source of pharyngeal arch skeleton. We cannot rule out a community effect, however, wherein smaller groups of individual basibranchial 2-forming cells are more responsive to cues from the host environment, as can occur following transplantation of coherent groups of neural crest cells (Trainor and Krumlauf 2000). Stone (1932) performed heterotopic transplantations of cranial mesoderm (with the surrounding ectoderm and endoderm) into locations in the trunk in the axolotl. These experiments resulted in the formation of ectopic gills, heart and a small rod of cartilage presumed to be basibranchial 2. Development of the ectopic basibranchial 2 was always accompanied by formation of the heart. The lack of positional restriction in the ability of cranial mesoderm to form head muscles by stage 21 in the axolotl agrees with results from comparable studies in mouse: cells transplanted across the anteroposterior axis of CPM generate structures typical of their host location (Trainor et al. 1994).

2.3.3 Retinoic acid-treated embryos lack basibranchial 2

Proper levels of retinoic acid (RA), a derivative of vitamin A, are required for multiple aspects of craniofacial development (Lohnes et al. 1994; Niederreither and Dollé 2008). To test the role of RA in patterning the axolotl pharyngeal skeleton, we treated embryos with all-trans RA. In zebrafish, excess RA inhibits formation of the posterior basibranchials (Laue et al. 2008). Strikingly, treatment of white (dd) axolotl embryos with 0.05 μM RA results in the absence of basibranchial 2 but not basibranchial 1 (n = 31/33; Figure 2.3B). Furthermore, all six arches are present with normal anteroposterior patterning (Figure 2.3B). Basibranchial 1 remains intact at higher doses (n = 6/6; Figure 2.3C), whereas even at the lowest dose, 0.01 μM, basibranchial 2, while still present, is less robust than in controls (n = 9/9; Supplemental Figure 3). This implies that RA restricts basibranchial 2 progenitors.

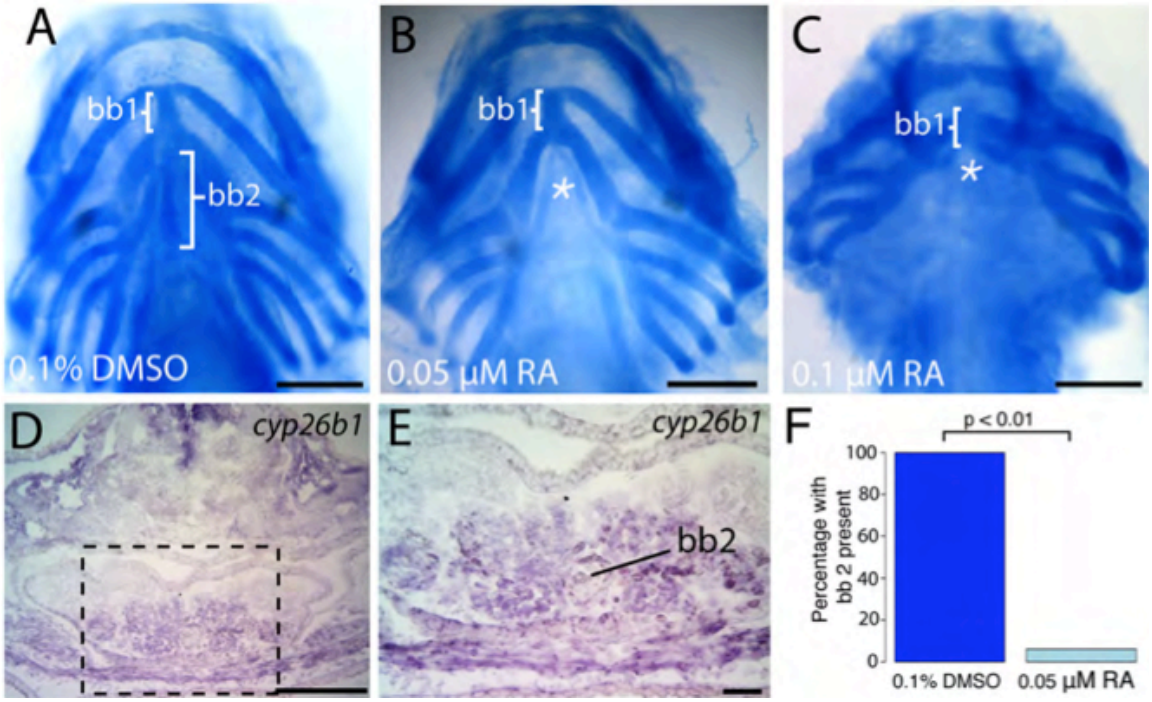

Figure 2.3 | Exogenous retinoic acid (RA) disrupts the mesoderm-derived pharyngeal skeleton. (A–C) Alcian-blue staining of craniofacial cartilages at stage 45 following treatment with 0.1% DMSO (A, control), 0.05 μM RA (B), and 0.1 μM RA (C). Ventral views, anterior is at the top. Brackets depict positions of basibranchials 1 and 2. Asterisks in B and C indicate normal position of missing basibranchial 2. (D—E) Transverse section of a stage-44 *cyp26b1* in situ hybridization. Dashed rectangle in D is enlarged in E. (F) Frequency of basibranchial 2 in control group (0.1% DMSO) and following treatment with 0.05 μM RA. The p-value is based on a 2-sample t-test.

In zebrafish, RA does not have a posteriorizing influence in the location of myocardial progenitors, but instead controls progenitor density (Keegan et al. 2005). Xenopus embryos exposed to increased RA before cardiac differentiation have reduced levels of *Nkx2.5* (Jiang et al. 1999). At the low concentrations used in our RA experiments, RA does not appear to have a posteriorizing effect on the pharyngeal skeleton, but instead it has a potent repressive function in the mesoderm-derived component of the axolotl pharyngeal skeleton. The Cyp26 cytochrome P450 enzymes degrade RA, acting to control RA levels in cells and tissues (reviewed by Blomhoff and Blomhoff 2006). We examined the expression of both *cyp26b1* and *cyp26c1*. Although no significant expression of *cyp26c1* is found in the midline where basibranchial 2 forms (data not shown), *cyp26b1* is expressed in the ventral midline of larvae (Figure 2.3D—E). This is consistent with the presence of an RA gradient in the

head, with concentration increasing from medial to lateral positions (Laue et al. 2008).

2.4 Discussion

2.4.1 Neural crest-mesoderm boundary in the pharyngeal skeleton

The embryonic derivation of the cranium has significant implications regarding vertebrate origins and relationships (including assessments of skull bone homologies), the flexibility of developmental programs, and the diagnosis and treatment of craniofacial anomalies (Cerny et al. 2006; Darwin 1859; Kimmel et al. 2001; Kuratani 1997; Kuratani et al. 1997; Matsuoka et al. 2005; Schneider 1999; Trainor and Krumlauf 2000). The dual embryonic origin of the skull from both neural crest and mesoderm has been well documented in two widely used amniote models, chicken and mouse. The corresponding pharyngeal skeletons, however, are derived largely from neural crest, and this pattern has generally been extrapolated to all vertebrates. Yet, the pharyngeal skeleton has changed dramatically in the course of vertebrate evolution in relation to feeding, respiration, vocalization and hearing, and amniotes account for only a small portion of that diversity. Fate mapping in multiple lineages is needed to determine the degree to which the neural crest-mesoderm boundary is evolutionarily conservative or labile (Piekarski et al. 2014). Whereas fate mapping and genetic analysis of neural crest has yielded insight into the degree of conservation of embryonic origin and the neural crest-mesoderm boundary in anamniotes (Epperlein et al. 2000; Ericsson et al. 2008; Olsson et al. 2001; Olsson and Hanken 1996; Falck et al. 2002; Horigome et al. 1999; Kague et al. 2012; Mongera et al. 2013; McCauley and Bronner-Fraser 2003; Ota et al. 2007; Schmidt et al. 2011), fate mapping of cranial mesoderm has received far less attention (Kuratani et al. 2004; Davidian and Malashichev 2013; Schilling and Kimmel 1994). Cranial mesoderm fate maps are particularly important for structures of dual origin, such as the otic capsule and stapes (Noden 1982; Thompson et al. 2012).

The dual embryonic origin of the pharyngeal skeleton in the axolotl provides an additional morphological frontier to study the boundary between neural crest and mesoderm. If the pharyngeal skeleton is defined to include laryngeal cartilages, then the boundary appears to

vary even among amniotes. In the chicken, cricoid and arytenoid cartilages are derived from lateral mesoderm at the level of the otic placode and first somite, as inferred from quail-chick chimaeras (Noden 1986, 1988) and more recently from retroviral labeling (Evans and Noden 2006). In contrast, genetic fate-mapping in the mouse indicates a neural crest origin of cricoid, arytenoid and thyroid cartilages (Matsuoka et al. 2005), although aspects of these findings are controversial (Sánchez-Villagra and Maier 2006). Notwithstanding these interspecific differences in its exact location, the neural crest-mesoderm boundary in the pharyngeal skeleton of amniotes is typically placed in the laryngeal cartilages. Our fate mapping in the axolotl, however, shifts the boundary anteriorly to include basibranchial 2, a prominent element in many fishes and amphibians that is absent or significantly transformed in the reduced pharyngeal skeleton of amniotes.

Our heterotopic transplantations suggest that mesoderm that forms basibranchial 2 and the heart is specified earlier in development than mesoderm that forms skeletal muscle. The neural crest-mesoderm boundary remains stable when cartilage-forming mesoderm cells are moved into the mandibular arch; basibranchial 2-forming cells appear unable to form neural-crest derived cartilages following such experimental treatment. And while chondrogenic progenitors maintain their ”normal” fate at late-neurula stages, skeletal muscle progenitors demonstrate equivalent potential along the anteroposterior axis. The earlier specification of basibranchial 2 progenitors in the heart field and negative regulation by retinoic acid (RA) offers a potential explanation for the curious absence of neural crest cells from the ventromedial pharyngeal skeleton. Future studies, including clonal analysis, are needed to determine the precise relationship between the second heart field, including the outflow tract, and the formation of basibranchial 2.

2.4.2 Evolution of basibranchial 2 and the urohyal

Our fate-mapping results confirm the recent report of a mesodermal derivation of basibranchial 2 in the axolotl (Davidian and Malashichev 2013). We further show that cranial mesoderm that forms this cartilage cannot substitute for neural crest in forming other cartilages of the pharyngeal skeleton, and that basibranchial 2 differs from the rest of the

pharyngeal skeleton in its response to exogenous RA. These distinctive features of basibranchial 2 are consistent with the hypothesis that this element both develops and evolved independently from the remainder of the pharyngeal skeleton. Jarvik (1963) proposed that basibranchial 2 is not derived from neural crest, but instead forms as a developmental unit with the somite-derived tongue musculature. If this hypothesis is true, then the mesodermal origin of basibranchial 2 and its differential sensitivity to RA may be linked to the somitic signalling environment provided by the surrounding tongue musculature. According to Jarvik, basibranchial 2 in urodeles is the homolog of the urohyal of piscine sarcopterygians, including the basal taxon Eusthenopteron. The urohyal is an unpaired median skeletal element in bony fishes that lies caudal to the basibranchial (Figure 2.4).

Like basibranchial 2, the urohyal in sarcopterygians forms first as cartilage, which then ossifies endochondrally (Arratia and Schultze 1990). A bony urohyal is also present in teleosts, although it typically forms by intramembranous ossification. In bichirs (*Polypterus* spp.), which are neither teleosts nor sarcopterygians, the urohyal appears to ossify as three distinct ventral tendon bones, although relatively little is known regarding pharyngeal ossification in this evolutionarily conservative sister taxon to all other actinopterygians (Arratia and Schultze 1990). Recent fate-mapping studies demonstrate a neural-crest contribution to the entire pharyngeal skeleton in the zebrafish, including the urohyal (Kague et al. 2012). This result is consistent with the claim that the teleost urohyal, which forms as an ossification of the sternohyoideus tendon, is not homologous to the urohyal of piscine sarcopterygians (Arratia and Schultze 1990). If the zebrafish urohyal is homologous to basibranchial 2 of the axolotl, then developmental system drift (True and Haag 2001) may offer an explanation for the differing germ-layer origin and mode of ossification between these two elements. Given this complex phylogenetic distribution of alternate developmental trajectories and unresolved homologies, we can propose at least three possible scenarios for the evolution of the mesodermal derivation of basibranchial 2 and, possibly, the urohyal (Figure 2.4). First, it evolved in basal osteichthyans but later was lost independently in at least some teleosts and amniotes (hypothesis 1). Alternatively, it originated coincident with evolution of endochondral ossification of the urohyal of sarcopterygians and later was lost in at least some

amniotes (hypothesis 2). Finally, mesodermal derivation of basibranchial 2 may simply be a synapomorphy unique to urodeles, and possibly other amphibians (hypothesis 3). Parallel, independent evolution of this feature also remains a possibility, if it is present, for example, in piscine sarcopterygians.

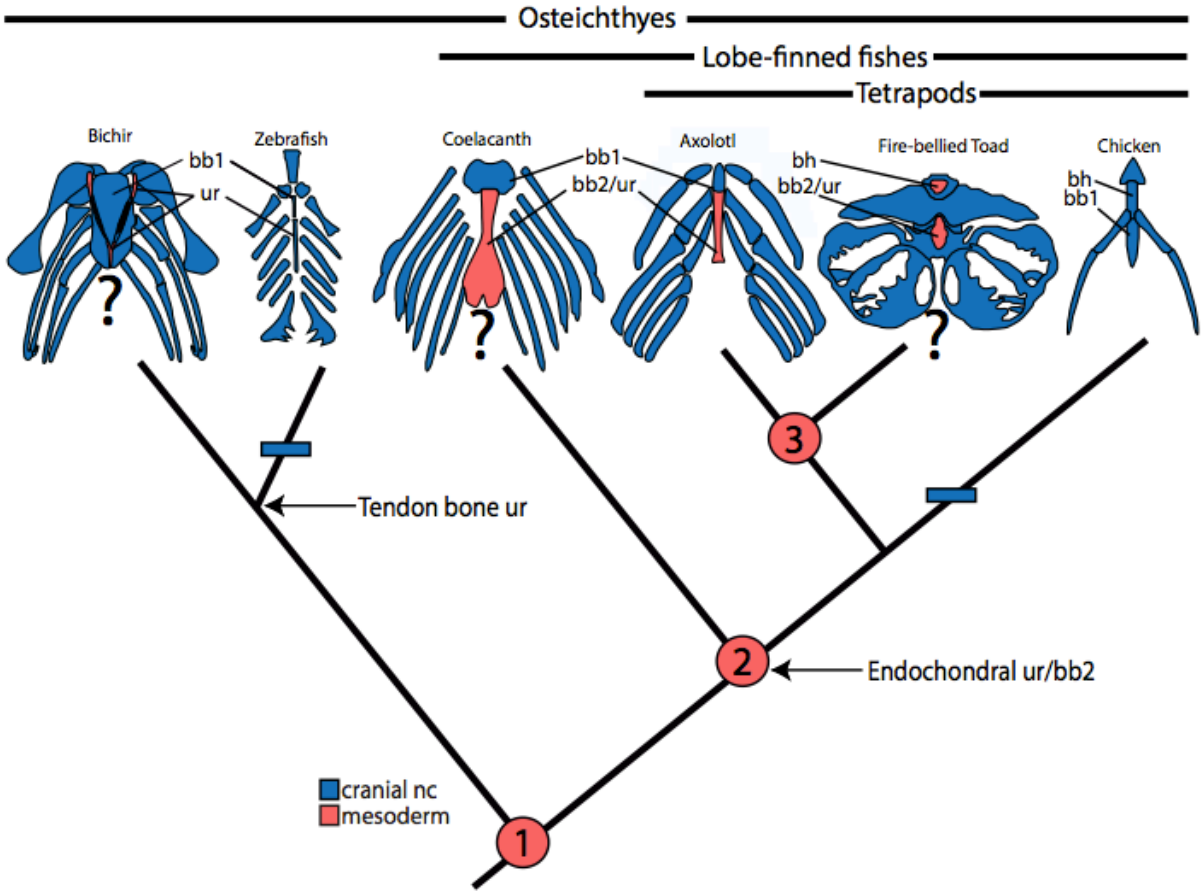

Figure 2.4 | Evolution of pharyngeal skeleton origins. Simplified osteichthyan phylogeny depicting cranial neural crest and cranial mesoderm contributions to the hyoid and branchial arches. The mesodermal contributions to coelacanth (modified from Forey, 1998), toad and bichir (modified from Arratia and Schultze, 1990) are hypothesized (question marks). Red circles represent gain of mesodermal contribution to the pharyngeal skeleton in three alternate hypotheses. Blue bars indicate loss of mesodermal contribution according to hypothesis 1 or 2. The urohyal in teleosts and bichirs, which forms by intramembranous ossification within tendon ("Tendon bone ur"), may not be homologous to the urohyal in sarcopterygians, which ossifies endochondrally within cartilage (" Endochondral ur/bb2"). In hypothesis 1, derivation of bb2/ur from cranial mesoderm is an osteichthyan synapomorphy, which later was lost independently in teleosts (e.g., zebrafish) and amniotes (chicken). In hypothesis 2, mesodermal contribution to the pharyngeal skeleton is a sarcopterygian synapomorphy, which later was lost in amniotes. In hypothesis 3, mesodermal contribution to the pharyngeal skeleton is an amphibian synapomorphy.

Homology of basibranchial 2 and the urohyal, at least across sarcopterygians, is further supported by their strikingly similar morphology. Both basibranchial 2 of the axolotl and the urohyal of the coelacanth are elongate bones that articulate anteriorly with basibranchial 1 and expand caudally to terminate in a bifid tip. Each element also serves as an attachment site for ventral branchial musculature, although the muscle origins and insertions may vary, especially among salamanders (Kleinteich and Haas 2011). For example, the sternohyoideus muscle inserts on the dorsal surface of the urohyal in the coelacanth (Millot and Anthony 1958) and on the dorsal side of basibranchial 2 in the axolotl (Piekarski and Olsson 2007). In the absence of lineage-tracing data from piscine sarcopterygians, hypotheses 2 and 3 are equally parsimonious. Nevertheless, we favor hypothesis 2, primarily because it associates two developmental innovations at the origin of sarcopterygians: mesodermal origin of median elements of the pharyngeal skeleton, and endochondral ossification of the urohyal/basibranchial 2. If this hypothesis is correct, then these features represent the ancestral condition for lobe-finned fishes. A specific prediction that follows is the mesodermal derivation of the urohyal in piscine sarcopterygians. If the urohyal of teleosts is not homologous to the urohyal of sarcopterygians (Arratia and Schultz 1990), then such a distinctive mode of development of the urohyal of sarcopterygians and the basibranchial 2 of urodeles would not require an evolutionary change in the embryonic derivation of homologous elements. Rather, the urohyal preformed in cartilage would represent a neomorphic element unique to sarcopterygians that evolved by incorporating cranial mesoderm closely associated with the heart field.

Neural crest has played a critical role in vertebrate craniofacial development and evolution (Northcutt 2005; Abitua et al. 2012). According to the ”New Head” hypothesis, the origin of the head during the transition of vertebrates to active predation from a more passive protochordate ancestor involved morphological innovations derived from the neural crest and epidermal placodes, as well as muscularization of lateral plate mesoderm (Gans and Northcutt 1983). Neural crest derivation of the pharyngeal skeleton in general has been known for well over a century (Platt 1893). Basibranchial 2 of the axolotl, however, is a surprising example of a functional component of the pharyngeal feeding apparatus that

originates instead from cranial mesoderm. In aquatic feeding salamanders, basibranchial 2 is the attachment site of muscles that pull the center of the hyobranchial apparatus forward and open the mouth (Deban and Wake 2000). It is an interesting exception to the more typical association of neural crest with skeletal structures involved in feeding. Tracing its origin and phylogenetic diversity sheds light on whether basibranchial 2 was always linked to the neural crest-derived pharyngeal skeleton, or, if it was not, on how this element came to be integrated with the pharyngeal skeleton following its initial evolution.

Contributions: E. Sefton performed cranial mesoderm transplantations, retinoic acid treatments and in situ hybridizations. N. Piekarski conducted neural crest transplantations.

Chapter 3

Evolution of cheek bones in amphibians and reptiles: insights from lineage tracing in the axolotl (*Ambystoma mexicanum*)

Abstract

The vertebrate skull is a complex structure that arises from three embryonic sources– cranial mesoderm, neural crest and somitic mesoderm. The contribution of cranial mesoderm to the bony skull has been documented in two amniote models, the mouse and the chicken. The dominant bone of the cheek, the squamosal, is derived from neural crest in both species. In the chicken, however, a postero-dorsal component of the squamosal receives an additional contribution from cranial mesoderm. Additional data from an anamniote model permits comparisons in a wider phylogenetic context and provides evidence regarding the extent of evolutionary conservation in the embryonic derivation of the skull during vertebrate history. To delineate the extent of cranial mesoderm derivation of the skull in Ambystoma mexicanum, we utilize GFP-transgenic axolotls, which permit long-term fate mapping. Our

Contributions: E. Sefton performed cranial mesoderm transplantations, cryosections and antibody stains. Victoria Lellis assisted in cryosections and antibody stains.

results provide the first fate map of osteogenic cranial mesoderm in an anamniote. We show the postero-dorsal squamosal bone in the axolotl is derived from cranial mesoderm, as in the chicken. This lends support to the hypothesis that the batrachian squamosal is a compound bone. The neural crest-derived squamosal is fused to a mesoderm-derived bone, likely either the tabular or supratemporal. We propose that this fusion evolved convergently in archosaurs and amphibians. In mice, it has previously been proposed that the tabular bones fuse to the postparietals during development. Distinct patterns of fusion could thus explains the incongruent origin of the squamosal between mouse and chicken/axolotl: in mammals, the tabulars fused to the medial postparietal bone, while in amphibians and reptiles, the supratemporals/tabulars fused to the laterally adjacent squamosal.

3.1 Introduction

In vertebrates, cranial mesoderm is an unsegmented mesenchymal cell population adjacent to the neural tube that fills the core of each pharyngeal arch following the migration of cranial neural crest (reviewed by Noden and Francis-West 2006; Noden and Trainor 2005). Cranial mesoderm contributes to head and heart musculature as well as cartilage and bone of the skull. The resulting interface between mesoderm- and neural crest-derived components bears developmental, clinical and evolutionary significance (Gross and Hanken 2008).

Mesodermal contribution to the bony skull has been documented in the chicken through quail-chick chimeras and retroviral labeling (Evans and Noden 2006; Noden 1988; Couly et al. 1993). Transgenic lines, including *Mesp1-Cre/R26R* and *Myf5-Cre/R26R*, have been used to examine mesodermal derivation of the mouse skull (Yoshida et al. 2008; Hosokawa et al. 2007; McBratney-Owen et al. 2008). There are no published reports that directly address the contributions of cranial mesoderm to the adult bony skull of actinopterygians, although a transgenic paraxial mesoderm line was recently produced for the zebrafish (Mongera and NÃijsslein-Volhard 2013). In the chicken, the posterior portion of the frontal bone and the entire parietal bone, which together comprise the cranial vault, are derived from cranial mesoderm (Evans and Noden 2006; although see Couly et al. 1993 for an alternative claim).

In the mouse, however, the neural crest-mesoderm interface is largely between frontal and parietal bones (Jiang et al. 2002; Yoshida et al. 2008), although a few mesoderm cells are found in the otherwise neural crest-derived frontal (Deckelbaum et al. 2012).

The fate maps of chicken and mouse also differ in the derivation of the squamosal, a prominent part of the temporal series of bones that form the "cheek." In the chicken, cranial mesoderm forms a postero-dorsal portion of the squamosal (Evans and Noden 2006), whereas in mice the squamosal is derived solely from neural crest (Jiang et al. 2002) (Fig. 3.1). While differing fate maps in the skull vault have garnered much attention (Noden and Trainor 2005; Gross and Hanken 2008; Noden and Schneider 2006; Gross and Hanken 2005; Hanken and Gross 2005), the contrasting derivation of the squamosal between mouse and chicken has received little attention.

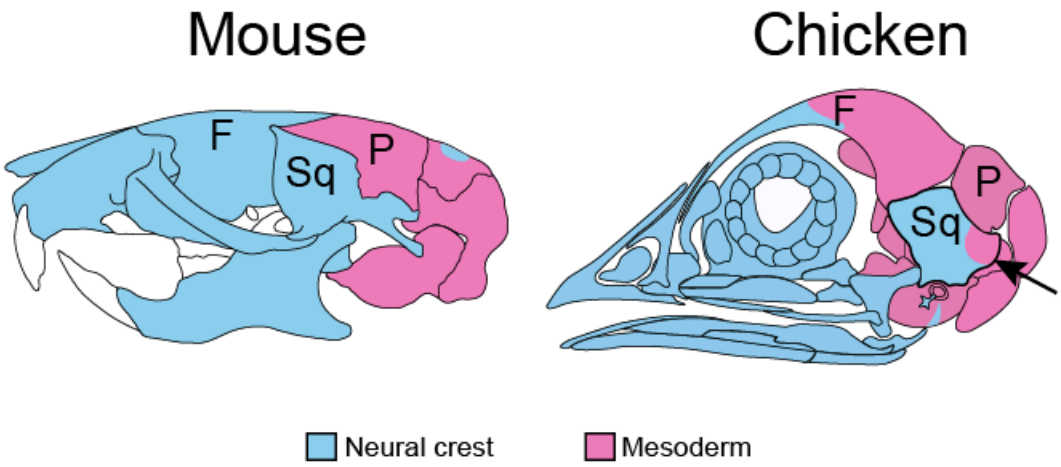

Figure 3.1 | Differing derivation of the squamosal in chicken and mouse. In the mouse, the squamosal is derived entirely from neural crest. In the chicken, the squamosal receives a contribution from cranial mesoderm in the postero-dorsal region (arrow). F, frontal; P, parietal; Sq, squamosal. Mouse fate map based on refs. 7 and 11. Chicken fate map from ref. 4.

The homology and evolutionary history of the squamosal has been contentious (Alcalde and Basso 2013; Huxley 1864; Gaupp 1895; Thyng 1906; Schoch 2014). In addition to the cheek bones, early tetrapods possessed a temporal series including the intertemporal, supratemporal and tabular, with the tabular forming the lateral occiput of the skull (Romer 1949). The tendency towards simplification of the dermal tetrapod skull is a repeated trend

in vertebrate evolution (Esteve-Altava et al. 2012; Gregory 1935). Lissamphibian skulls have lost of numerous bones in comparison to the heavily ossified skulls of temnospondyls, which often overshadows other characters in phylogenetic analyses of lissamphibian origins (Schoch and Milner 2004). The loss of bones in batrachians (a clade that includes frogs and salamanders), including the tabular, supratemporal, postfrontal and jugal, has been associated with their paedomorphic morphology (Milner 1988; Roĉek and Rage 2000; Smirnov 1995). Although initially without developmental evidence, it was proposed that the tetrapod squamosal bone resulted from the fusion of two independent bones (Allis 1919; Bütschli 1910). Embryonic studies subsequently documented that the squamosal in numerous anurans and salamanders develops from two or three distinct centers of ossification (Reinbach 1939; Lebedkina 1979; Sedra 1949; Wiens 1989; Griffiths 1954a). The arrangement of ossification centers led to the hypothesis that the anuran and urodele squamosal is the product of fusion to a dorsal bone in the temporal series overlying the otic capsule (Reinbach 1939; Lebedkina 1979; Griffiths 1954a). Fused bones, however, do not necessarily present more than one ossification center during ontogeny, as the original ossification centers may have fused over evolutionary time (Lebedkina 1979; Griffiths 1954b; Roĉek 1988).

A similar instance of fusion has been documented in a group of Paleozoic amphibians: in the lepospondyl order Adelospondyli, just one bone is located where the squamosal, tabular, supratemporal and intertemporal bones are typically found (Andrews and Carroll 1991). This bone is termed the tabular-squamosal, although it is not possible to determine from existing data if the tabular and/or the supratemporal are involved in the fusion (Andrews and Carroll 1991; Carroll 2009).

The existence of structures derived from both cranial mesoderm and neural crest, such as the axolotl viscerocranium (Davidian and Malashichev 2013; Sefton et al. 2015) and the chicken frontal bone (Deckelbaum et al. 2012), demonstrates the necessity of fate-mapping cranial mesoderm to more completely characterize the neural crest-mesoderm boundary. Here, we use the axolotl, *Ambystoma mexicanum*, to fate-map cranial mesoderm to the bony skull in a urodele amphibian. The neural crest contribution to the skull in the axolotl is highly similar to that in amniotes (Piekarski et al. 2014), but the nature and extent

of mesodermal contributions are yet to be described in this species or any other living amphibian. We find a cranial mesoderm contribution to the dorsal squamosal; comparisons with chicken fate mapping shed light on the convergence of bone fusion in amphibians and archosaurs.

3.2 Materials and Methods

Axolotl husbandry and embryos

Green fluorescent protein (GFP) transgenic (Sobkow et al. 2006) and white mutant (dd) embryos were acquired from the Ambystoma Genetic Stock Center at the University of Kentucky or from the colony in the Hanken laboratory at the Museum of Comparative Zoology. Animals were staged (Bordzilovskaya et al. 1989; Nye et al. 2003) and reared in 20% Holtfreter solution.

Embryonic Grafting of cranial mesoderm

Prior to grafting, watchmakers forceps were used to manually remove the jelly coat. Transplantations were performed in sterile 100% Holtfreter solution on 2% agar-coated dishes as previously described (Sefton et al. 2015). Tungsten needles were used to transplant segments of cranial mesoderm from GFP-positive white mutant donor embryos into stage-matched white mutant hosts. Transplantations were unilateral and performed during stages 16–22. Cranial mesoderm was artificially divided into six regions (Fig. 3.2A). Following extirpation of a region of host mesoderm, GFP-positive donor mesoderm of similar size was grafted in its place. To avoid contamination with neural crest, transplantations were carried out before ventrally migrating cranial neural crest cells had reached the level of paraxial mesoderm. Chimeras were raised up to 6 months; animals younger than stage 53 were not used to analyze bone derivation. Animals were anesthetized in tricaine methanesulfonate (MS-222; Sigma-Aldrich, St. Louis, MO) and then fixed in 4% paraformaldehyde at 4 ℃ for 48 h.

Sectioning and Immunohistochemistry

Animals were rinsed in PBS and transferred to 15% sucrose for several hours, then 30% sucrose overnight, and finally a 1:1 solution of 30% sucrose and Optimal Cutting Temperature compound (OCT; Electron Microscopy Sciences, Hatfield, PA). They were then transferred to pure OCT and embedded in plastic molds in OCT utilizing a dry-ice ethanol bath and stored at -80 ℃. 12–16 μm transverse serial cryosections were made on a Leica CM 3050S cryostat.

Sections were blocked with 5% normal goat serum in PBT for 2 hr at room temperature and then incubated with rabbit polyclonal anti-GFP ab 290 (1:3000; Abcam, Cambridge, MA) overnight at 4 ℃. AlexaFluor-488 goat anti-rabbit was used as a secondary antibody (1:1000; Life Technologies, Carlsbad, CA). Sections were stained with 0.5% alizarin red for 3 min, rinsed in PBS and stained with DAPI (0.1–1 μg/ml in PBS) to label cell nuclei.

12/101 skeletal muscle marker was applied to some sections (1:100; Developmental Studies Hybridoma Bank, Iowa City, IA), followed by AlexaFlour 568 goat anti-mouse secondary (1:500; Life Technologies, Carlsbad, CA).

3.3 Results and Discussion

We use a GFP transgenic strain of the Mexican axolotl (Sobkow et al. 2006) to map derivatives of embryonic cranial mesoderm to bone and cartilage in the axolotl skull. Cranial mesoderm was divided into six regions (Fig. 3.2A). Five of the six regions were skeletogenic in at least one transplant, although many of the transplants from these regions only gave rise to muscle (Table 3.1). Region 1 contributed to the crista trabeculae (not shown) (orbital cartilage–(de Beer 1937; Goodrich 1958). We have previously shown that two lateral regions, 5 and 6, give rise to the endochondral basibranchial 2, or urohyal, of the viscerocranium (Davidian and Malashichev 2013; Sefton et al. 2015) but do not contribute to either the dermatocranium or the neurocranium.

Regions 2 and 3 both contribute to the otic capsule and to cells at the base of the stapes (Fig. 3.2B–C). In the axolotl, the developing stapedial cartilage is initially continuous with the periotic cartilage, but these two elements later separate (Parker and Bettany 1877). It

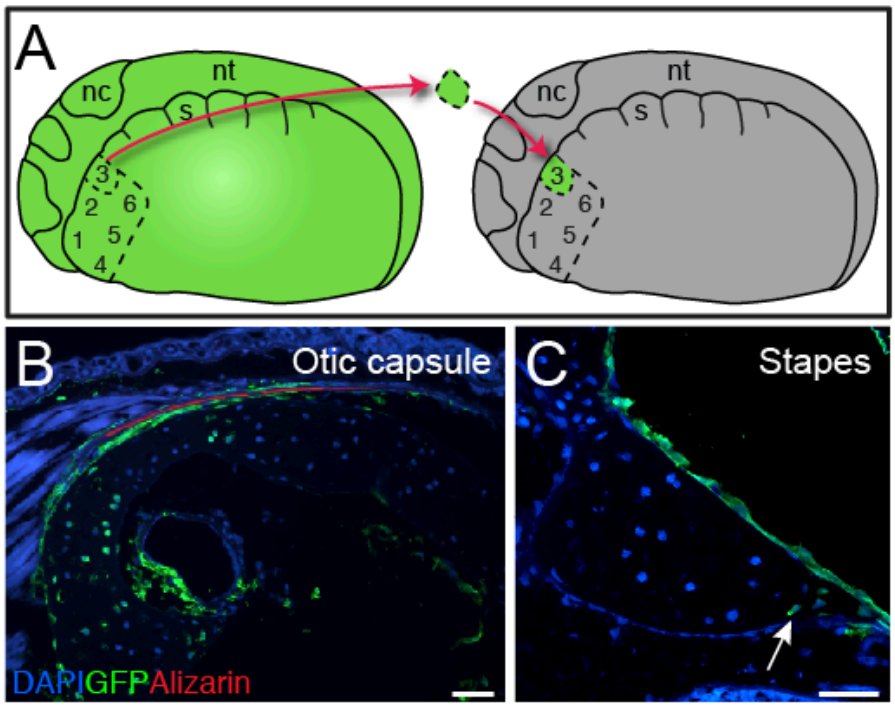

Figure 3.2 | Transplantation strategy and cranial mesoderm derivation of the cartilaginous skull. (A) Schematic of transplant regions (1–6) in a GFP+ stage-21 embryo and a stage-matched white (d/d) host (drawn with the epidermis removed). (B, C) The otic capsule and a few cells at the base of the stapes (arrow) are derived from cells in region 3. Transverse sections through the otic region. nc, neural crest; nt, neural tube; s, somite. Scale bar: 100 μm.

is possible that some of the mesodermally derived otic cartilage is retained at the edges of the base of the stapes as separation occurs. A partially mesodermal origin of the columella, a homologue of the stapes, is reported in chicken (Smith 1904; Noden 1986), although other studies in chicken claim the stapes is entirely neural-crest derived (Le Lièvre 1978; Couly et al. 1993). Based on genetic lineage tracing, the footplate of the stapes is partially derived from mesoderm in mouse (Thompson et al. 2012). Otic capsule ablation in the spotted salamander, *Ambystoma maculatum*, results in defects in the base and shaft of the stapes, although in these experiments the otic capsule was interpreted as the signaling center for stapes development rather than the source of the stapes itself (Toerien 1963). Our results suggest that the defects in the stapes that follow otic capsule ablation are due, at least in part, to the mesodermal origin of the base of the stapes.

Cranial mesoderm from all three paraxial regions contributes to the parietal bone (Fig.

Table 3.1 | Surgeries in *Ambystoma*: labelled bones and cartilages following cranial mesoderm transplantation.

		Skeletal elements							
Transplant type[a]	No. Survived[b]	par	sq	ps	os[c]	oc	st[d]	bb2	cm
Region 1	13	4		1	5				13
Region 2	14	2	2	4		3	2		14
Region 3	18	4	9	11		16	3		14
Region 4	8								6
Region 5	8							2	6
Region 6	9							2	1
Region 5 + 6	15							13	10

[a] See Figure 1A for regions
[b] to stage 53 or later (up to 6 months)
[c] posterior os
[d] base of stapes

Abbreviations: par, parietal; sq, squamosal; ps, parasphenoid; os, orbitosphenoid; oc, otic capsule; st, stapes; bb2, basibranchial 2; cm, cranial muscle

3.3A–C); regions 1 and 3 form rostral and caudal portions of the parietal, respectively. Overall, the derivation of the cranial vault in the axolotl closely resembles that in the mouse, with the neural crest-mesoderm boundary primarily between the frontal and parietal. Chicken fate maps by different research groups have reported conflicting locations of the neural crest-mesoderm interface in the skull vault: either in the mid-frontal (Noden 1978; Le Lièvre 1978) or between the parietal and supraoccipital (Couly et al. 1993). Both of these locations differ from the location in axolotl and mouse, where the parietal is entirely mesoderm derived and neural crest contributes to the full length of the frontal. Using developmental origin as one criterion for homology, these results raise the possibility that the chicken 'frontal' might instead be considered a 'frontoparietal', as previously suggested (Noden and Trainor 2005; Noden and Schneider 2006). In the palate, we also found the the posterior parasphenoid is derived from cranial mesoderm (Fig. 3.3E, F).

Posterior cranial paraxial mesoderm contributes to the dorsalmost portion of the squamosal bone in the axolotl, as it does in chicken (Fig. 3.4; Evans and Noden 2006). The rest of the squamosal in axolotl and chicken is derived from neural crest, which is the source of the entire squamosal in mouse (Le Lièvre 1978; Noden 1978; Couly et al. 1993; Köntges and

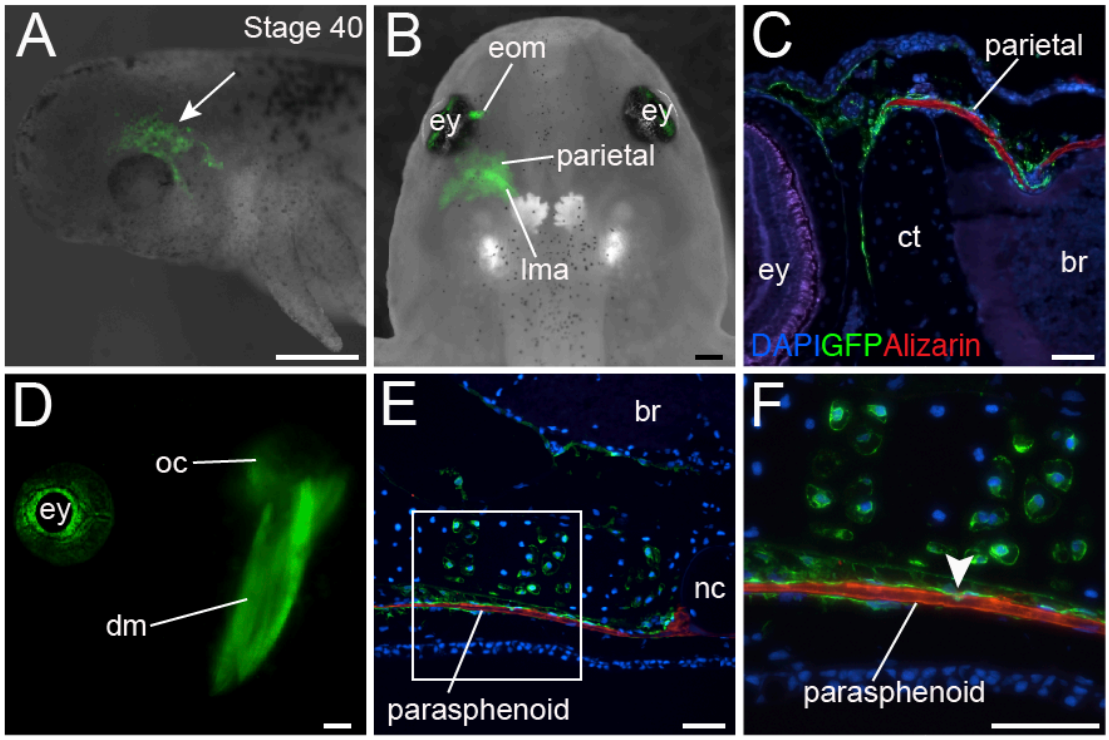

Figure 3.3 | Contribution of cranial mesoderm to the skull roof and palate.. (A) Stage-40 embryo that received a unilateral (left) graft from region 1 at stage 19. Lateral view, anterior to the top. (B) Recipient in (A) at stage 54. Extraocular muscle (eom), the levator mandibulae anterior muscle (lma) and the parietal bone are labeled. The retinal pigmented epithelium of the eye (ey) is autofluorescent, not GFP labeled. (C) The periosteum surrounding the parietal bone is GFP-labeled in transverse section at stage 56. Cross section through the eye (ey) region. (D) Stage-57 juvenile that received a graft from region 2 at stage 21. Labeling is present in the depressor mandibulae (dm), which opens the jaw, the cartilaginous otic capsule (oc) and the parasphenoid bone (visible in cross section). (E–F) The parasphenoid bone is labeled in transverse sections of juvenile axolotls. Boxed area in left panel is shown at higher magnification on the right. Cross section through the otic region. Scale bar: A, C, E and F–100 μm; B, D–500 μm.

Lumsden 1996; Morriss-Kay 2001; Jiang et al. 2002). The squamosal in Xenopus is derived from neural crest, although fate maps of cranial mesoderm have not been produced (Gross and Hanken 2004; Piekarski et al. 2014).

In zebrafish, neural crest does not contribute to the supratemporal, which suggests a mesodermal origin of this bone (Kague et al. 2012). Fusion of bones in the skull would provide a stronger, continuous attachment surface for cranial musculature (Schoch 2014). In lissamphibians, it has been proposed that the dorsal ossification center is homologous to the supratemporal (Reinbach 1939; Lebedkina 1979; Griffiths 1954a; Jarvik 1967; Schoch 2014)

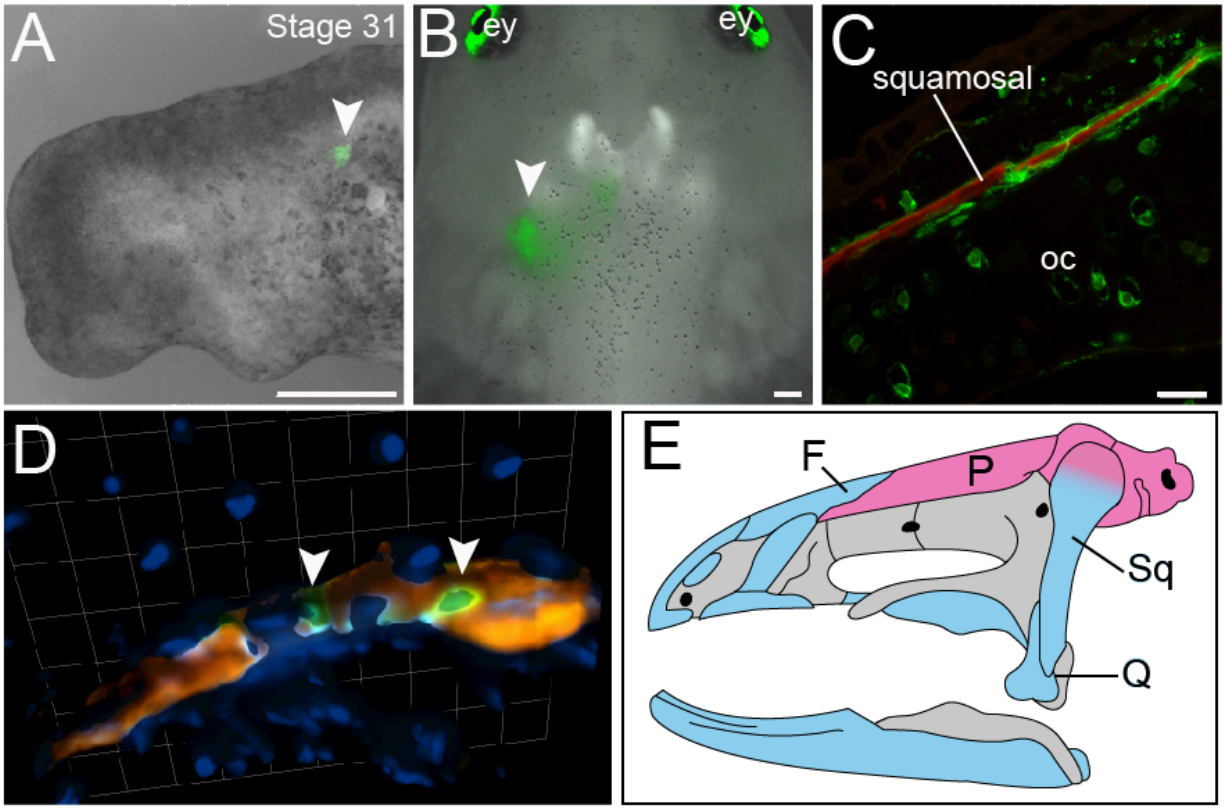

Figure 3.4 | Cranial mesoderm forms the dorsal cheekbone in *A. mexicanum*. (A) Stage-31 embryo that received a unilateral graft of GFP-labeled paraxial cranial mesoderm (arrowhead) just anterior to somite 1 at stage 21. (B) Recipient in (A) at stage 57. Dorsal view, anterior to the top. Labeling in cartilaginous otic capsule visible (arrowhead). (C) Periosteum surrounding the dorsal portion of the squamosal bone is GFP-labeled in cross section through the otic region. (D) 3D reconstruction of labeling in squamosal bone, indicating labeling of cells within the bone (arrowheads). In transverse sections, GFP-positive cells are green; DAPI-stained nuclei are blue and the alizarin-stained bone matrix is red. (E) Mesodermal contribution to the axolotl skull. Mesoderm, pink; neural crest, blue; cartilage, gray. Scale bar: A, B–500 μm; C–100 μm; D–one unit, 30 μm.

or the tabular (Alcalde and Basso 2013). Our fate-mapping data supports the hypothesis that the dorsal ossification center that contributes to the adult squamosal is homologous to the supratemporal (or tabular). Our data cannot distinguish between these alternatives. Most early tetrapods and temnospondyls, e.g., *Apateon*, possessed both supratemporals and tabulars (Fig. 3.5). The early Jurassic caecilian Eocaecilia retains a separate bone medial to the squamosal, but it is uncertain if this bone is the supratemporal or the tabular (Jenkins et al. 2007). Based on the anterior location of the dorsal ossification center in the squamosal, Schoch (2014) recently proposed its homology with the supratemporal and not with the

more posteriorly located tabular.

Both the tabular and the supratemporal are reduced or lost in synapsids and diapsids. The tabular tends to be lost prior to the supratemporal in diapsid evolution; the reverse is true in synapsids (Parrington 1937). Here, we review the presence of the supratemporal and tabular in diapsids (Fig. 3.5). In reptiles, the squamosal generally extends on to the surface of the otic capsule (Howes and Swinnerton 1901). The supratemporal is found in the stem diapsid *Youngina*, different authors have proposed either presence or absence of the tabular (Carroll 1981; Evans 1980). The tabular and supratemporal were present ancestrally in lepidosauromorphs, including *Paliguana* (Carroll 1975), but the tabular is absent in rhynchocephalians and squamates (Gauthier et al. 1988). The supratemporal is absent in adult *Sphenodon*; its presence in hatchlings is unresolved (Howes and Swinnerton 1901; Rieppel 1992). A supratemporal is present in the Triassic sphenodontian *Clevosaurus* (Robinson 1973; Fraser 1988) as well as in most extant squamates, in which it has acquired a new function in association with cranial kinesis (Evans 2008). Resolving the embryonic origin of the squamosal in squamates that have a discrete supratemporal, such as the lizard *Anolis*, might reveal if the tabular is truly absent in squamates or if instead it is fused with the squamosal.

The tabulars are absent in all archosauromorphs, while the supratemporal is present in both *Prolacerta* (Modesto and Sues 2004) and the archosauriform *Proterosuchus* (Cruickshank 1972). The supratemporal is absent in *Euparkeria*, crocodiles and dinosaurs (including avians). Examination of embryonic ostrich, chicken and penguin material did not reveal a second dorsal ossification center (Brock 1935). Thus, it was presumed that the avian squamosal lacks any supratemporal or tabular component (Brock 1935). While it is possible that critical embryonic stages were missing in determining centers of ossification, the two ancestral ossification centers may have merged such that they are no longer independently visible. The anuran frontoparietal, for example, forms from a single center of ossification in multiple lineages (Sedra 1949; Trueb 1970). The squamosal of at least some anurans and urodeles exhibits a secondary fusion wherein a discrete dorsal center fuses with ventral ossification(s) (Reinbach 1939; Sedra 1949; Lebedkina 1979; Wiens 1989; Wild 1997,

1999; Perotti 2001; Alcalde and Basso 2013). However, not all frog species possess a distinct dorsal ossification center, and there can be significant variation within a single genus. In *Bufo*, for example, a discrete dorsal ossification center is present in *B. calamita*, *B. regularis* and *B. bufo* (although the timing of its appearance varies), whereas the dorsal ossification center is absent in *B. calamita* (Griffiths 1954a). Thus, species may show varying degrees of ossification center fusion (Lebedkina 1979). It has been proposed that heterochronic shifts can lead to an alteration in the number of ossification centers (Smirnov et al. 2008).

Retroviral labeling of cranial mesoderm in the chicken has identified a postero-dorsal region of the squamosal that is derived from cranial mesoderm (Evans and Noden 2006). The mesodermal origin of the postero-dorsal squamosal in chickens could be explained by fusion of the supratemporal to the squamosal in archosaurs. Given that a second, dorsal ossification center has not been observed in avian embryos (Brock 1935), we suggest that the apparent absence of a postero-dorsal ossification center represents an instance of "fusion primordiale" (Dugès 1834) with the squamosal, wherein the discrete ossification centers have themselves fused over time (Fig. 3.6). We propose that the squamosal bone in axolotl and in chicken retains evidence of this fusion in its dual embryonic origin. In mice, the mesoderm-derived tabular bones fuse to the medial postparietal to form the adult interparietal (Koyabu et al. 2012); concomitantly, the squamosal has no reported mesoderm component (Jiang et al. 2002; McBratney-Owen et al. 2008). This study provides evidence of how simplification of the temporal region might have arisen repeatedly in distinct tetrapod lineages i.e not through true loss (failure to ossify), but through fusion to the adjacent squamosal.

We derive a fate map of osteogenic cranial mesoderm in the axolotl, which includes contributions to the parietal, occipito-otic, posterior parasphenoid, and the base of the stapes. Broadly speaking, the nature and extent of mesodermal contribution to the bony skull closely resembles that reported for amniotes. Cranial mesoderm in axolotl also contributes to a dorsal component of the squamosal, which supports the proposed homology between the dorsal ossification center in batrachians and the supratemporal of earlier tetrapods. Moreover, we propose that the mesoderm-derived component of the avian squamosal (Evans and Noden 2006) is likewise homologous to the supratemporal, which might have fused to the

squamosal early in archosaur evolution. Absence of a discrete "supratemporal" ossification center in avians suggests either a more advanced state of fusion than is seen in many amphibians or that critical embryonic stages have not been examined. Independent fusion of the supratemporal/tabular and squamosal in stem amphibians, batrachians, and archosaurs indicates a recurring tendency towards consolidation of these bones during tetrapod evolution.

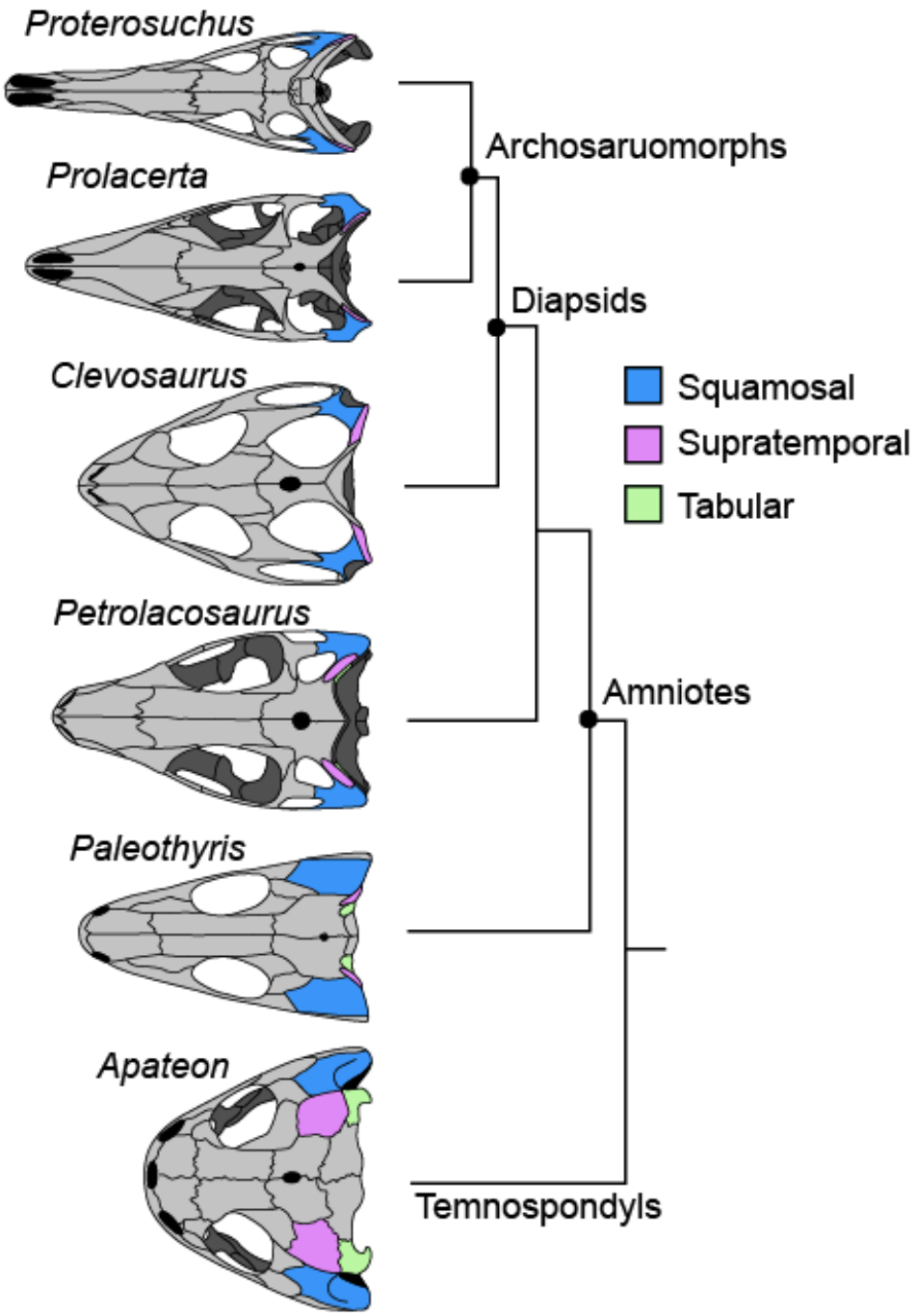

Figure 3.5 | Squamosal and temporal series in amphibians and reptiles. The distribution of the supratemporal bone in dissorophoid temnospondyls, stem diapsids and stem archosaurs indicates repeated, independent loss of this element in tetrapod vertebrates. Skulls are redrawn from the following references: *Apateon* (Fröbisch and Schoch 2009); *Paleothyris* (Carroll 1969); *Petrolacosaurus* (Reisz 1977); *Clevosaurus* (Fraser 1988); *Prolacerta* (Gow 1975); *Proterosuchus* (Cruickshank 1972).

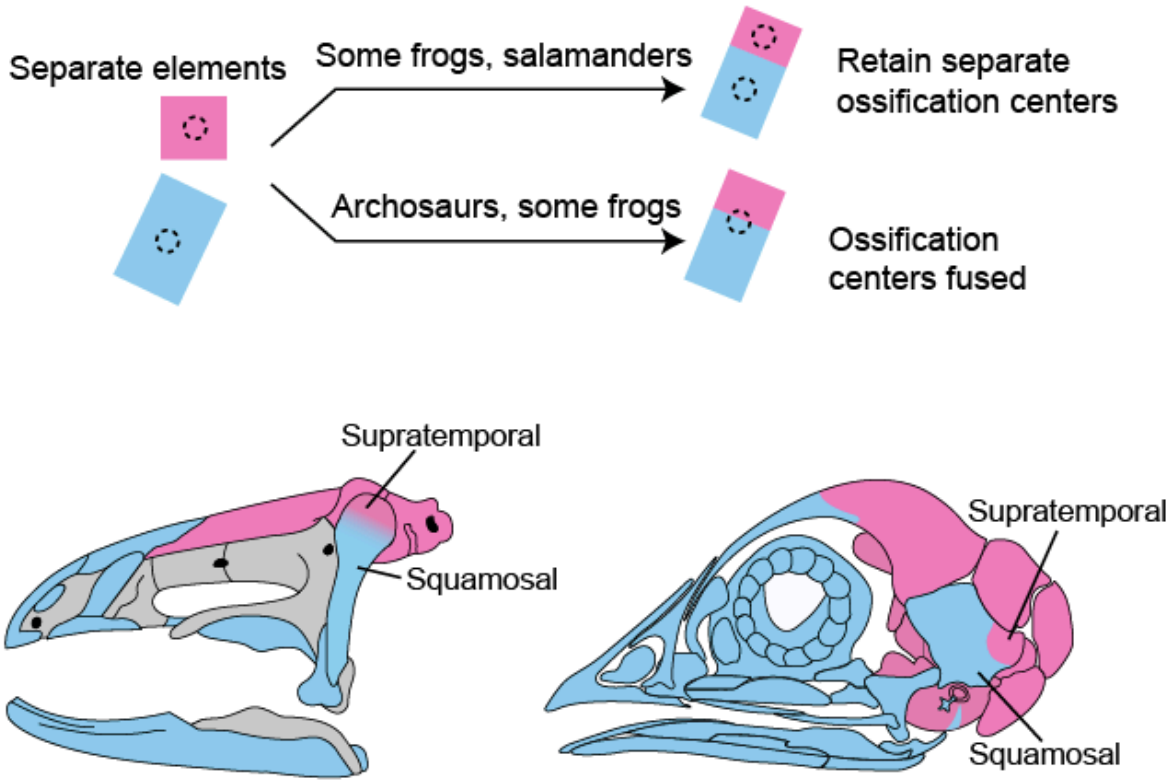

Figure 3.6 | Hypothesis of supratemporal incorporation into the squamosal in amphibians and archosaurs. The squamosal is partially derived from cranial mesoderm in both axolotl and chicken. This mesoderm-derived portion (red) may be homologous to the supratemporal of earlier tetrapods. In numerous amphibians, there is a discrete dorsal ossification center (dotted circle) within the mesoderm-derived portion, in addition to a ventral center within the crest-derived portion (blue). In birds and at least some frogs, the entire squamosal develops from a single ossifcation center. Chicken fate-map is based on ref. 4.

Chapter 4

Evolution of the head-trunk interface in tetrapod vertebrates

Abstract

Vertebrate neck musculature spans the transition zone between head and trunk. The extent to which the cucullaris muscle is a cranial muscle allied with the gill levators of anamniotes or is instead a trunk muscle is an ongoing debate. Novel computed tomography datasets reveal broad conservation of the cucullaris in gnathostomes, including coelacanth and caecilian, two sarcopterygians previously thought to lack it. Lateral plate mesoderm (LPM) adjacent to occipital somites is a recently identified source of cervical musculature in two amniote models, chicken and mouse. We fate-map this mesoderm in the axolotl (*Ambystoma mexicanum*), which retains external gills, demonstrating its contribution to posterior gill-levator muscles and the cucullaris. Accordingly, LPM adjacent to the occipital somites should be regarded as posterior cranial mesoderm. The axial position of the head-trunk border in axolotl is congruent between LPM and somitic mesoderm, unlike in chicken, and possibly other amniotes.

4.1 Introduction

The evolution of a mobile neck was a key innovation at the origin of tetrapods (Daeschler et al. 2006). It involved expansion of muscles, some derived from the head (cranial muscles) and some from the trunk, to support the skull apart from the pectoral girdle and permit a greater range of movement of the head relative to the rest of the body. Cranial muscles support a range of functions, including feeding, respiration, vision, facial expression and vocalization. They are distinct from trunk muscles in genetic regulation and susceptibility to disease (Noden 1983a; Noden et al. 1999; Sambasivan et al. 2009; reviewed by Bismuth and Relaix 2010; Diogo et al. 2015; Noden and Francis-West 2006; Tzahor 2009). Developmentally, they are non-somitic, arising instead from cranial paraxial and splanchnic mesoderm (Couly et al. 1992; Noden 1983a; Evans and Noden 2006; reviewed by Noden and Trainor 2005). Cranial muscle regulatory factors include *Isl1*, *Tbx1*, *MyoR*, *Capsulin* and *Pitx2*, which operate in specific muscle groups (Hacker and Guthrie 1998; Sambasivan et al. 2009; Lu et al. 2002; Mootoosamy and Dietrich 2002; Harel et al. 2009). In contrast, formation of trunk muscle is *Pax3*-dependent (Tajbakhsh et al. 1997).

The domain of the vertebrate neck contains two muscle groups: the ventral hypobranchial muscles and the dorsal cucullaris. Hypobranchial muscles are derived from occipital somites, which form the hypoglossal cord and migrate towards the tongue (Noden 1983a; OâĂŹRahilly and Müller 1984). The number of occipital somites contributing to cranial structures varies among species, however. Somites 2 and 3 form both hypobranchial musculature and the occipital arch in the axolotl (Piekarski and Olsson 2007, 2013), whereas in chicken the boundary of contribution to hypobranchial muscles and the posterior skull is within somite 5.

The cucullaris muscle, a feature of gnathostomes, connects the head to the pectoral girdle, thus spanning the transition zone between cranial and trunk myogenic signaling regimes (Kuratani 1997). It is suggested to be homologous to the trapezius and sternocleidomastoid in amniotes (Lubosch 1938). In sharks and the Queensland lungfish, the cucullaris elevates the gill arches and the pectoral girdle. It originates near the skull and continues caudally and

ventrally to insert on the scapular region of the pectoral girdle; a ventral fascicle extends to the posteriormost branchial bar (Edgeworth 1926, 1935; Allis 1917; Vetter 1874; Greenwood and Lauder 1981). The cucullaris is a thin muscle, and it can be difficult to visualize its three-dimensional position vis-à-vis adjacent skeleton and musculature. Hence, it is poorly described in many taxa with regard to both its shape and its relation to other cranial and trunk musculature. It is innervated by the accessory ramus of the vagus (X) nerve in anamniotes, but primarily by the accessory (XI) nerve in amniotes (Edgeworth 1935). The connective-tissue component of hypobranchial muscles and the ventrolateral neck is derived from neural crest in chicken (Le Lièvre and Le Douarin 1975). The cucullaris in chickens is reported to have somite-derived connective tissue (Noden, 1983a). The derivation of connective-tissue components of the mouse spinotrapezius has not been resolved, as both lateral plate mesoderm (Durland et al. 2008) and neural crest (Matsuoka et al. 2005) are reported sources.

While a somitic derivation of the hypobranchial muscles is widely accepted, the embryonic origin of the cucullaris is controversial (reviewed by Tada and Kuratani 2015; Ericsson et al. 2013). Historically, the cucullaris was considered a branchiomeric cranial muscle based in part on its anatomical relation to the gill levators (Vetter 1874; Edgeworth 1935; Piatt 1938). Subsequent fate mapping of anterior somites in chicken and axolotl, though, demonstrated a somitic (trunk) contribution (Noden 1983a; Couly et al. 1993; Huang et al. 1997, 2000; Piekarski and Olsson 2007). More recent fate mapping in chicken and genetic analysis in mouse reveal that the trapezius is primarily a lateral plate mesoderm-derived structure that employs a cranial, rather than trunk, myogenic program (Theis et al. 2010; Lescroart et al. 2015).

These data leave unresolved whether the lateral plate origin of the cucullaris is the result of a posterior shift of the head myogenic program or if instead head mesoderm extends caudally into the region adjacent to the anterior somites. To distinguish between these hypotheses, it is important to define the posterior limit of myogenic cranial mesoderm in an organism with a relatively conservative cervical and branchial region. Amniote branchial arch musculature is reduced in comparison to that of piscine sarcopterygians and aquatic

salamanders such as the axolotl, which has a relatively plesiomorphic arrangement of cranial muscle. Moreover, axolotls possess bushy external gills and their associated musculature, which likely were present in the larvae of Paleozoic tetrapods, as well as a robust gill skeleton, which was present in the earliest limbed stem tetrapods (Schoch and Witzmann 2011).

Here, we address this problem from a combined morphological and developmental perspective. In the axolotl, we report a shared cranial (branchiomeric) morphology and myogenic program of gill-levator muscles and the cucullaris and locate the head-trunk boundary within unsegmented cranial mesoderm. In addition, we use micro-computed tomography (CT) to describe the morphology of the cucullaris and gill levators in a phylogenetically diverse series of gnathostome taxa, including limbless caecilians and the coelacanth, the sister taxon to all other extant lobe-finned fishes. In previous studies, the cucullaris was investigated largely by gross dissection. In many species, however, the cucullaris is a thin, superficial muscle embedded in several layers of fat and connective tissue. It can be difficult to expose without damaging its *in situ* context with respect to the trunk and the pectoral girdle. Our CT-based reconstructions reveal such three-dimensional relationships without tissue disruption.

In those taxa that have both branchial levators and a cucullaris, the cucullaris invariably appears to be in series with the levators, suggesting that it is a serial homolog and thus supporting a cranial muscle identity. Likewise, in the axolotl, although the cucullaris in adults assumes a large, triangular "trapezius-like" morphology, the larval cucullaris is clearly in series with the levators. The ubiquity of the cucullaris further supports the hypothesis that it is a critical and indispensible component of the head/trunk connection in gnathostomes. We thus undertook to study the development of tissues in the transitional region spanned by the levators and cucullaris by extending modern fate-mapping techniques and gene-expression analysis of cranial mesoderm to the axolotl. We show that unsegmented mesoderm adjacent to the anterior three somites contributes to the cucullaris as well as to the gill-levator muscles in a manner consistent with their apparent serial homology, which supports the categorization of the cucullaris as a branchiomeric muscle. Cranial mesoderm markers, including isl1 and tbx1, also are expressed in the developing cucullaris region. We

argue that the posterior limit of cranial mesoderm extends caudally to the axial level of somite 3 and this head trunk boundary is consistent between the somites and lateral plate mesoderm in the axolotl. We discuss the importance of posterior cranial mesoderm in the evolution of the vertebrate neck.

4.2 Materials and Methods

Contrast staining and micro computed tomography (CT) scans

CT scans were prepared from anatomical specimens of *Hydrolagus* sp. (MCZ 164893), *Polypterus bichir* (MCZ 168418) and *Protopterus* sp. (MCZ 54055) from the Museum of Comparative Zoology at Harvard University, as well as *Typhlonectes natans* (YPM HERA 012618) and *Monodelphis domestica* (YPM MAM 10713) from the Yale Peabody Museum of Natural History at Yale University. *Latimeria chalumnae* (AMNH 32949h) was obtained from the American Museum of Natural History. For contrast staining, specimens were immersed in 5% Lugol solution in 70% ethanol for 7–10 d at room temperature. Specimens were washed in 70% ethanol for 2 d, changing solution daily. Three-dimensional images were taken using an XRA-002 microCT scanner (X-Tek) at the Center for Nanoscale Systems at Harvard University. Reconstructions were performed with VGStudio Max 2.0 (Volume Graphics).

Magnetic Resonance Imaging (MRI) data for coelacanth

MRI data for *Latimeria chalumnae* (SIO 75-347) from the Scripps Institution of Oceanography were obtained from the Digital Fish Library hosted by the University of California, San Diego, through the generosity of Lawrence Frank and Rachel Berquist.

Fate-mapping in *Ambystoma mexicanum*

White mutant (dd), GFP+ white mutant and albino (aa) embryos of the Mexican axolotl (*Ambystoma mexicanum*) were obtained from the Ambystoma Genetic Stock Center at the University of Kentucky and from the Hanken laboratory breeding colony at Harvard University. Before grafting, embryos were decapsulated manually by using watchmaker forceps and

then staged (Bordzilovskaya et al. 1989; Nye et al. 2003). Explants of unsegmented cranial mesoderm (stages 18–22) from donor embryos were grafted unilaterally into stage-matched hosts in place of comparable regions that had been extirpated. Stage-matched donors were of similar size and form. Explants were kept in place with a glass coverslip for several minutes to promote healing. In heterotopic transplantations, anterior cranial mesoderm from regions that contribute to mandibular or hyoid arch musculature was partially extirpated in hosts. In one set of heterotopic experiments, GFP+ mesoderm adjacent to somite 2 was moved into either region 1 or region 2 of host anterior cranial mesoderm (integrating into either the mandibular or hyoid arch). In a second set of experiments, GFP+ mesoderm adjacent to somite 5 was transplanted into host anterior cranial mesoderm.

Immunohistochemistry and sectioning

Fixation, embedding and sectioning were performed as previously described for *A. mexicanum* (Sefton et al. 2015). For GFP labeling, sections were incubated with rabbit polyclonal anti-GFP ab290 (1:2000; Abcam, Cambridge, MA), followed by AlexaFluor-488 goat anti-rabbit (1:500; Life Technologies, Carlsbad, CA). Sections were also stained with DAPI (0.1–1 Îijg/ml in PBS) to label cell nuclei. Some sections were stained with the skeletal muscle marker 12/101 monoclonal antibody (1:100; Developmental Studies Hybridoma Bank, Iowa City, IA). Additionally, desmin (1:100; Monosan, PS031; Uden, Netherlands) was used to label muscle in stage-40 embryos. Acetylated alpha-tubulin (1:100; Sigma, T6793; St. Louis, MO) was used to detect developing axons, followed by AlexaFluor-568 goat anti-mouse (1:500; Life Technologies, Carlsbad, CA).

Optical Projection Tomography (OPT) of *Ambystoma mexicanum*. A specimen for OPT (Sharpe et al. 2002) was stained with 12/101 followed by AlexaFluor-568 goat anti-mouse as described above. Clearing and embedding were performed at the University of Washington, where the larva was dehydrated in ethanol, cleared in 1:2 benzyl alcohol/benzylbenzoate and imaged with a Bioptonics 2100M scanner.

RNA in situ hybridization

Albino (aa) embryos were used for in situ hybridization. Antisense riboprobes were syn-

thesized from the cloned fragment (DIG RNA labeling kit; Roche Diagnostics, Indianapolis, IN). In situ hybridization was performed as previously described (Henrique et al. 1995), with the addition of an MAB-T wash overnight at 4°C (100 mM maleic acid, 150 mM NaCl, pH 7.5, 0.1% Tween 20). Hybridization was performed at 65°C. Primers are included in Supp. Table 2. Amplified PCR fragments were subcloned into the pCR II vector (Life Technologies).

4.3 Results

4.3.1 Morphology and Conservation of Cranial muscle

New soft-tissue-contrast staining methods for high-resolution CT afforded us the opportunity to examine the volumetric anatomy of muscles in a sample of vertebrates spanning Gnathostomata (Fig. 4.1; Appendix B.1–8). In Chondrichthyes, such as the chimaera, the cucullaris is a massive muscle that may incorporate anterior gill levators; it may not be strictly homologous, in its entirety, with the cucullaris of osteichthyans. In piscine osteichthyans, such as bichir and lungfish, the cucullaris is a thin, strap-like muscle, sometimes called the "protractor pectoralis." (e.g., Greenwood and Lauder 1981). It diverges from the anterior gill levators, but otherwise it is in series with them and is located in the same connective tissue sheath, as well as sharing muscle fibers with more anterior muscles. It originates from the posterior region of the head and inserts on the pectoral girdle and, when present, the top of the fifth gill arch. In some amphibians and in amniotes, the cucullaris is a large wedge-shaped muscle, sometimes termed the trapezius (Owen 1866; Edgeworth 1935; Gegenbaur et al. 1878). This morphology is seen clearly in an *Anolis* lizard and in an opossum, which exhibits the primitive mammalian condition (Fig. 4.1F).

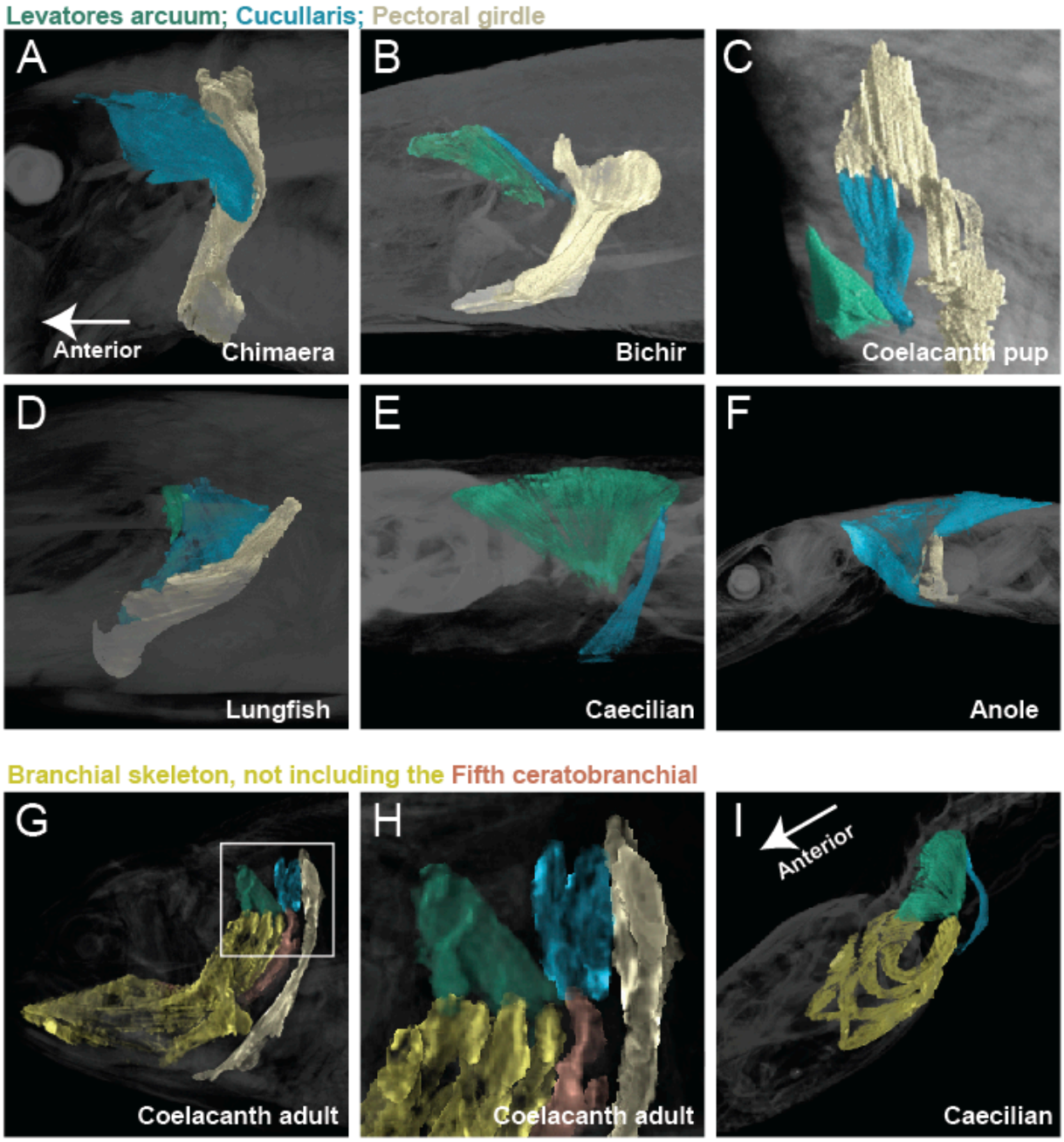

Figure 4.1 | Cranial muscle evolution based on contrast-stained CT scans and an MRI scan (coelacanth adult). (A–F) Left lateral views of gill-levator musculature and the cucullaris (or its homologue) in representative gnathostomes, showing its insertion on the pectoral girdle (except in caecilians, where it inserts on ventral fascia). (G, H) Left lateral views of gill levators and the cucullaris in relation to the branchial skeleton in a coelacanth. Box in G is enlarged in H. (I) Left dorsolateral view of the cucullaris in a caecilian. The cucullaris attaches to the posteriormost gill arch in the coelacanth. The gill-levator musculature is shaded green, the cucullaris blue, and the pectoral girdle white. In the lower panels, the fifth ceratobranchial is in pink and the anterior branchial skeleton in yellow.

The cucullaris has not been described in the musculoskeletally conservative coelacanth, nor in the limbless caecilian amphibians. Greenwood and Lauder (1981) reported the cucullaris absent from the coelacanth, based on novel dissections. Millot and Anthony (1958), however, had earlier briefly described in the coelacanth a fifth gill levator that originates on the anocleithrum of the pectoral girdle, unlike the first four gill levators, which originate in the otic region. We examined this muscle in both a CT scan of a contrast-stained coelacanth pup and an MRI (magnetic resonance imaging) scan of an adult. The muscle is larger than previously described, with several heads originating on the pectoral girdle (Fig. 4.1B, G–H). It is angled differently from the other levators but its fibers remain in close association with them and extend from the anocleithrum to insert on the fifth ceratobranchial. In the adult, an anterior portion of this muscle extends dorsally to attach on the fascia of the epaxial musculature (Fig. 4.1H). Based on its morphology and location, we regard the fifth gill levator as the homolog of the cucullaris. Accordingly, the coelacanth cucullaris retains the ancestral connection between the posteriormost branchial bar and the shoulder girdle, which is seen in at least some sharks and lungfish (Edgeworth 1926, 1935; Allis 1917; Vetter 1874; Greenwood and Lauder 1981). Even though actinopterygians lack an ossified fifth gill arch, the cucullaris in these taxa sometimes joins the fibers of the posteriormost gill levator (Greenwood and Lauder 1981). Similarly, even though the cucullaris in the coelacanth lacks a dorsal connection to the head, it does attach to the dorsal fascia posterior to the cranium, and it connects the pectoral girdle to the cranial skeleton, specifically the branchial skeleton.

In the caecilian *Typhlonectes natans* we examine the m. levator arcus branchiales complex, previously described in *Dermophis mexicanus* (Bemis et al. 1983). It is also termed the m. cephalodorsosubpharyngeus (Wilkinson and Nussbaum 1997; Lawson 1965). Based on our examination, the m. levator arcus branchiales complex is a triangular structure that originates from the otic capsule and dorsal trunk muscle fascia with a ventral insertion on the the posteriormost ceratobranchial (Fig. 4.1E, I). A posterior division of the muscle, termed the pars posterosuperficialis by Wilkinson and Nussbaum (1997), inserts on the on fascia separating the rectus abdominus and the interhyoideus. Based on the topographical relationships of the posterior m. levator arcus branchialis complex, we homologize and syn-

onymize the posterior division with the cucullaris. It is unclear if part of the anterior division might also be considered part of the cucullaris as well, connecting to the transformed gill levator musculature.

The cucullaris and its homologs comprise a highly conserved connection between head and trunk. In general, the cucullaris is intimately associated, and sometimes partially continuous, with the gill levators, which are unambiguously cranial (branchiomeric) muscles. In numerous taxa, it attaches to both the skull and the gill skeleton, both cranial elements.

Mesoderm adjacent to anterior somites forms the cucullaris and gill levators

In amphibians, the cucullaris has also been termed the protractor pectoralis (Ziermann and Diogo 2013) or the trapezius (Piatt 1938). In juvenile axolotls, the cucullaris resembles the ancestral osteichthyan condition and is morphologically similar to and in series with the anterior gill levators, whereas in adults it expands into a broad, thin sheet (Fig. 4.2A, B). Given the conservative morphology of branchiomeric musculature in the axolotl (Ericsson et al. 2004; Ericsson and Olsson 2004; Ziermann and Diogo 2013), we began fate-mapping head mesoderm that contributes to the pharyngeal arches. In chicken and axolotl, mesoderm from somites 1 and 2 contributes to the cucullaris (Piekarski and Olsson 2007). In chicken, however, the majority of the cucullaris is derived from lateral plate mesoderm adjacent to the occipital somites (Theis et al. 2010). Consequently, we suspected that the axolotl cucullaris might also have a dual origin from both somitic and unsegmented mesoderm.

We transplanted GFP+ mesoderm adjacent to the first three somites into a white (d/d) host (Fig. 4.2C; Appendix B.9). By stage 35, GFP+ cells were visible dorsal to the developing gill buds in the region of the presumptive gill muscles, the cucullaris and the dilatator laryngis (Fig. 4.2D–G). In cross section, labeled cells were present throughout the length of the cucullaris but absent from the somitic hypobranchial or epaxial muscles, thus indicating little if any somitic contamination (Fig. 4.2H–I). Additional transplants were performed for three regions of cranial mesoderm anterior to the first somite. In most of these transplants, the first gill-levator muscle originated from mesoderm just anterior to the first somite, whereas the posterior three gill levators arose from unsegmented mesoderm at the level of somites 1–3 (Figure 4.5A; Table 4.1).

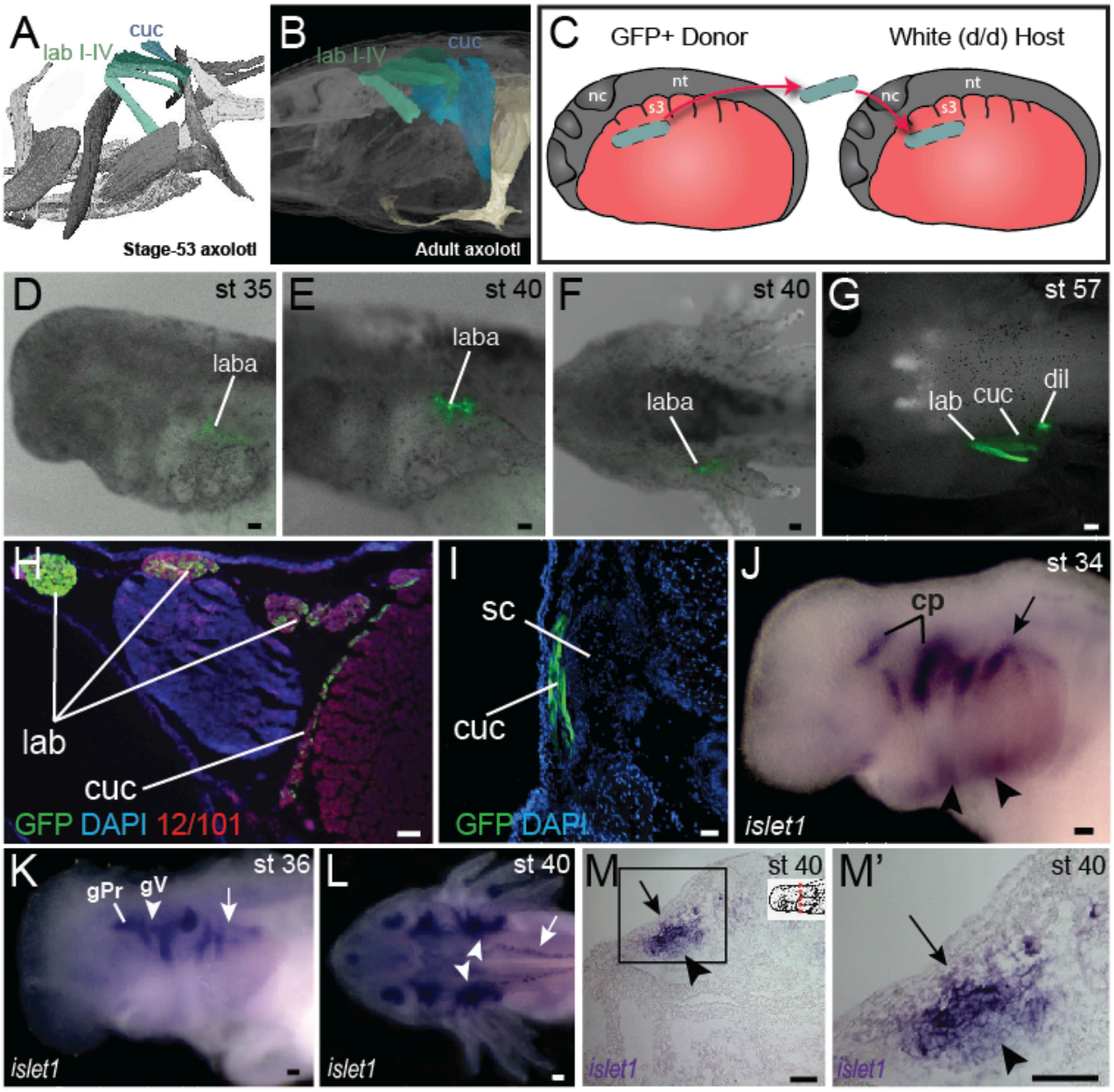

Figure 4.2 | Development of the cucullaris muscle in the axolotl. (A, B) Morphology of the developing cucullaris, with the four gill-levator muscles (lab I–IV) shaded light green and the cucullaris (cuc) blue. More-posterior muscles are shaded dark green. Anterior is to the left. (A) Dorsolateral view of an OPT scan of a juvenile axolotl stained with the 12/101 muscle antibody. (B) Contrast-stained CT scan of an adult axolotl in lateral view. The cucullaris is expanded into a broad sheet that inserts on the scapula. (C) Schematic depiction of an orthotopic transplantation of unsegmented mesoderm lateral to somites 1–3 at stage 21. Lateral views; anterior is to the left. nc, neural crest; nt, neural tube; s3, somite 3. (D–I) GFP labeling following stage-21 transplantation of unsegmented mesoderm lateral to somites 1–3. (D–F) Labeling of the levator arcuum branchiarum anlagen (laba) dorsal to the developing gills is visible in lateral (D, E) and dorsal (F) views. Anterior is to the left. (G) Gill-levator muscles (levator arcuum branchiarum, lab) of arches 3 and 4, the cucullaris (cuc) and the dilatator laryngis (dil) are labeled in a juvenile axolotl. Dorsal view; anterior is to the left.

Figure 4.2 | Continued. (H–I) Transverse sections through the posterior occipital region (H) and anterior trunk (I) of juvenile axolotl. GFP labeling is visible in the gill levators and anterior cucullaris (H) and in the posterior cucullaris near its attachment with the scapula (I; sc). Lateral is to the left; dorsal is to the top. (J–M') *isl1* expression in albino embryos. (J) At stage 34, *isl1* is expressed in ventral mesoderm, in the developing heart region (arrowheads) and around the dorsal cranial placodes (cp). Arrow indicates several stripes of expression dorsal to the developing gills. (K) At stage 36, *isl1* marks the profundal (gPr)/trigeminal (gV) placode region and earlier expression is maintained dorsal to the gills (arrow). (L) At stage 40, *isl1* is expressed in neurons within the dorsal spinal cord (arrow) and in the gill-levator region (arrowheads). Dorsal view. (M, M') Transverse section of a stage-40 embryo with *isl1* expression in the dorsal gill region (arrows), placode and associated ganglia (arrowheads). Box in M is enlarged in M'. Scale bars, 100 μm, except G, 500 μm.

Table 4.1 | Surgeries in *Ambystoma*: number of mesoderm transplants and muscles labeled.

		Cranial and cervical muscles									
Transplant type	No. Survived[a]	lme	lma	im	ih	bhe	dm	ldb	lab	cuc	dil
Region 1	16	14	8	9							
Region 2	20	2	3	4	13	6	10	1			
Region 3	32[b]				1	4	20	6[c]	9[d]		
LPM s1-3	14							13[e]	13[f]	13	8
LPM s4	3										
LPM s1-3 into CM (heterotopic)	7[g]	3	1		1		3		2		
LPM s5 into CM (heterotopic)	10				1						

[a] To stage 43 or later
[b] of these, 9 were labeled only in the otic capsule
[c] all in ldb 1
[d] 6 in only lab 1, 2 in lab 1-2, and 1 in lab 1-4
[e] 2 in ldb 1-3, 7 in ldb 2-3, and 4 in only ldb 3
[f] 2 in lab 1-4, 8 in lab 2-4, 2 in lab 3-4, 1 in lab 4 only
[g] 3 into region 1 and 4 into region 2

Key to mesoderm regions:

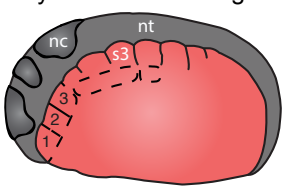

Abbreviations: LPM s, lateral plate mesoderm adjacent to somite; CM, cranial mesoderm; lme, levator mandibulae externus; lma, levator mandibulae anterior; im, intermandibularis posterior; bhe, branchiohyoideus externus; dm, depressor mandibulae; ldb, levatores et depressores banchiarum; lab, levatores arcus branchiarum; cuc, cucullaris; dil, dilatator laryngis

4.3.2 *Isl1* is expressed in the gill levator and cucullaris region

Transcription factors involved in cranial muscle development are expressed in gill levator/cucullaris muscle territory. At neurula and tailbud stages, *isl1* is expressed in anterior cranial mesoderm associated with the second heart field (Appendix B.10; Sefton et al. 2015). In subsequent stages, *isl1* expression expands dorsally to encompass the entire dorsoventral length of the gills, but later (stage 34) it is reduced near the heart and appears in the developing cranial placodes (Fig. 4.2J–L). From stage 36 through at least stage 40, stripes of expression are present dorsal to the developing gills, including the levator anlage (Fig. 4.2K–M'). The head muscle gene *tbx1* (sequences of *tbx1*, *msc* and *pitx2* by pers. comm. from J. Whited, B. Haas and L. Peshkin) is expressed in the developing gill muscle region at stages 35 and 38 (Appendix B.11). By stage 38, *msc* is also expressed in the gill region. Unlike *isl1*, expression of *tbx1* and *msc* extends distally into the external gills (Appendix B.11).

4.3.3 Molecular regionalization of mandibular and hyoid arch muscles

Two genes reveal substantial genetic heterogeneity within the phylogenetically conserved amphibian adductor complex. In axolotl, jaw adductor muscles include the levator mandibulae externus (lme) and the levator mandibulae anterior (lma); the latter muscle is also called the pseudotemporalis (Ziermann and Diogo 2013). Both of these muscles develop within the mandibular arch (Fig. 4.3B, I). We examined expression of *lhx2*, a LIM-domain transcription factor involved in pharyngeal muscle specification in the mouse (Harel et al. 2012). As seen in mouse and Xenopus, *lhx2* is expressed in axolotl in the brain and eye (Fig. 4.3; Appendix B.12; Viczian et al. 2006; Atkinson-Leadbeater et al. 2009). At stage 34, *lhx2* is expressed in the mesodermal core of the pharyngeal arches (Fig. 3E, F), but by stage 40 it becomes more restricted to specific muscle groups, including the lme and ventral hyoid arch musculature (Fig. 4.3G, H). Expression of *lhx2* was not visible in the lma at stage 40. At stage 38, the anlage of the lma is located posterior to the eye (Fig. 4.3I). By stage 40, this region expresses *isl1*, including the superficial lma and developing ganglia, while we were

unable to see expression of isl1 in the lme (Fig. 4.3J–K").

A third gene provides an additional example of genetic heterogeneity in cranial muscle development. In mouse, *Pitx2* is broadly expressed in developing muscle; it is necessary to specify mesoderm of the mandibular arch but not of the hyoid arch (Shih et al. 2007a, b). In axolotl, as in chick, *pitx2* is expressed in anterior ectoderm and mesoderm from neurula stages through at least tailbud stages (Fig. 4.4E, F; Appendix B.12; Bothe and Dietrich 2006). A stripe of expression in hyoid arch mesoderm and in the migrating hypobranchial muscle precursors also appears by stage 34 (Fig. 4.4E). It is maintained in hyoid arch derivatives and by stage 40 is concentrated in the hyoid musculature, including the depressor mandibulae and branchiohyoideus externus (Fig. 4.4F; Appendix B.12K, M). The depressor mandibulae anlage (dma) is in the dorsal/proximal pharyngeal arch at stage 35 (Fig. 4.4B, C) and then extends to insert on Meckel's cartilage at stage 42 (Ericsson and Olsson 2004). At stage 40, *pitx2* expression is not apparent in branchial arch muscles, although it is strongly expressed in tongue musculature (Appendix B.12L, M).

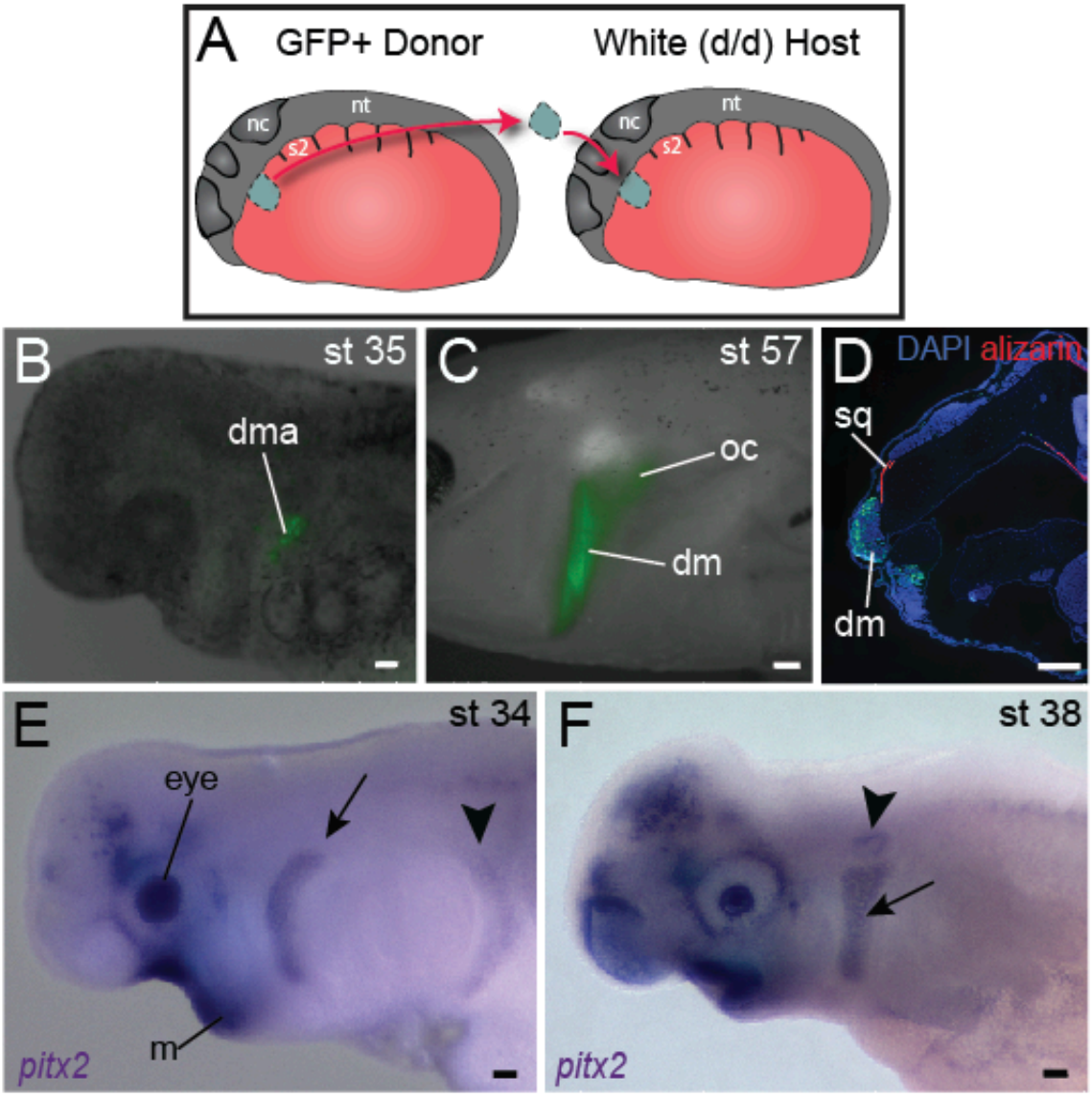

Figure 4.3 | Origin of the mandibular depressor muscle and expression of pitx2 in the hyoid arch. (A) Schematic depiction of orthotopic transplantation of cranial mesoderm. nc, neural crest; nt, neural tube; s2, somite 2. Somite 1 is small and triangular in shape. (B) GFP labeling of dorsal hyoid-arch mesoderm at stage 35 following transplantation at stage 20 includes the anlage of the depressor mandibulae (dma). (C) Specimen in (B) at stage 57, with labeling of the depressor mandibulae (dm) and otic capsule (oc). (D) Labeling of the depressor mandibulae in a transverse section through the jaw region of a stage-57 juvenile axolotl. sq, squamosal bone. Dorsal is to the top; lateral is to the left. (E) At stage 34, *pitx2* is expressed in the eye, the ventral mandibular arch (m), the hyoid arch (arrow) and more faintly in migrating somitic cells (arrowhead). (F) At stage 38, *pitx2* expression is maintained in the hyoid arch (arrow) and is also present in the otic vesicle (arrowhead). Scale bars, 100 μm, except C, 500 μm.

4.3.4 Heterotopic transplantation between lateral plate and cranial mesoderm

We investigated the myogenic properties of lateral plate mesoderm adjacent to the somites to determine if local signals in the cranial mesoderm of the mandibular and hyoid arch regions could instruct lateral plate mesoderm at various axial levels to adopt cranial muscle fate. Myogenic lateral plate mesoderm in the cucullaris region adjacent to somite 2 was transplanted into anterior cranial mesoderm following extirpation of a region of host mesoderm (Fig. 4.5A). Transplanted cells were incorporated into both dorsal and ventral mandibular arch or hyoid arch muscle (Fig. 4.5B, C"). These muscles displayed normal innervation from the mandibular branch of the trigeminal nerve (Fig. 5.5C, C") and the facial nerve, respectively. Local cues appear sufficient to pattern myogenic lateral plate mesoderm in the cucullaris region and to promote mandibular or hyoid arch muscle development.

Next, more posterior lateral plate mesoderm, adjacent to somite 5, was transplanted heterotopically to mandibular arch mesoderm at stage 21 (Fig. 4.5D). While transplanted cells were present among mandibular arch structures, in 9 of 10 larvae they did not incorporate into muscle (Fig. 4.5E). Neither mandibular nor hyoid arch mesoderm appears sufficient to pattern posterior non-myogenic lateral plate mesoderm to promote muscle formation.

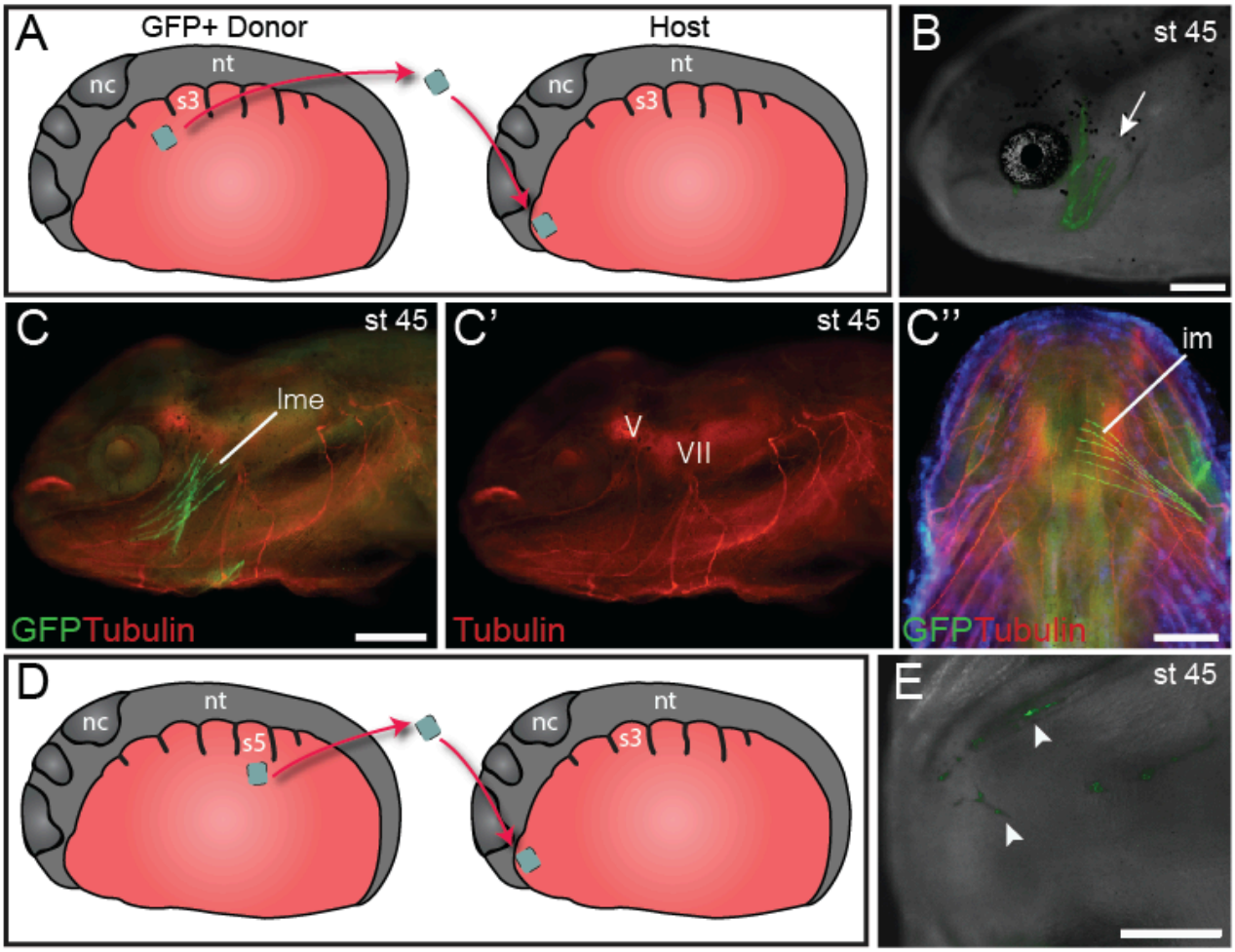

Figure 4.4 | Heterotopic transplantation of lateral plate mesoderm. (A) Schematic depiction of a caudal-to-cranial heterotopic transplantation of lateral plate mesoderm from somite level 2 (donor) to mandibular arch mesoderm (host). Lateral views; anterior is to the left. nc, neural crest; nt, neural tube; s3, somite level 3. (B–C") Stage-45 larva following heterotopic transplantation shown in (A). (B) GFP+ cells contribute to mandibular arch muscles (arrow). Lateral view; anterior is to the left. (C) Lateral plate mesoderm contributes to the levator mandibulae externus (lme). (C') Innervation of the levator mandibulae externus by the mandibular branch of the trigeminal nerve (V) is normal. VII, facial nerve. (C") The intermandibularis (im), a ventral mandibular muscle, is also labeled. Ventral view; anterior to the top. (D) Schematic depiction of a caudal-to-cranial heterotopic transplantation of lateral plate mesoderm from somite level 5 (s5) to mandibular arch mesoderm. (E) Stage-45 larva following heterotopic transplantation shown in (D). Ventral view; anterior is to the left. No muscle fibers are formed, but labeled cells contribute to cranial vasculature (arrowheads). Scale bars, 100 μm.

4.4 Discussion

4.4.1 Phylogenetic distribution of the cucullaris

We provide evidence from comparative morphology, embryonic fate mapping and gene expression that the cucullaris is a branchiomeric muscle in series with the gill levators and that it is stably conserved across gnathostomes as a link between head and trunk. Accordingly, we propose the fifth gill levator of the coelacanth is homologous to the cucullaris, which, as in some sharks, rays and lungfish, attaches the pectoral girdle to the posteriormost gill bar (Edgeworth 1935; Greenwood and Lauder 1981). We regard this interpretation of data from coelacanth, viz., the cucullaris has reduced its dorsal attachment to the head/expaxial muscle fascia, more parsimonious than an earlier claim that the cucullaris is absent and that a gill levator has entirely shifted its origin from the head to the pectoral girdle (Millot and Anthony 1958). In the larval caecilian *Ichthyophis kohtaoensis*, the fourth gill levator is substantially larger than the anterior three levators (Kleinteich and Haas, 2007). The cucullaris could potentially develop from the caudalmost gill levator, as has been suggested in urodeles (Edgeworth 1935). The cucullaris of caecilians, lacking an insertion to the absent shoulder girdle, instead has evolved a patent connection between the otic capsule (as well as the dorsal trunk fascia) and fascia associated with ventral trunk musculature. It is unclear if the anterior portion of the levator arcus branchiales complex, which inserts on the posteriormost gillbar, is also part of the cucullaris or instead represents gill levators that did not degenerate following metamorphosis. If the former is the case, this unusual configuration may express an ancestral potential of the cucullaris to attach to the gill skeleton, and it evokes reports that the paired fin/limb apparatus has surprising developmental resemblance to the gill arches (Gillis et al. 2009).

The cucullaris has evolved to perform distinct functions in different lineages. In placoderms, for example, it may have depressed the head (Trinajstic et al. 2013). The morphology of the cucullaris in sharks and rays suggests the muscle in gnathostomes originates ancestrally from the pectoral girdle and inserts on two parts of the cranial skeleton: the posterior

gill bar and the caudal region of the head. The connection to the gill arches was likely lost in early tetrapods (but possibly later reappeared in caecilians), while an alternate attachment to the clavicle evolved in some lineages. The cucullaris is purportedly absent in turtles and snakes, but recent work suggests that it may be present in both groups. In turtles, it has been proposed that the muscle originates on the shell (carapace), which incorporates parts of the pectoral girdle (Lyson et al. 2013). In snakes, the pectoral girdle is absent and the origin of the cucullaris has concomitantly shifted to the body wall (Tsuihiji et al. 2006).

4.4.2 Cucullaris development in the axolotl

The cucullaris is located in a complex transition zone between head and trunk; in the axolotl, this complexity is reflected in the muscleâĂŹs dual embryonic derivation from both somitic and cranial mesoderm. An origin from both the caudal branchial levator and somites was suggested in the yellow-spotted salamander based on serial sections and dissection (Piatt 1938). Our finding that unsegmented mesoderm adjacent to the anterior somites forms the posterior gill-levator muscles, a laryngeal muscle, the levatores et depresores branchiarum and the cucullaris indicates that the posterior limit of cranial mesoderm is at somite 3. The presence of labeled cranial mesoderm cells in a laryngeal muscle in axolotl betrays the deep phylogenetic conservation of a relationship between the cucullaris and laryngeal muscles, which is revealed in a recent analysis demonstrating that mouse laryngeal muscles are clonally related to the trapezius and absent following mutation of the gene *Tbx1* (Lescroart et al. 2015). Moreover, expression of the genes *isl1* and *tbx1* in the gill-levator region suggests these muscles develop through the cranial muscle regulatory network, consistent with their classical anatomical classification as cranial muscles. The LIM homeodomain protein *Isl1* is required for normal second heart field (SHF) development and its expression in SHF progenitors is downregulated following differentiation (Cai et al. 2003). Genetic fate mapping in mouse demonstrates a large contribution of *Isl1*-positive cells to the ventral intermandibular muscle and the cucullaris (Nathan et al. 2008; Theis et al. 2010).

Our analysis of cranial mesoderm markers in axolotl provides additional evidence for substantial genetic heterogeneity in cranial muscle development, as in the mouse and chicken

(Nathan et al. 2008; Dong et al. 2006; Kelly et al. 2004; Marcucio and Noden 1999). Surprisingly, our data reveal that differentiation of mandibular adductor muscles is present in amphibians at the level of gene expression. At prehatching stages, *isl1* is expressed in the anterior adductor, while *lhx2* is expressed primarily in the external adductor.

4.4.3 Evolution of the Head-Trunk Boundary

In the axolotl embryo, somites and pharyngeal arches occur at the same post-otic axial level, which is a basic feature of morphologically conservative vertebrates (Kuratani 1997). Lateral plate mesoderm adjacent to somites 1 and 2 is located in the intermediate region between head and trunk and is important for morphogenetic movements associated with the migration of hypobranchial muscle progenitors (Lours-Calet et al. 2014). The head-trunk interface at the paraxial level is marked by the path of circumpharyngeal neural crest cells as they migrate ventral to the occipital somites to form the circumpharyngeal ridge caudal to the pharynx (Kuratani 1997). Specialized muscles occur at this paraxial level, including the trapezius/cucullaris and, in axolotls, the gill levators.

Our finding that the posterior gill-levator muscles and the cucullaris originate from cranial mesoderm adjacent to the first three somites supports categorization of the cucullaris as a branchiomeric muscle. Moreover, it may help explain why lateral plate mesoderm in the embryonic âĂŸtrunkâĂŹ in chicken has myogenic capacity. Our fate-mapping data suggest that this mesoderm, which gives rise to the cucullaris in amniotes, is not a novel source of musculature, but instead is cranial mesoderm associated with the most posterior pharyngeal arch (5th, 6th or 7th, depending on species). We propose that, in the axolotl, somite 3 is the posterior limit of mesodermal contribution to cranial structures in both paraxial and lateral mesoderm (Fig. 4.6A). In our heterotopic transplantations, cranial mesoderm that forms the cucullaris is able to follow the myogenic program of cranial muscles in the mandibular and hyoid arches. Although the chicken lacks many of the cartilages and muscles associated with the posterior pharyngeal arches in other tetrapods, it retains cucullaris progenitors in the same anatomical position as in the axolotl (Fig. 4.6B).

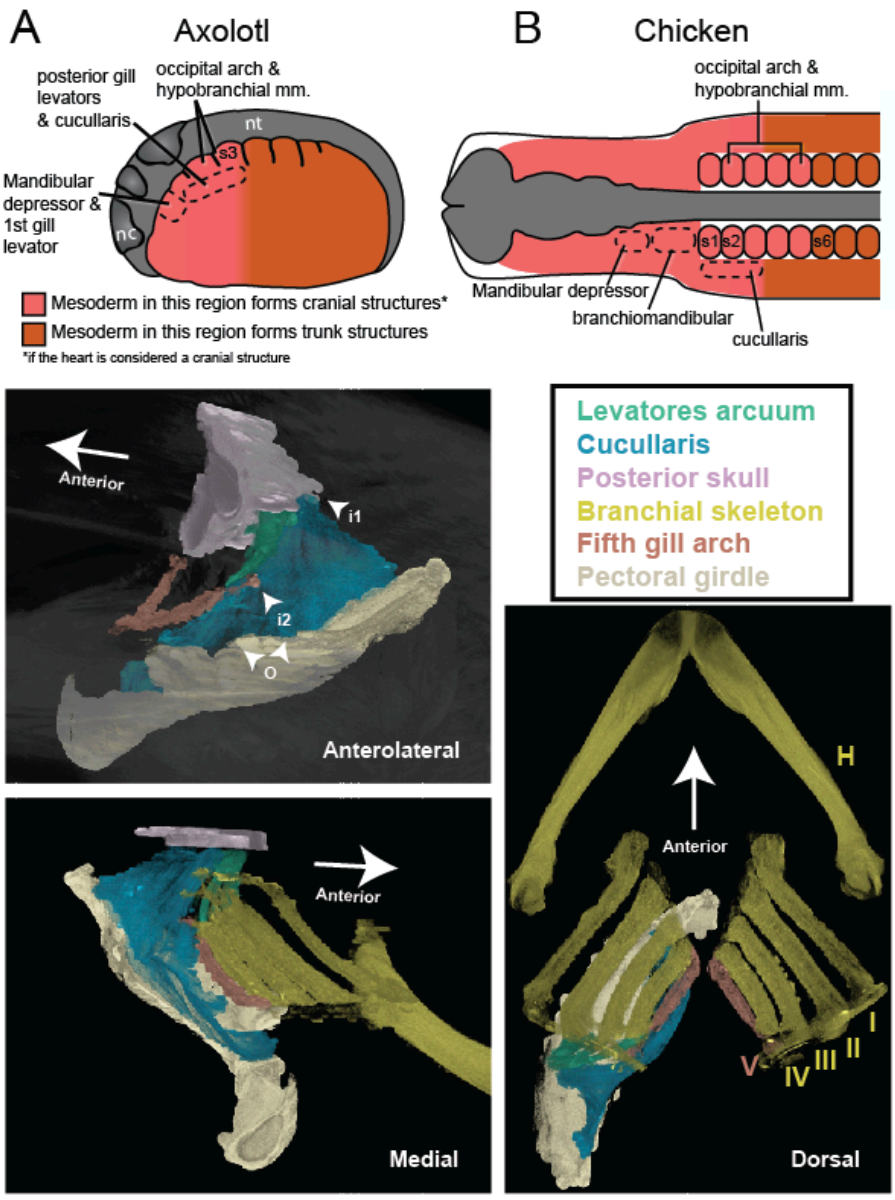

Figure 4.5 | The cucullaris and the transition zone between the head and trunk. (A) In the axolotl embryo, the head-trunk boundary in unsegmented mesoderm is closely congruent with that in the somites. Paraxial and lateral mesoderm anterior to somite 3 form cranial structures (including the heart). The illustration depicts a stage-21 embryo with epidermis removed; anterior to the left. Somite fate-mapping data are from Piekarski and Olsson (2007, 2013). (B) In the chicken, the axial level of the head-trunk boundary in somitic mesoderm is posterior to the border in unsegmented mesoderm. Somite fate-mapping data are from Noden (1983a; hypobranchial mm.) and Couly (1993); cucullaris data are from Theis et al. (2010); mandibular depressors and branchiomandibular data are from Noden (1983) and Evans and Noden (2006). (C–E) Contrast-stained CT images of the lungfish branchial skeleton, pectoral girdle, posterior skull, gill levators and cucullaris. All structures except the branchial skeleton are segmented on the left side only. The anterolateral view depicts only the fifth gill arch, with its attachment to the cucullaris; the body is rendered transparent. The lungfish cucullaris retains the ancestral tripartite attachment: origin from the pectoral girdle (o) and insertions on the posterior skull (i1) and fifth ceratobranchial (i2).

The head-trunk boundary in the axolotl is congruent between cranial mesoderm and somitic mesoderm, but in the chicken (and probably other amniotes) the head-trunk boundary in somites is posterior to that in unsegmented cranial mesoderm (Fig. 4.6A–B; Couly et al. 1993; Piekarski and Olsson 2013; Huang et al. 2000). It remains to be determined whether this congruence, as seen in the axolotl, is the plesiomorphic condition for tetrapods. Heterotopic transplantations in chicken suggest that somitic mesoderm has greater regional plasticity than lateral plate mesoderm. Somites that contribute to the posterior skull are able to generate vertebrae when transplanted to a more posterior position, independent of *Hox* gene expression (Kant and Goldstein 1999), whereas caudal cranial mesoderm that gives rise to the cucullaris is unable to generate muscle when transplanted to a more posterior location (Theis et al. 2010). It will be of interest to determine the mechanisms responsible for the incorporation of somites into the posterior skull during tetrapod evolution and to determine if the posterior limit of cranial mesoderm is less evolutionarily labile than somitic contribution to cranial structures.

Contributions: E. Sefton performed cranial mesoderm transplantations, antibody stains, section analysis, in situ hybridization, and OPT scan preparation and subsequent segmentation. T. Cox at the University of Washington Small Animal Tomographic Analysis Facility performed the OPT scan. B.-A.S. Bhullar contrast stained and CT-scanned specimens. B.-A.S. Bhullar and E. Sefton analyzed CT scans. Z. Mohaddes carried out in situ hybridizations and cryosectioning.

Chapter 5

New Transgenic lines for fate-mapping mesoderm and neural crest in *Xenopus tropicalis*

The world always seems brighter when you've just made something that wasn't there before.
-Neil Gaiman (2004)

Abstract

Frogs and salamanders possess distinct pectoral girdles; the frog retains a dermal bone, the cleithrum, which was present in early tetrapods, whereas the salamander pectoral girdle is entirely endochondral. It is unclear to what extent neural crest contributes to dermal elements of the shoulder, which is otherwise derived from mesoderm. To assess mesodermal and neural crest contribution to the skull and shoulder girdle, we sought to generate two transgenic lines to indelibly label mesoderm and neural crest in *Xenopus tropicalis*. For neural crest, we generated a *sox10-Cre* line, and for mesoderm, a *bra-Cre* line. Cells were labeled through Cre/loxP recombination in two reporter lines, one of which is a brainbow line. We are still in the process of characterizing these inducer lines and will determine if

they can provide a new perspective in tracing the boundary between the head and neck.

5.1 Introduction

One of the most striking features associated with the evolution of the tetrapod body plan is the separation of the shoulder girdle from the skull by a mobile neck (Daeschler et al. 2006; Shubin et al. 2015). The cleithrum, a dermal bone, forms a major component of the shoulder girdle in early tetrapods such as *Acanthostega* and *Tulerpeton*. It was eventually lost independently in amphibian and amniote lineages, as the endochondral elements proceeded to form the bulk of the shoulder girdle (Kardong 2002; Matsuoka et al. 2005; McGonnell 2001). Frogs are the only lineage of extant tetrapods to retain the cleithrum (Fig. 5.1). Prior work on anuran shoulder girdle development has focused on the timing of chondrogenesis and ossification (Shearman 2005, 2008). The neural crest-mesoderm boundary has not been examined in the anuran shoulder girdle.

A model of macroevolutionary change in musculoskeletal morphology, the scaffold model, has recently been proposed to explain shoulder girdle development. Genetic lineage tracing in the mouse has revealed that part of the scapular spine is derived from neural crest (Matsuoka et al. 2005). This neural crest-derived population is interpreted as the "ghost" of the cleithrum, wherein the embryonic origin of muscle connective tissue and its skeletal attachment region form a highly conserved "connectivity code" on the basis of muscular scaffolds (Köntges and Lumsden 1996; Matsuoka et al. 2005). This hypothesis been criticized, as a portion of the scapular spine is hypothesized to be a neomorphic feature in therians (Sanchez-Villagra and Maier 2006; Jenkins 1979).

In the axolotl, a salamander, neural crest makes no contribution to the shoulder girdle, providing no evidence for a connectivity code in urodeles (Epperlein et al. 2012). Axolotls, however, do not possess any dermal bone in their shoulder girdle. The differing morphologies of the shoulder girdle in frogs and salamanders, particularly the presence of dermal elements in the frog, presents a unique opportunity to compare the mesoderm and neural crest boundaries and evaluate a potential connectivity code in a tetrapod with a cleithrum.

Here, we take a transgenic fate-mapping approach to evaluate both neural crest and mesodermal contributions to the shoulder girdle. This analysis will test the hypothesis that neural crest contributes to elements of the shoulder girdle, especially the clavicle and cleithrum in *Xenopus tropicalis*. If the cleithrum, including its region of attachment to the connective tissue of the cucullaris, is not derived from neural crest, then this would contradict the muscular scaffold model defined by a conserved pattern of connectivity (Matsuoka et al. 2005). Long-term fate-mapping in the zebrafish indicated the cleithrum is not derived from neural crest (Kague et al. 2012), although this condition may not be representative of the condition in lobe-finned fishes; the zebrafish parasphenoid, for example, receives no neural crest contribution, while the anterior portion is derived from neural crest *X. laevis*, axolotl, and chicken (Couly et al. 1993; Piekarski et al. 2014; Kague et al. 2012). Deriving a fate map for the anuran clavicle and cleithrum would determine to what extent the dermal shoulder girdle is a part of the developmental program of the head (Matsuoka et al. 2005).

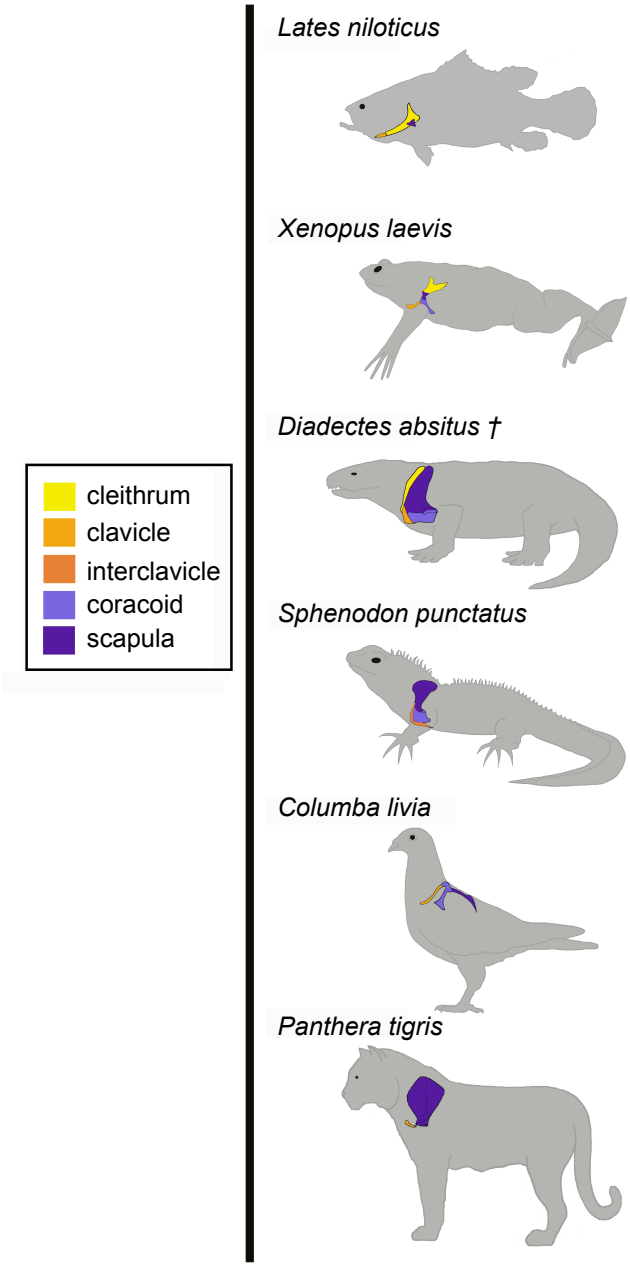

Figure 5.1 | Schematic depiction of dermal and endochondral elements of the pectoral girdle in a range of gnathostomes. The cleithrum (yellow) is a substantial component of the shoulder girdle in most actinopterygians, such as *Lates niloticus*, while the endochondral elements are comparatively small. The cleithrum is present in extant frogs and the stem amniote *Diadectes*. The endochondral scapula and coracoid (dark and light purple) are the primary elements in the pectoral girdle of extant amniotes.

5.2 Materials and Methods

Animal husbandry

Xenopus tropicalis were cared for and maintained in the Khokha lab aquatics facility, in accordance with Yale University Institutional Animal Care and Use Committee protocols, and the Hanken lab, with procedures approved by the Harvard University/Faculty of Arts and Sciences Standing Committee on the use of Animals in Research and Teaching. Embryos for injection were obtained through *in vitro* fertilization and raised in 1/9 MR (Modified Frog Ringers) with 100 μg/ml gentamycin.

Transgenic lines

To generate *Tg(sox10:Cre-cry:GFP-I-SceI)* (abbreviated to *sox10-Cr*e) a 4.8 kb promoter was subcloned using the pTransgenesis system (Love et al. 2011). This promoter has not been well characterized, although a sox10-GFP line has been made that demonstrates expression in migrating cranial neural crest (R. Kerney, personal communication). Primers used: 5'- AAGTCGACCATGAGCCTGGCCTA-3' and 5'- AAATGCATTTCC-AAGAGCGATGTGATTGG-3'. *Tg(bra:Cre-cry:GFP-I-SceI)* was also generated using pTransgeneis (Fig. 5.2). The 4.3 kb *bra* promoter and the pTransgenesis set were kindly provided by the European Xenopus Resource Center at the University of Portsmouth. Transgenic lines were made using I-*Sce*I Meganuclease transgenesis (Ishibashi et al. 2012). The *Tg(CMV-loxP-CFP-loxP-mCherry-I-SceI)* line was a gift of Raphael Thuret in Enrique Amaya's laboratory. The *Brainbow1.0* line was generated by Mustafa Khokha.

Image aquisition

Images were taken using a Leica DMRE fluorescence compound microscope and a Leica stereomicroscope.

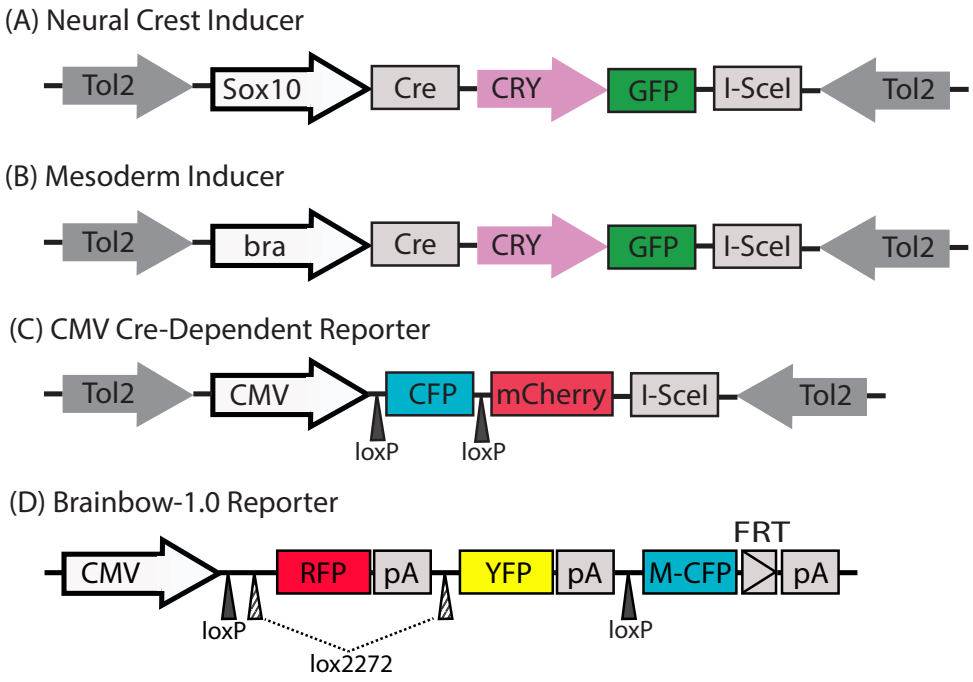

Figure 5.2 | Cre-dependent system to label *sox10+* and *bra+* cells. (A) An inducer transgenic line under the control of a *sox10* promoter. (B) Inducer line with the *bra* promoter. Both inducer lines can be screened through GFP expression in the lens. (C) Reporter line in which, when crossed with an inducer line, Cre recombinase acts on loxP sites to replace CFP expression with mCherry under control of the constitutively active CMV promoter. (D) Cre-dependent Brainbow 1.0 reporter line, in which Cre chooses between two potential excision events, loxP or lox2272. Recombination changes expression to either YFP or M-CFP.

5.3 Results

Xenopus Brachyury, a member of the T-box transcription factor family, is required for normal mesoderm development (Conlon et al. 1996). It is expressed throughout the marginal zone "the prospective mesoderm" and is subsequently present in the involuting mesoderm around the blastopore and the notochord (Smith et al. 1991). The *bra* promoter was inserted into a construct that fate maps via Cre-loxP recombination, where a floxed transgene is

removed by Cre. This results in the conditional activation of another transgene lying downstream of the distal loxP site (Lakso 1992). I-*Sce*I transgenesis was used to generate an *X. tropicalis* reporter line that expresses cyan fluorescent protein (CFP) ubiquitously in the absence of Cre recombinase, although this line has not been characterized in detail (Love et al. 2011). In the presence of Cre, recombination will result in mCherry replacing CFP. In the inducer line, a gamma crystalline lens-specific promoter driving GFP allows for the selection of transgenic animals. In the reporter line, the "constitutively active" promoter cyotomegalovirus (CMV) drives CFP expression. Flanked by loxP sites, CFP will be excised in the presence of Cre, resulting in the permanent expression of mCherry.

Double-transgenic tadpoles from *bra-Cre* X *CMV-loxP-CFP-loxP-mCherry* were expected to have fluorescing blue bodies, fluorescing green lenses, and red in mesoderm-derived cells. Expression was visible in the myotomes by stage 36 (Fig. 5.3A). This expression was maintained in older stages, but there was minimal expression in the cranial muscles, indicating only partial labeling of cranial mesoderm (Fig. 5.3C). These tadpoles were raised to post-metamorphic stages, fixed and cryosectioned. Expression was present in some neural crest-derived cartilages (data not shown), indicating additional, unexpected Cre activity. The *bra-Cre* line has not yet been crossed to the *Brainbow1.0* reporter.

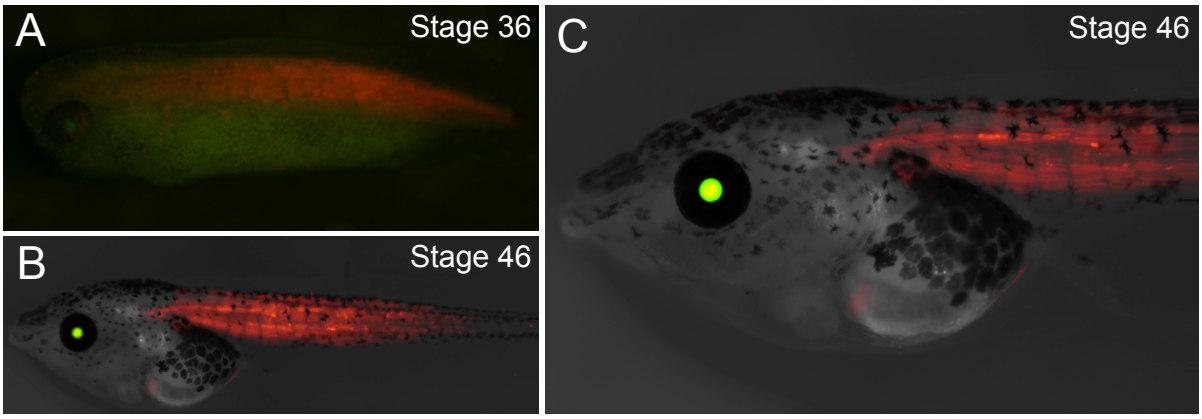

Figure 5.3 | Expression of mCherry and GFP in double-transgenic embryos from *bra-Cre* X *CMV-loxP-CFP-loxP-mCherry*. mCherry expression is visible in the myotomes, but not in cranial muscle.

Variable expression with different reporter lines

The transcriptional modulator Sox10 labels early neural crest cells and the peripheral nervous system (Kuhlbrodt et al. 1998). The *sox10* promoter has been used to successfully fate map neural crest in zebrafish (Kague et al. 2012; Mongera et al. 2013; Mongera and Nüsslein-Volhard 2013). Double-transgenic tadpoles from *sox10-Cre* X *CMV-loxP-CFP-loxP-mCherry* show scattered expression throughout the skin but strong expression in the olfactory capsules and in the stomodeum (Fig. 5.4A–C). Expression was also present in scattered but numerous myotomal cells (Fig. 5.4D)—approximately 75 per flank at stage 45. No mCherry expression was visible in the ceratobranchials of the pharyngeal skeleton.

Expression was distinct in double-transgenic tadpoles from *sox10-Cre* X *Brainbow1.0*. At stage 46, no expression was visible, suggesting transcripts had not accumulated in sufficient number to be seen. By stage 56, expression was evident in pharyngeal cartilages, including the planum orbitale, palatoquadrate and ceratobranchials (Fig. 5.4E, F, H). Additionally, expression could be detected in the central core of the barbels (Fig. 5.4G). These tadpoles were raised to stage 66, following the completion of metamorphosis. However, expression could not be detected post-metamorphosis, suggesting CMV stops initiating new transcripts by stage 66 and transcripts become less visible as the metamorphosing tadpole grows. A similar occurrence has been documented in *X. laevis* transgenic lines (Kerney et al. 2012).

5.4 Discussion

The same *sox10-Cre* driver line produced strikingly different results when crossed with distinct reporter lines. The differences between reporter lines could be due to variation in the reporter gene expression or inconsistent recombination. In mice, not all reporter lines have a uniform domain of gene expression (Heffner et al. 2012). Individual alleles can display differential sensitivity to Cre-mediated recombination (Schmidt-Supprian and Rajewsky 2007).

The gender of the parent can also influence Cre expression; in some transgenic mouse lines, a Cre female transmits the protein to oocytes causing early deletions (Matthaei 2007;

Heffner et al. 2012). Moreover, expression in unexpected tissues could be due to a number of factors. The Cre driver strains are constructed with a discrete portion of the proximal promoter. Thus, the subset of enhancers and repressors included in this region might result in more widespread expression. Alternatively, it could also reflect genuine expression of the driver gene.

Transgene expression patterns might also be influenced by integration site effects (Heffner et al. 2012). The site the DNA integrates into the genome is random. The local environment of the integration site for either the promoter or the inducer construct may influence expression (Matthaei 2007). For all transgenic lines examined herein except *Brainbow1.0*, the number of integration sites in the genome is expected to be rare due to the size of I-*Sce*I. I-*Sce*I is reported to integrate as a single copy or low copy number into mostly a single site in the genome (Thermes et al. 2002). Brainbow, by contrast relies on the integration of multiple transgene copies in tandem to produce color mixtures (Livet et al. 2007). The greater copy number in the *Brainbow1.0* reporter line may better reflect the expression of Cre in the inducer line.

To further characterize these lines, focusing on the *Brainbow1.0* reporter line, we will continue analyzing double-transgenic tadpoles at different stages using both freshly frozen sections and confocal imaging. The cleithrum appears at stages 58–60 in X. laevis (Trueb and Hanken 1992). We will need to determine to what extent transcripts are still visible in double transgenic *sox10-Cre* X *Brainbow1.0* at this stage, as they are absent/difficult to visualize at stage 66.

Contributions: E. Sefton generated constructs for injection. R. Kerney provided the *sox10* promoter. E. Sefton and J. Griffin injected 1-cell stage embryos for I-*Sce*I meganuclease transgenesis. J. Griffin screened tadpoles. E. Sefton analyzed expression.

Chapter 6

Conclusion

The fate map generated in this dissertation delineates the contribution of cranial mesoderm to the skull and cranial muscles in the axolotl. I demonstrated neural crest contribution to an element in the pharyngeal skeleton and the skull vault. Moreover, this work identifies the posterior limit of myogenic cranial mesoderm, indicating that lateral plate mesoderm adjacent to anterior somites contributes to true cranial muscles, including the gill levators. Cells in this region express cranial muscle markers. Lastly, I generated two novel transgenic lines to fate map neural crest and mesoderm in the diploid tropical clawed frog. In this chapter, I discuss the broader implications of my results and future directions to build upon this work.

6.1 Conservation and divergence in the embryonic origin of the skull

The fate of most skeletal structures in the axolotl is highly conserved with amniote models, with a few notable exceptions discussed further below. This contrasts with the frog *Xenopus laevis*, where differences in the embryonic derivation of the bony skull are striking compared to the axolotl, chicken, and mouse; although it remains to be seen if other frog

species demonstrate a similar pattern to *X. laevis*, the unique origin of the skull may be linked to the extensive remodeling of the skull in metamorphosis (Piekarski et al. 2014). The case of *X. laevis* and other examples (Spemann 1915; de Beer 1971; Hall 1995) indicate that homologous structures in the vertebrate head can develop via nonhomologous developmental processes. Thus, to what extent can embryonic origin shed light on homologies? Although embryonic derivation is not an inherent or necessary part of character identity, it can be a means to examine what Gunter Wagner terms âĂIJhistorical residuesâĂİ that point to hypotheses regarding homology (Wagner 2014). The skull of extant tetrapods has undergone a dramatic reduction in the number of elements compared to early tetrapods such as *Ichthyostega*. In urodeles and anurans, the skull is far more lightly built, with increased fenestration and emargination of the cheek (Schoch 2014). It is unclear clear, however, which bones have been lost through a failure to ossify (truncated developmental trajectory) or, alternatively, have been lost through fusion of proximate anlagen during early stages of development. Studying the embryonic origin of the skull can suggest patterns of loss and fusion, especially when considering elements of dual origin.

Previous studies in frogs and salamanders have shown that the pharyngeal skeleton is not entirely derived from neural crest (Stone 1926; Olsson and Hanken 1996). I demonstrate a mesodermal origin of the urohyal in the axolotl, also termed basibranchial 2. The axolotl urohyal progenitors are closely associated with the second heart field, based on both transplantation experiments and early expression of *isl1*. Furthermore, we find that ectopic retinoic acid signaling inhibits the formation of the urohyal. Future work examining this lineage in a clonal analysis would shed light on the relationship of these two structures. It would also be of interest to explore the role Wnt/-catenin signaling to this lineage of cells, as Wnt signaling is also involved in restricting the cardiac progenitor pool (Ueno et al. 2007). Given differences in origin, mode of development and muscle attachments, this element is likely not homologous with the urohyal in teleosts (as suggested by Arratia and Schultze 1990). We describe multiple hypotheses for the evolution of mesodermal contribution to the pharyngeal skeleton (Figure 2.4). Based on the similar morphology, muscle attachment and development (endochondral ossification) of the urohyal in *Latimeria chalumnae* to the uro-

hyal/basibranchial 2 in salamanders, it would be interesting to test the mesodermal origin of the urohyal in piscine sarcopterygians.

My data from axolotl provide evidence that embryonic derivation (either cranial neural crest or mesoderm derived portions of the skull) are in general highly conserved among three tetrapod lineages: mammals, birds and urodeles. This similarity likely represents an ancestral pattern of osteocranium embryonic development present in their common tetrapod ancestor, if not even earlier, in bony fishes (Piekarski et al. 2014). Comparison of the detailed fate maps for axolotl and chicken reveals the high degree of similarity between these two distantly related species (Figure 3.6). Even though axolotl and chicken have significantly different cranial morphologies and are separated by more than 300 million years of evolution, they share a nearly identical pattern of embryonic derivation of the skull. Less detailed fate-map data for the mouse also are highly similar. One important consequence for the cranial vault is that the boundary between CNC- and mesoderm-derived bones is located in approximately the same anatomical positionâĂŤalong the posterior margin of the orbitâĂŤin all three vertebrates (Jiang et al. 2002; Evans and Noden 2006).

I found the squamosal is a compound bone, with both a mesoderm and neural crest contribution, in the axolotl. This supports the homology of the mesoderm-derived dorsal portion of the squamosal to the supratemporal, an element independently lost in lissamphibians, mammals and archosaurs. Intriguingly, the postero-dorsal region of the chicken squamosal is likewise derived from mesoderm, unlike in mice (Evans and Noden 2006; Yoshida et al. 2008; Jiang et al. 2002). The supratemporal is present in stem diapsids, numerous extant lepidosaurs, and stem archosaurs; the tabular by contrast is largely absent. In synapsids, the supratemporal is absent in early lineages, while the tabular persists and has been proposed to fuse to the postparietals in extant mammals (Koyabu et al. 2012). We propose that the supratemporal convergently fused to the squamosal in archosaurs and amphibians, which explains differences between between the mouse and chicken/axolotl fate maps. It also clarifies how the skull has been repeatedly simplified in the cheek region: not through a failure to ossify, but fusion of the bone primordia early in development.

Instead of the supratemporal, it is possible the tabular has fused to the supratemporal

(reviewed by Alcalde and Basso 2013). Lepidosaurs are an intriguing lineage on which to test this hypothesis, as many species have retained a discrete supratemporal, although the squamosal has been highly modified in lepidosaurs for its role in cranial kinesis (Evans 2008). Lentivral lineage tracing has recently been developed for the lizard *Anolis* (Tschopp et al. 2014). If the squamosal in *Anolis* is derived from both neural crest and mesoderm, this would point to a possible early fusion of the tabular primordia to the squamosal during embryonic development. An entirely neural crest derivation of the *Anolis* squamosal would suggest the tabular does not ossify in lepidosaurs.

These hypotheses of homology and the evolution of the vertebrate skull rely on both comparative anatomy and lineage tracing. The use of lineage tracing addresses homology from the perspective of embryonic cell populations. How similar is the gene expression profile and gene regulatory network in the two distinct primordia of the squamosal bone? In mice, the neural crest-derived frontal and mesoderm-derived parietal display distinct osteogenic potentials and regenerative capacity that appears to be mediated by increased canonical Wnt signaling in the frontal bone (Quarto et al. 2009). It will be interesting to compare the Wnt and fibroblast growth factor signaling in the mesoderm and neural crest-derived portions of the squamosal bone.

6.2 Cranial muscle development and evolution of the head-trunk boundary

I also examined the origin of cranial muscles, establishing the posterior limit of myogenic cranial mesoderm at the axial level of somite 3. This extends the caudal limit of cranial mesoderm into what is typically considered the embryonic trunk, indicating lateral plate mesoderm adjacent to the occipital somites should be regarded as cranial mesoderm. I created a gene expression map of cranial muscles in the axolotl, which demonstrates heterogeneous gene expression in the mandibular adductor complex. Data from gene expression analysis, fate-mapping and comparative anatomy demonstrate a close relationship of the cucullaris to the gill levator musculature. While the axolotl cucullaris receives some contri-

bution from somitic mesoderm (Piekarski and Olsson 2007), most of the muscle is derived from cranial mesoderm. This suggests the evolution of the neck involved the expansion of a cranial muscle to join the pectoral girdle to the cranium.

It is unclear what mechanisms mediate the posterior limit of myogenic cranial mesoderm. Detailed analyses of *Hox* gene expression patterns in lateral plate mesoderm may shed light on the head-trunk boundary in unsegmented mesoderm. Moreover, It will be of interest to determine the functional role of cranial mesoderm genes with distinct expression patterns, such as a potential role for *pitx2* in dorsal hyoid arch musculature. The advent of genome editing technology in the axolotl will aid in such analyses (Flowers et al. 2014).

Lastly, we generated two transgenic lines of *Xenopus tropicalis* by using promoters for lineage tracing mesoderm (*brachyury*) and neural crest (*sox10*). Analysis of these lines is still preliminary, but we find expression differences depending on the reporter line. Fluorescence appears to more faithfully represent the sox10 expression when crossed with the *Brainbow1.0* reporter, as compared to the *Tg(CMV-loxP-CFP-loxP-mCherry-SceI* line. If these lines prove sufficiently specific and provide robust expression, it would provide a valuable resource to the *Xenopus* community.

6.3 Summary

This dissertation examined the role of cranial mesoderm in forming the bony skull and cranial muscles in the axolotl *Ambystoma mexicanum*. The axolotl is a valuable model to examine the pattern of embryonic origin in the context tetrapod head evolution. Urodeles are a have evolved independently for over 150 million years, although in many respects their body plan has remained morphologically stable (Gao and Shubin 2001). Future work studying the morphogenesis of bones, cartilage and muscles in the amphibian head will further our understanding of how complex structures are modified during evolution.

Appendix A

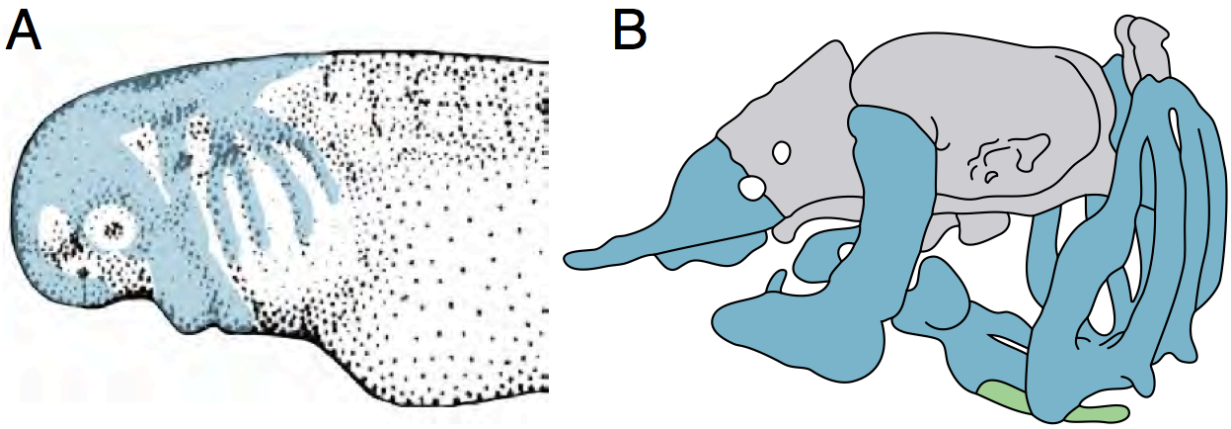

Figure 6.1 | Fate map and morphology of the salamander pharyngeal skeleton. (A) Drawing of a stage-33 *Ambystoma mexicanum* embryo showing streams of migrating neural crest (blue). Lateral view, anterior is to the left. (B) Schematic of a larval *A. maculatum* neurocranium and pharyngeal skeleton. Neural crest-derived cartilages are shaded blue. The second basibranchial (green) is the only pharyngeal skeleton component that is not derived from neural crest. Lateral view, anterior is to the left. Drawing in B is modified from Stone (1926).

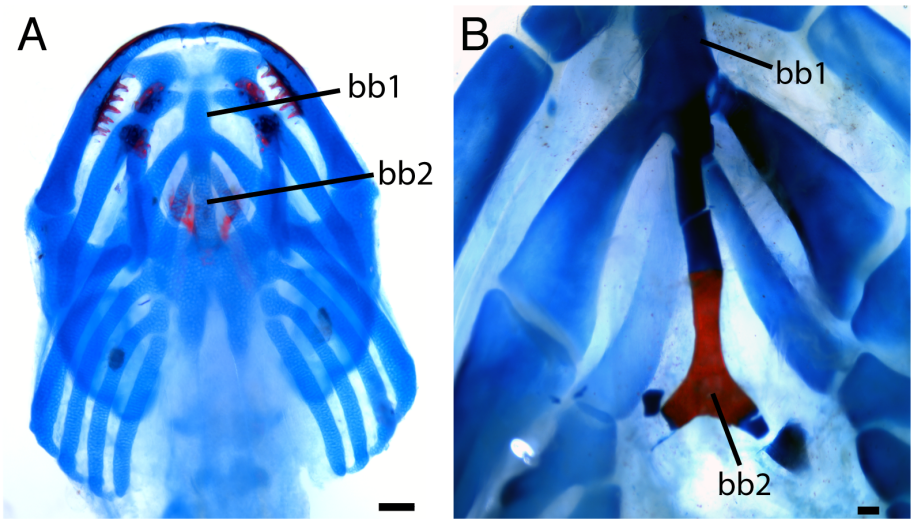

Figure 6.2 | Ossification of the axolotl basibranchial 2/urohyal.. (A) Cleared and stained pharyngeal skeleton of *A. mexicanum* at stage 46. Both first and second basibranchials (bb1, bb2) are cartilaginous. Ventral view, anterior is to the top. Cartilages are blue; bones and teeth are red. (B) Adult pharyngeal skeleton. The second basibranchial is now ossified. Scale bars: C—100 μm, D—2 mm.

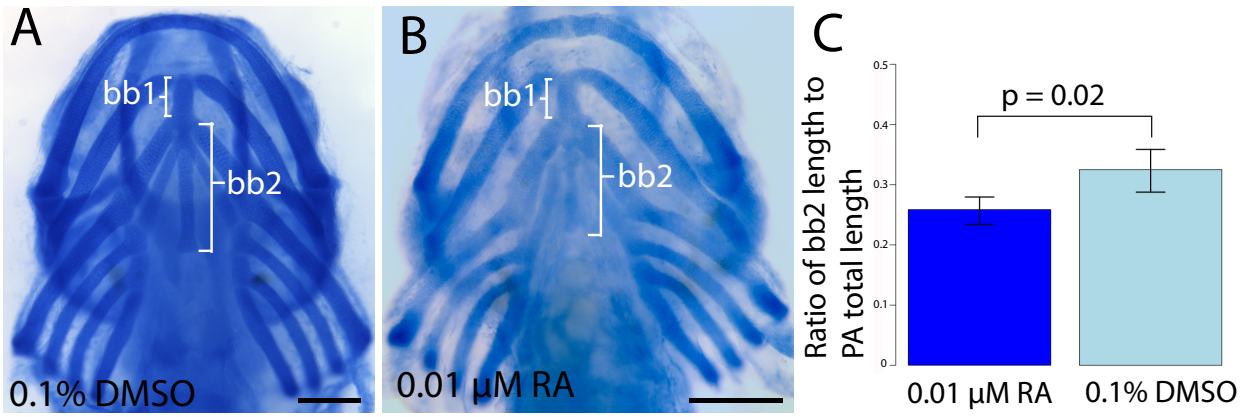

Figure 6.3 | Effect of retinoic acid (RA) on pharyngeal skeleton morphology. (A, B) Alcian-blue staining of cranial cartilages at stage 45. Ventral views, anterior is at the top. (C) Ratio of second basibranchial length to pharyngeal arch (PA) skeleton total length in the control group (0.1% DMSO; n = 12) and following treatment with 0.01 μM RA (n = 9). The p-value is based on a 2-sample t-test. Error bars indicate s.e.m. Scale bar: 500 μm.

Appendix B

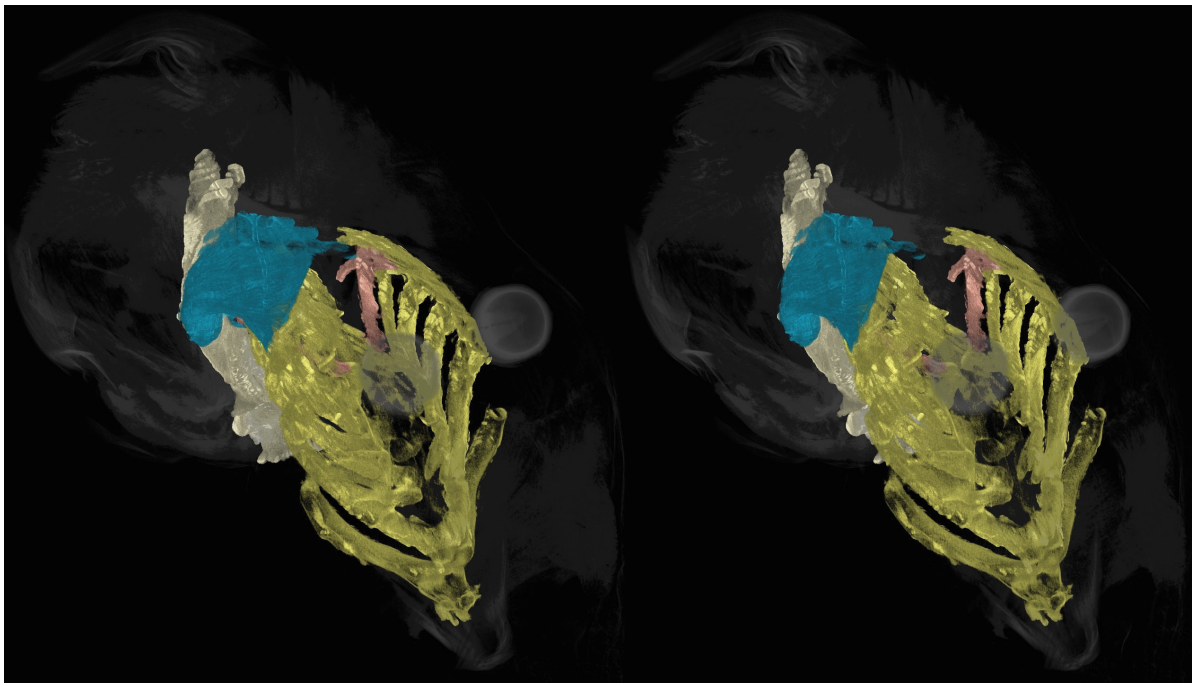

Figure 6.4 | Chimaera cucullaris morphology. Stereo image of chimaera with skeletal elements and muscles segmented. The cucullaris inserts on the 5th branchial bar in addition to the shoulder girdle. Levatores arccum in green. Cucullaris in blue. Gill skeleton in yellow (except for 5th branchial bar). 5th branchial bar in pink. Shoulder girdle in light gray. Stereo created in VGStudio Max v2.2.

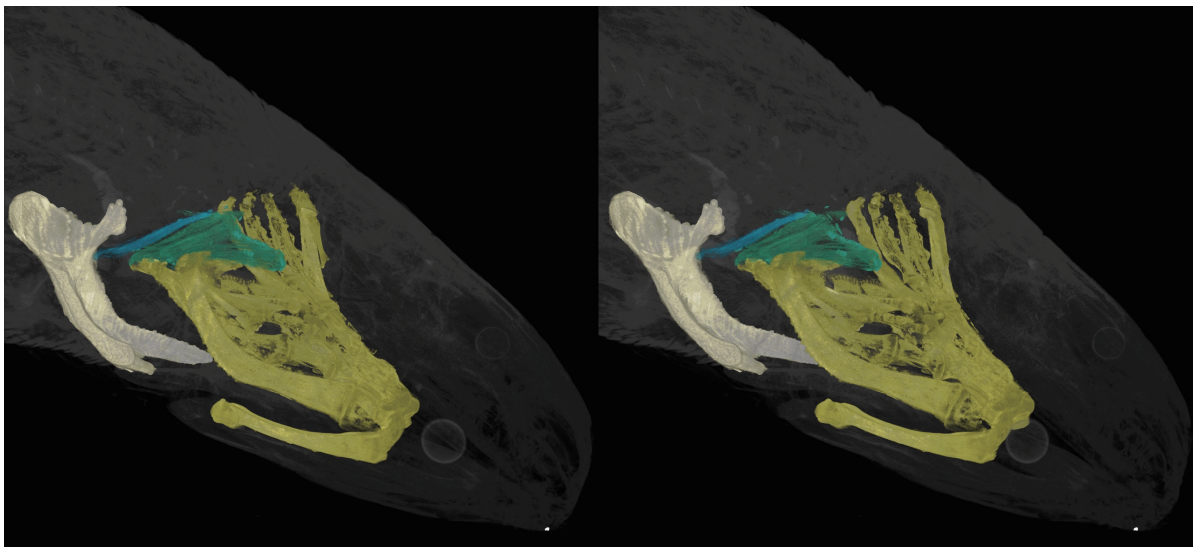

Figure 6.5 | Bichir cucullaris morphology. Stereo image of bichir with skeletal elements and muscles segmented. Levatores arccum in green. Cucullaris in blue. Gill skeleton in yellow. Shoulder girdle in light gray. Stereo created in VGStudio Max v2.2.

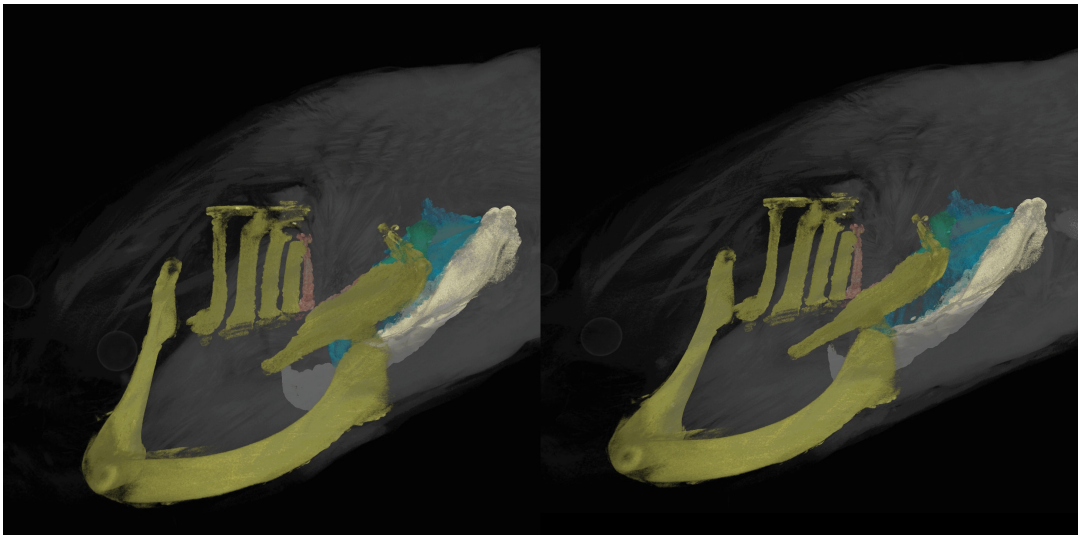

Figure 6.6 | Lungfish cucullaris morphology. Stereo image of lungfish with skeletal elements and muscles segmented. The cucullaris inserts on the 5th branchial bar in addition to the shoulder girdle. Levatores arccum in green. Cucullaris in blue. Gill skeleton in yellow (except for 5th branchial bar). 5th branchial bar in pink. Shoulder girdle in light gray. Stereo created in VGStudio Max v2.2.

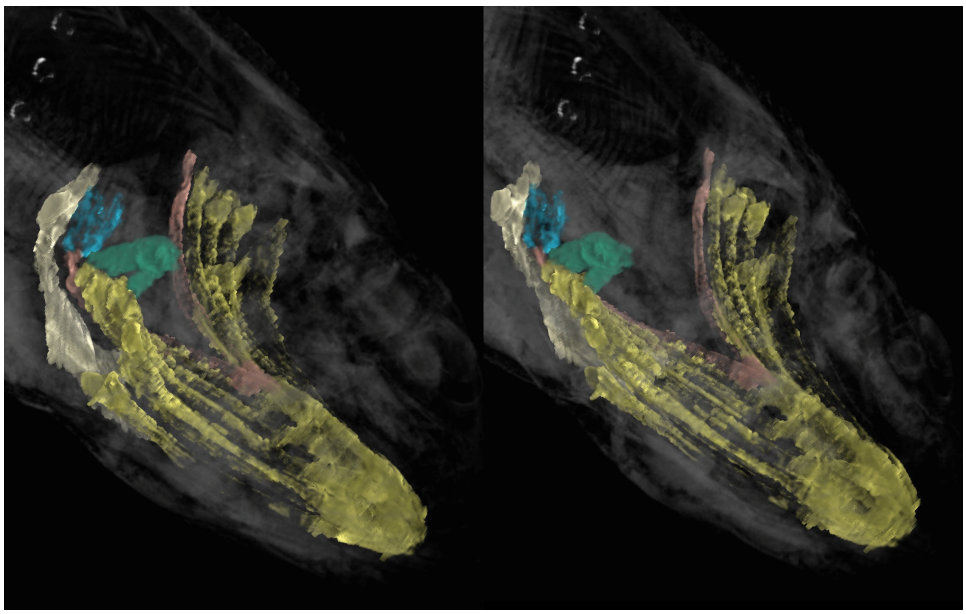

Figure 6.7 | Coelacanth cucullaris morphology. Stereo image of coelacanth based on MRI scan with skeletal elements and muscles segmented. The cucullaris inserts on the 5th branchial bar in addition to the shoulder girdle (but has lost the dorsal attachment to the head). Levatores arccum in green. Cucullaris in blue. Gill skeleton in yellow (except for 5th branchial bar). 5th branchial bar in pink. Shoulder girdle in light gray. Stereo created in VGStudio Max v2.2.

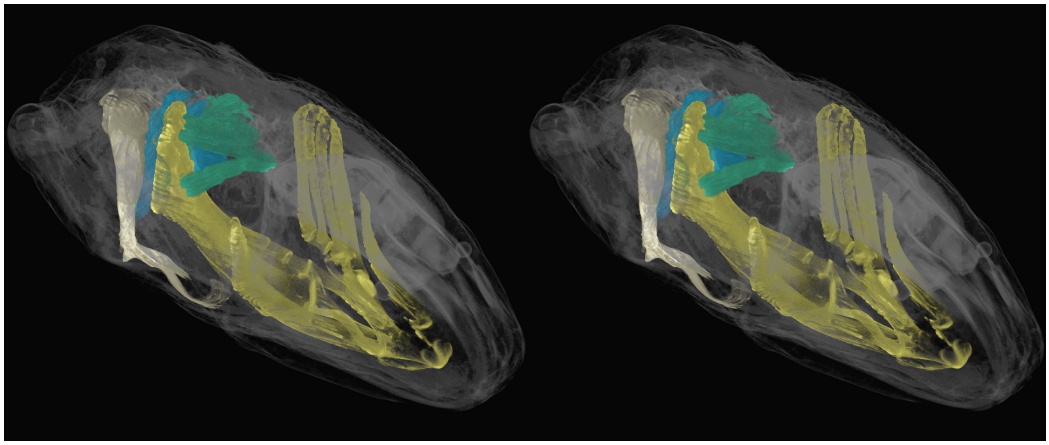

Figure 6.8 | Axolotl cucullaris morphology. Stereo image of axolotl with skeletal elements and muscles segmented. Levatores arccum in green. Cucullaris in blue. Gill skeleton in yellow. Shoulder girdle in light gray. Stereo created in VGStudio Max v2.2.

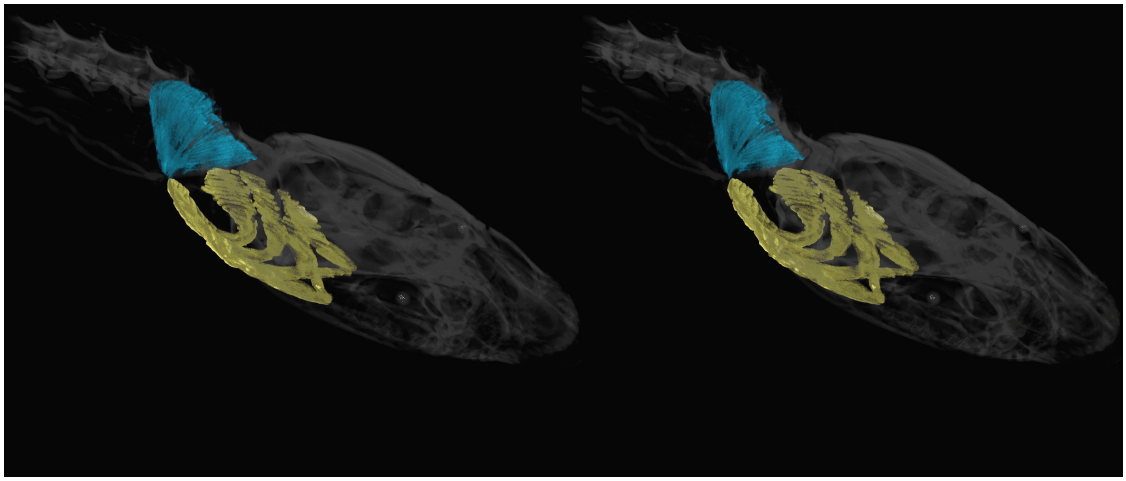

Figure 6.9 | Caecilian cucullaris morphology. Stereo image of caecilian with skeletal elements and muscles segmented. With the shoulder girdle absent, the cucullaris inserts ventrally on the posteriormost ceratobranchial. Cucullaris in blue. Gill skeleton in yellow. Stereo created in VGStudio Max v2.2.

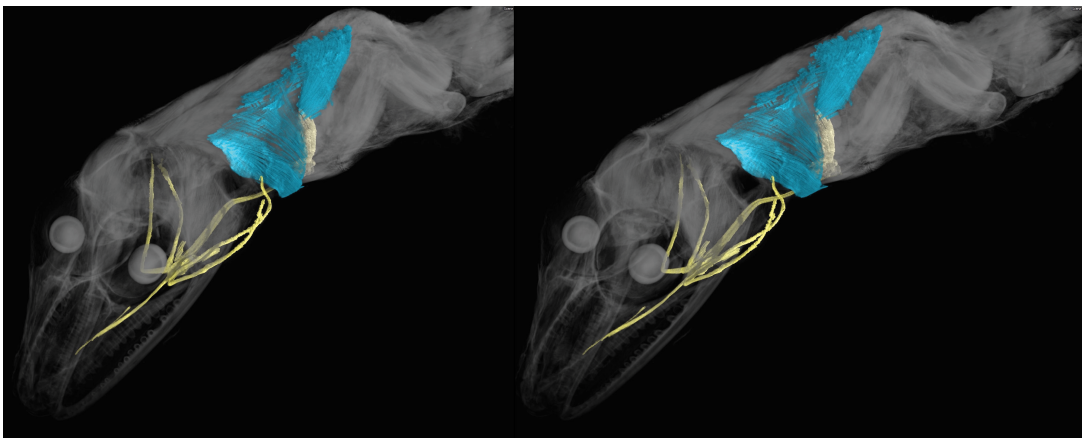

Figure 6.10 | Anole cucullaris morphology. Stereo image of anole with skeletal elements and muscles segmented. Cucullaris in blue. Gill skeleton in yellow. Shoulder girdle in light gray. Stereo created in VGStudio Max v2.2.

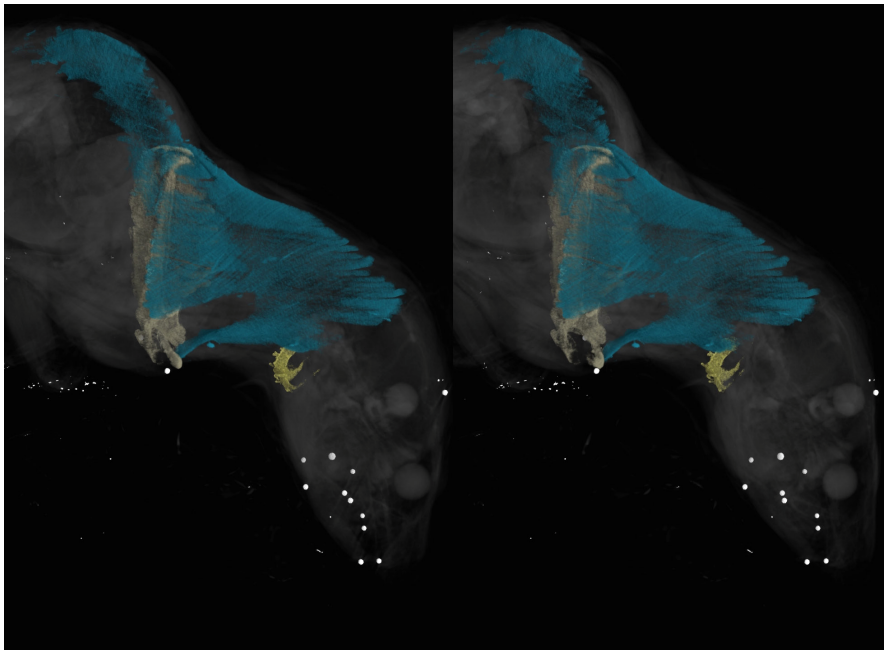

Figure 6.11 | Opossoum cucullaris morphology. Stereo image of opossum with skeletal elements and muscles segmented. Cucullaris in blue. Hyoid elements in yellow. Shoulder girdle in light gray. Stereo created in VGStudio Max v2.2.

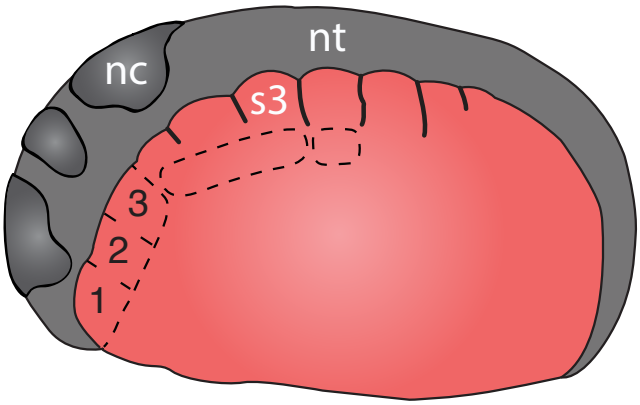

Figure 6.12 | Mesoderm fate-mapping in *A. mexicanum* embryos. Boundaries between regions 1 and 2 and 2 and 3 are approximate. s3, somite 3; nc, neural crest, nt, neural tube. Anterior is to the left; dorsal is to the top.

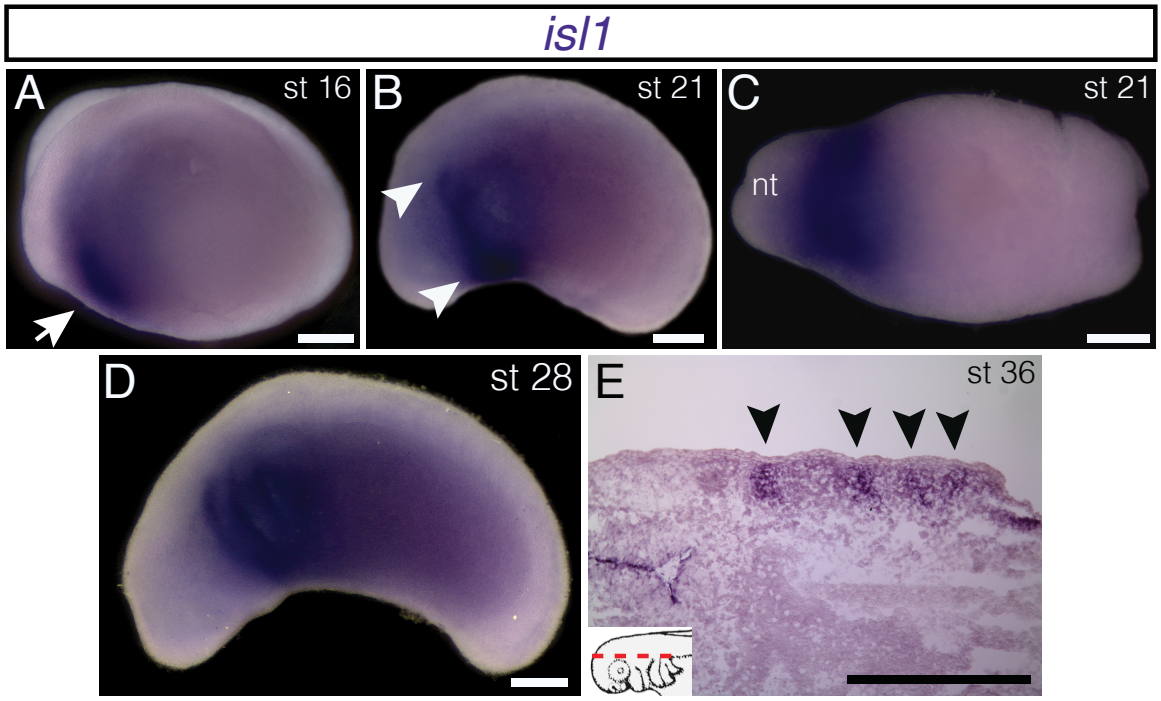

Figure 6.13 | Additional stages of embryonic isl1 expression in *A. mexicanum*. (A) At stage 16, *isl1* is expressed in the region of the developing heart field (arrow). (B) By stage 21, expression has expanded dorsally (arrowheads). (C) Ventral region of *isl1* at stage 21. nt, neural tube. (D) *isl1* expression at stage 28, including the branchial arches. (E) Frontal section dorsal to the developing gill arches at stage 36. Inset panel indicates plane of section (dashed red line). Lateral is to the top. A, B and D, lateral views; C, ventral view. Anterior is to the left in all panels. Scale bars, 500 μm.

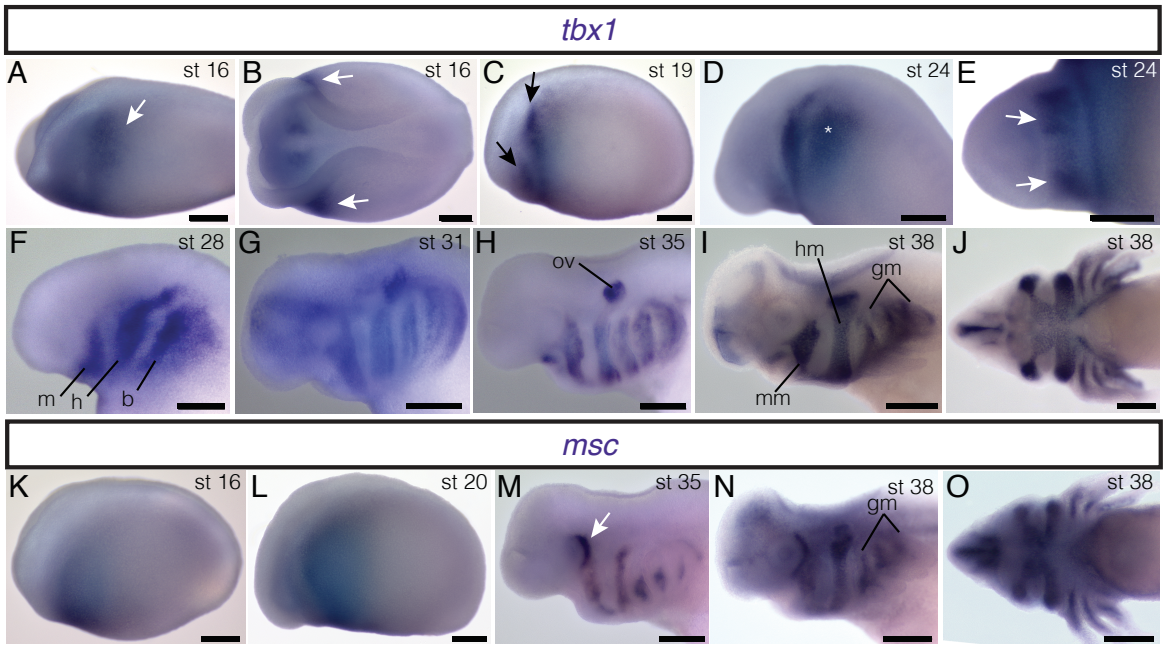

Figure 6.14 | Embryonic expression of *tbx1* and *msc* in *A. mexicanum*. All embryos are depicted in lateral view except for E, J and O, which are ventral views; anterior is to the left. (A—B) Bilateral stripes of tbx1 expression (arrows) are present in mid-neurula stages. (C) Two bilateral stripes of tbx1 expression are visible (arrows). (D) *tbx1* is expressed in the region of the developing branchial arches (asterisk). (E) Patches of *tbx1* expression in mandibular arch in ventral view (arrows). (F—G) *tbx1* is expressed in mandibular (m), hyoid (h) and branchial (b) regions. (H) *tbx1* is expressed in the otic vesicle (ov). (I—J) At stage 38, *tbx1* is expressed in developing muscle groups. mm, mandibular arch muscle; hm, hyoid arch muscle; gm, gill musculature. (K—L) *msc* is expressed anteriorly at neurula stages. (M) Patch of *msc* expression just posterior to the eye (arrow). (N) *msc* is expressed in the gill arch muscles (gm). (O) *msc* expression seen in ventral view. Scale bars, 500 μm.

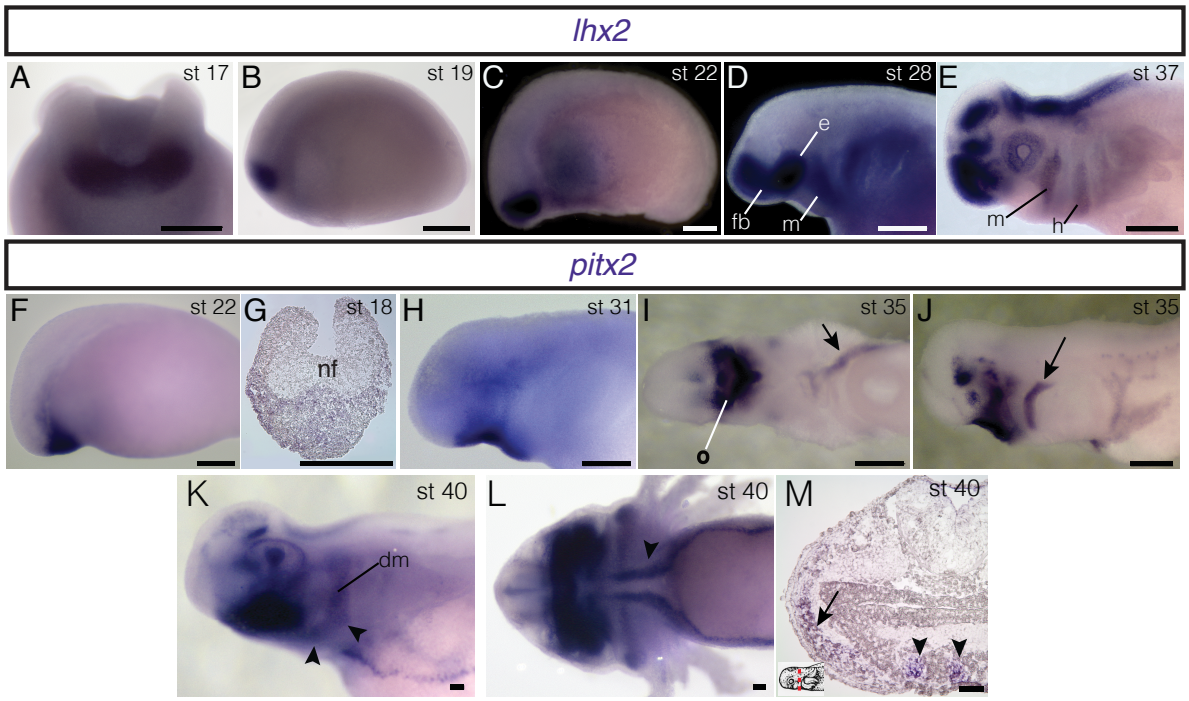

Figure 6.15 | Embryonic expression of *lhx2* and *pitx2* in *A. mexicanum*. (A, B) In neurula stages, *lhx2* is expressed in anterior neurectoderm. A, anterior view, dorsal is to the top. B, lateral view, anterior is to the left. (C) *lhx2* is expressed in cranial mesoderm at stage 22,. (D) *lhx2* is expressed in the mandibular (m), hyoid (h) and branchial arch mesoderm as well as the eye field (e) and forebrain (fb) during middle-tailbud stage. (E) *lhx2* expression is maintained in the eye, and brain, as well as in mandibular and hyoid arches. (F) *pitx2* is expressed in anterior cranial mesoderm. (G) Transverse section through the anterior neural folds (nf) indicates expression through the ectoderm and mesoderm at neurula stages. (H) At stage 31, *pitx2* is expressed in oral ectoderm. (I) At stage 35, *pitx2* is expressed asymmetrically in the left lateral-plate mesoderm (arrow) and oral region (o); ventral view. (J) *pitx2* is also expressed in hyoid arch mesoderm (arrow) at the same stage; lateral view. (K). At stage 40, *pitx2* is strongly expressed in mandibular arch derivatives, including the lme. It is also present in two hyoid arch muscles, the branchiohyoideus externus (bhe; arrowheads) and the depressor mandibulae (dm). (L) *pitx2* is expressed in the tongue muscles; ventral view, anterior is to the left. (H) Transverse section at stage 40 shows *pitx2* expression in the tongue muscles (arrowheads) and hyoid arch musculature (arrow). Dorsal is to the top, lateral is to the left. Inset panel indicates plane of section (red dashed line). C—F, H, J—K, lateral view; anterior is to the left. Scale bars A—J, 500 μm; scale bars K—M, 100 μm.

References

Abitua, P. B., E. Wagner, I. A. Navarret, and M. Levine. 2012. Identification of a rudimentary neural crest in a non-vertebrate chordate. *Nature* 492 (7427):104–107. doi: 10.1038/nature11589.

Abzhanov, A. 2013. von Baer's law for the ages: lost and found principles of developmental evolution. *Trends Genet* 29 (12):712–722. doi: 10.1016/j.tig.2013.09.004.

Alcalde, L., and N. G. Basso. 2013. Old and new hypotheses about the homology of the compound bones from the cheek and otico-occipital regions of the anuran skull. *Zool* 116 (4):232–245. doi: 10.1016/j.zool.2013.03.002.

Allis, E. P. 1917. The homologies of the muscles related to the visceral arches of the gnathostome fishes. *Q J Microsc Sci* 62 (247):303–406.

Allis, E. P. 1919. On the homologies of the squamosal bone in fishes. *Anat Rec* 17 (2):73–87. doi: 10.1002/ar.1090170202.

Andrews, S. M., and R. L. Carroll. 1991. The order Adelospondyli: Carboniferous lepospondyl amphibians. *Trans Roy Soc Edin, Earth Sci* 82 (3):239–275.
doi: http://dx.doi.org/10.1017/S0263593300005332.

Arratia, G., and H. P. Schultze. 1990. The urohyal: development and homology within osteichthyans. *J Morphol* 203 (3):247–282. doi: 10.1002/jmor.1052030302.

Atkinson-Leadbeater, K., G. E. Bertolesi, J. A. Johnston, C. L. Hehr, and S. McFarlane. 2009. FGF receptor dependent regulation of Lhx9 expression in the developing nervous system. *Dev Dynam* 238 (2):367–375. doi: 10.1002/dvdy.21850.

Bemis, W. E., K. Schwenk, and M. H. Wake. 1983. Morphology and function of the feeding apparatus in *Dermophis mexicanus* (Amphibia: Gymnophiona). *Zool J Linn Soc* 77 (1):75–96. doi: 10.1111/j.1096-3642.1983.tb01722.x.

Birchmeier, C., and H. Brohmann. 2000. Genes that control the development of migrating muscle precursor cells. *Curr Opin Cell* Biol 12 (6):725–730. doi: 10.1016/S0955-

0674(00)00159-9.

Bismuth, K., and F. Relaix. 2010. Genetic regulation of skeletal muscle development. *Exp Cell Res* 316 (18):3081–3086. doi: 10.1016/j.yexcr.2010.08.018.

Blomhoff, R., and H. K. Blomhoff. 2006. Overview of retinoid metabolism and function. *J Neurobiol* 66 (7): 606–630. doi: 10.1002/neu.20242.

Bolker, J. A. 1992. "Constancy and variation in developmental mechanisms: an example from comparative embryology." In *Principles of organization in organisms*, edited by J. Mittenthal and A. Baskin, 73–85.

Bordzilovskaya, N. P., T. A. Dettlaff, S. T. Duhon, and G. M. Malacinski. 1989. "Developmental-stage series of axolotl embryos." In *Developmental biology of the axolotl*, edited by J. B. Armstrong and G. M. Malacinski, 201–219. New York: Oxford University Press.

Borue, X., and D. M. Noden. 2004. Normal and aberrant craniofacial myogenesis by grafted trunk somitic and segmental plate mesoderm. *Development* 131 (16):3967–3980. doi: 10.1242/dev.01276.

Bothe, I., and S. Dietrich. 2006. The molecular setup of the avian head mesoderm and its implication for craniofacial myogenesis. *Dev Dynam* 235 (10):2845–2860. doi: 10.1002/dvdy.20903.

Brade, T., S. Gessert, M. Kühl, and P. Pandur. 2007. The amphibian second heart field: *Xenopus islet-1* is required for cardiovascular development. *Dev Biol* 311 (2):297–310. doi: 10.1016/j.ydbio.2007.08.004.

Brock, G. T. 1935. The temporal bones in lizards, birds and mammal. *Anat Anz* 80:266–284.

Buckingham, M. 2006. Myogenic progenitor cells and skeletal myogenesis in vertebrates. *Curr Opin Genet Dev* 16 (5):525–532. doi: 10.1016/j.gde.2006.08.008.

Buckingham, M., S. Meilhac, and S. Zaffran. 2005. Building the mammalian heart from two sources of myocardial cells. *Nat Rev Genet* 6 (11):826–835. doi: 10.1038/nrg1710.

Burke, A. C. 2000. *Hox* genes and the global patterning of the somitic mesoderm. *Curr Top Dev Biol* 47:155–181. doi: 10.1016/S0070-2153(08)60725-5.

Bütschli, O. 1910. *Vorlesungen über vergleichende anatomie*. Leipzig: Engelmann.

Cai, C. L., X. Q. Liang, Y. Q. Shi, Y. Q., P. H. Chu, S. L. Pfaff, J. Chen, and S. Evans. 2003. Isl1 identifies a cardiac progenitor population that proliferates prior to differentiation and contributes a majority of cells to the heart. *Dev Cell* 5 (6):877–889. doi: 10.1016/S1534-5807(03)00363-0.

Capellini, T. D., G. Vaccari, E. Ferretti, S. Fantini, M. He, M. Pellegrini, L. Quintana, G. Di Giacomo, J. Sharpe, L. Selleri, and V. Zappavigna. 2010. Scapula development is governed by genetic interactions of Pbx1 with its family members and with Emx2 via their cooperative control of Alx1. *Development* 137 (15):2559–2569. doi: 10.1242/dev.048819.

Carroll, R. L. 1969. A Middle Pennsylvanian captorhinomorph, and the interrelationships of primitive reptiles. *J Paleontol* 43 (1):151–170.

Carroll, R. L. 1975. Permo-triassic "lizards" from the Karroo. *Palaeont Afr* 18:71–87.

Carroll, R. L. 1981. Plesiosaur ancestors from the upper Permian of Madagascar. *Phil T Roy Soc B* 293 (1):315–383. doi: 10.1098/rstb.1981.0079.

Carroll, R. L. 2009. *The rise of amphibians: 365 million years of evolution*. Baltimore: Johns Hopkins University Press.

Carroll, S. B., J. Gates, D. N. Keys, S. W. Paddock, G. E. Panganiban, J. E. Selegue, and J. A. Williams. 1994. Pattern formation and eyespot determination in butterfly wings. *Science* 265 (5168):109–114. doi: 10.1126/science.7912449.

Carvajal, J. J., D. Cox, D. Summerbell, and P. W. Rigby. 2001. A BAC transgenic analysis of the Mrf4/Myf5 locus reveals interdigitated elements that control activation and maintenance of gene expression during muscle development. *Development* 128 (10):1857–1868.

Cerny, R., I. Horáĉek, and L. Olsson. 2006. The trabecula cranii: development and homology of an enigmatic vertebrate head structure. *Anim Biol* 56 (4):503–518. doi: 10.1163/157075606778967801.

Chevallier, A., Kieny, M., Mauger, A. 1977. Limb-somite relationship: origin of limb musculature. *J Embryol Exp Morphol* 41:245–258.

Clarke, J. D., and C. Tickle. 1999. Fate maps old and new. *Nat Cell Biol* 1 (4):E103–9.

doi: 10.1038/12105.

Conlon, F. L., S. G. Sedgwick, K. M. Weston, and J. C. Smith. 1996. Inhibition of Xbra transcription activation causes defects in mesodermal patterning and reveals autoregulation of Xbra in dorsal mesoderm. *Development* 122 (8):2427–2435.

Cohen, S. M., G. Brönner, F. Küttner, G. Jürgens, and H. Jäckle. 1989. *Distal-less* encodes a homoeodomain protein required for limb development in *Drosophila*. *Nature* 338 (6214):432–434. doi: 10.1038/338432a0.

Cooke, J., and E. Zeeman. 1976. A Clock and wavefront model for control of the number of repeated structures during animal morphogenesis. *J Theor Biol* 58 (2):455–476.

Couly, G. F., P. M. Coltey, and N. M. Le Douarin. 1992. The developmental fate of the cephalic mesoderm in quail-chick chimeras. *Development* 114 (1):1–15.

Couly, G. F., P. M. Coltey, and N. M. Le Douarin. 1993. The triple origin of skull in higher vertebrates: a study in quail-chick chimeras. *Development* 117 (2):409–429.

Creuzet, S., G. Couly, and N. M. Le Douarin. 2005. Patterning the neural crest derivatives during development of the vertebrate head: insights from avian studies. *J Anat* 207 (5):447–459. doi: 10.1111/j.1469-7580.2005.00485.x.

Cruickshank, A. R. I. 1972. "The proterosuchian thecodonts." In *Studies in vertebrate evolution*, edited by K. A. Joysey and T. S. Kemp, 89–119. Edinburgh: Oliver and Boyd.

Daeschler, E. B., N. H. Shubin, and F. A. Jenkins. 2006. A Devonian tetrapod-like fish and the evolution of the tetrapod body plan. *Nature* 440 (7085):757–763. doi: 10.1038/nature04639.

Darwin, C. 1859. *On the origin of species by means of natural selection, or the preservation of favoured races in the struggle for life*. London: J. Murray.

Dastjerdi, A., L. Robson, R. Walker, J. Hadley, Z. Zhang, M. Rodriguez-Niedenführ, P. Ataliotis, A. Baldini, P. Scambler, and P. Francis-West. 2007. Tbx1 regulation of myogenic differentiation in the limb and cranial mesoderm. *Dev Dynam* 236 (2):353–363. doi: 10.1002/dvdy.21010.

Davidian, A., and Y. Malashichev. 2013. Dual embryonic origin of the hyobranchial apparatus in the Mexican axolotl (*Ambystoma mexicanum*). *Int J Dev Biol* 57: 821–828. doi: 10.1387/ijdb.130213ym.

Deban, S. M., and Wake, D. B. 2000. "Aquatic feeding in salamanders." In *Feeding: form, function and evolution in tetrapod vertebrates*, edited by K. Schwenk, 65–94. San Diego: Academic Press.

de Beer, G. R. 1937. *The development of the vertebrate skull*. Oxford: Clarendon Press.

de Beer, G. R. 1971. *Homology: an unsolved problem*, Oxford Biology Reader No. 11. London: Oxford University Press.

de Pinna, M. 1991. Concepts and tests of homology in the cladistic paradigm. *Cladistics* 7 (4):367–394. doi: 10.1111/j.1096-0031.1991.tb00045.x.

Deckelbaum, R. A., G. Holmes, Z. Zhao, C. Tong, C. Basilico, and C. A. Loomis. 2012. Regulation of cranial morphogenesis and cell fate at the neural crest-mesoderm boundary by engrailed 1. *Development* 139 (7):1346–1358. doi: 10.1242/dev.076729.

Dequéant, M.-L., and O. Pourquié. 2008. Segmental patterning of the vertebrate embryonic axis. *Nat Rev Genet* 9 (5):370–382. doi: 10.1038/nrg2320.

Dietrich, S. 1999. Regulation of hypaxial muscle development. *Cell Tissue Res* 296 (1):175–182.

Diogo, R., R. G. Kelly, L. Christiaen, M. Levine, J. M. Ziermann, J. L. Molnar, D. M. Noden, and E. Tzahor. 2015. A new heart for a new head in vertebrate cardiopharyngeal evolution. *Nature* 520 (7548):466–473. doi: 10.1038/nature14435.

Dong, F., X. Sun, W. Liu, D. Ai, E. Klysik, M.-F. Lu, J. Hadley, L. Antoni, L. Chen, A. Baldini, P. Francis-West, and J. F. Martin. 2006. Pitx2 promotes development of splanchnic mesoderm-derived branchiomeric muscle. *Development* 133 (24):4891–4899. doi: 10.1242/dev.02693.

Dugès, A. 1834. Recherches sur l'ordre des Acariens en général et la famille des Trombidiés en particulier. *Ann Sci Naturelles, Zool* 2:5–46.

Durland, J. L., M. Sferlazzo, M. Logan, and A. C. Burke. 2008. Visualizing the lateral

somitic frontier in the Prx1Cre transgenic mouse. *J Anat* 212 (5):590–602. doi: 10.1111/j.1469-7580.2008.00879.x.

Edgeworth, F. H. 1926. On the development of the coraco-branchiales and cucullaris in *Scyllium canicula*. *J Anat* 60 (3):298–308.

Edgeworth, F. H. 1935. *The cranial muscles of vertebrates*. London: Cambridge University Press.

Emlen, D. J., L. Corley Lavine, and B. Ewen-Campen. 2007. On the origin and evolutionary diversification of beetle horns. *Proc Natl Acad Sci USA* 104 Suppl 1:8661–8668. doi: 10.1073/pnas.0701209104.

Epperlein, H.-H., D. Meulemans, M. Bronner-Fraser, H. Steinbeisser, and M. A. J. Selleck. 2000. Analysis of cranial neural crest migratory pathways in axolotl using cell markers and transplantation. *Development* 127 (12):2751–2761.

Epperlein, H.-H., S. Khattak, D. Knapp, E. M. Tanaka, and Y. B. Malashichev. 2012. Neural crest does not contribute to the neck and shoulder in the axolotl (*Ambystoma mexicanum*). *PLoS ONE* 7 (12):e52244. doi: 10.1371/journal.pone.0052244.

Ericsson, R., R. Cerny, P. Falck, and L. Olsson. 2004. Role of cranial neural crest cells in visceral arch muscle positioning and morphogenesis in the Mexican axolotl, *Ambystoma mexicanum*. *Dev Dynam* 231 (2):237–247. doi: 10.1002/dvdy.20127.

Ericsson, R., J. Joss, and L. Olsson. 2008. The fate of cranial neural crest cells in the Australian lungfish, *Neoceratodus forsteri*. *J Exp Zool B (Mol Dev Evol)* 310 (4): 345–354. doi: 10.1002/jez.b.21178.

Ericsson, R., and L. Olsson. 2004. Patterns of spatial and temporal visceral arch muscle development in the Mexican axolotl (*Ambystoma mexicanum*). *J Morphol* 261 (2):131–140. doi: 10.1002/jmor.10151.

Ericsson, R., R. Knight, and Z. Johanson. 2013. Evolution and development of the vertebrate neck. *J Anat* 222 (1):67–78. doi: 10.1111/j.1469-7580.2012.01530.x.

Esteve-Altava, B., J. Marugán-Lobón, H. Botella, and D. Rasskin-Gutman. 2012. Struc-

tural constraints in the evolution of the tetrapod skull complexity: WillistonâĂŹs law revisited using network models. *Evol Biol* 40 (2):209–219. doi: 10.1007/s11692-012-9200-9.

Evans, D. J. R., and D. M. Noden. 2006. Spatial relations between avian craniofacial neural crest and paraxial mesoderm cells. *Dev Dynam* 235 (5):1310–1325. doi: 10.1002/dvdy.20663.

Evans, S. E. 1980. The skull of a new eosuchian reptile from the lower Jurassic of South-Wales. *Zool J Linn Soc* 70 (3):203–264. doi: 10.1111/j.1096-3642.1980.tb00852.x.

Evans, S. E. 2008. "The skull of lizards and tuatara." In *Biology of the Reptilia*, vol. 20, *The skull of Lepidosauria*, edited by C. Gans, A. S. Gaunt and K. Adler, 1–347. Ithaca, New York: Society for the Study of Amphibians and Reptiles.

Falck, P., J. Hanken, and L. Olsson. 2002. Cranial neural crest emergence and migration in the Mexican axolotl (*Ambystoma mexicanum*). *Zoology.* 105 (3):195–202. doi: 10.1078/0944-2006-00079.

Flowers, G. P., A. T. Timberlake, K. C. McLean, J. R. Monaghan, and C. M. Crews. 2014. Highly efficient targeted mutagenesis in axolotl using Cas9 RNA-guided nuclease. *Development* 141 (10):2165–2171. doi: 10.1242/dev.105072.

Forey, P. L. 1998. *History of the Coelacanth Fishes.* London: Chapman and Hall.

Fraser, N. C. 1988. The osteology and relationships of *Clevosaurus* (Reptilia, Sphenodontida). *Phil T Roy Soc B* 321 (1204):125–178. doi: 10.1098/rstb.1988.0092.

Fröbisch, N. B., and R. R. Schoch. 2009. The largest specimen of *Apateon* and the life history pathway of neoteny in the Paleozoic temnospondyl family Branchiosauridae. *Fossil Rec* 12 (1):83–90. doi: 10.1002/mmng.200800012.

Freeman, G. 1963. Lens regeneration from the cornea in *Xenopus laevis.* *J Exp Zool* 154 (1):39–65. doi: 10.1002/jez.1401540105.

Freund, R., D. Dorfler, W. Popp, and F. Wachtler. 1996. The metameric pattern of the head mesoderm - does it exist? *Anat Embryol* 193 (1):73–80.

Frohman, M. A., M. Boyle, and G. R. Martin. 1990. Isolation of the mouse Hox-2.9 gene; analysis of embryonic expression suggests that positional information along the anterior-

posterior axis is specified by mesoderm. *Development* 110 (2):589–607.

Gans, C., and R. G. Northcutt. 1983. Neural crest and the origin of vertebrates: a new head. *Science* 220 (4594):268–273. doi: 10.1126/science.220.4594.268.

Gao, K. Q., and N. H. Shubin. 2001. Late Jurassic salamanders from northern China. *Nature* 410 (6828):574–577. doi: 10.1038/35069051.

Gaupp, E. 1895. Beiträge zur morphologie des schädels III. Zur vergleichenden anatomie der schläfengegend am knöckernen wirbeltierschädel. *Morphol Arbeit* 4 (1):77–128.

Gauthier, J., R. Estes, and K. de Queiroz. 1988. "A phylogenetic analysis of Lepidosauromorpha." In *The phylogenetic relationships of the lizard families: essays commemorating Charles L. Camp*, edited by R. Estes and G. Pregill, 15–98. Palo Alto, CA: Stanford University Press.

Gegenbaur, C. 1870. *Grundzüge der vergleichenden anatomie*, 2nd edn. Leipzig: Wilhelm Engelmann.

Gegenbaur, C., F. Bell, and E. Lankester. 1878. *Elements of comparative anatomy*. London: Macmillan and Company.

Geoffroy Saint-Hilaire, E. 1818. *Pilosophie anatomique* (vol1) *des organes respiratoires sous le rapport de la determination et de l'indentitÃl de leurs piÃĺces osseusses*. Paris: JB BailliÃĺre.

Gessert, S., and M. KÃijhl. 2009. Comparative gene expression analysis and fate mapping studies suggest an early segregation of cardiogenic lineages in *Xenopus laevis*. *Dev Biol* 334 (2):395–408. doi: 10.1016/j.ydbio.2009.07.037.

Gillis, J. A., R. D. Dahn, and N. H. Shubin. 2009. Shared developmental mechanisms pattern the vertebrate gill arch and paired fin skeletons. *Proc Natl Acad Sci USA* 106 (14):5720–5724. doi: 10.1073/pnas.0810959106.

Goodrich, E. S. 1958. *Studies on the structure and development of vertebrates*. New York: Dover publications.

Gopalakrishnan, S., G. Comai, R. Sambasivan, A. Francou, R. G. Kelly, and S. Tajbakhsh.

2015. A cranial mesoderm origin for esophagus striated muscles. *Dev Cell* 34 (6):694–704. doi: 10.1016/j.devcel.2015.07.003.

Gow, C. E. 1975. The morphology and relationships of *Youngina capensis* Broom and *Prolacerta broomi* Parrington. *Paleont afr* 18:89–131.

Greenwood, P. H., and G. V. Lauder. 1981. The protractor pectoralis muscle and the classification of teleost fishes. *Bull Br Mus Nat Hist (Zool)* 41 (4):213–234.

Gregory, W. K. 1935. 'Williston's law' relating to the evolution of skull bones in the vertebrates. *Am J Phys Anthropol* 20 (2):123–152. doi: http://dx.doi.org/10.1002/ajpa.1330200202.

Griffiths, I. 1954a. On the "otic element" in Amphibia Salientia. *Proc Zool Soc Lond* 124 (1):35–50. doi: 10.1111/j.1096-3642.1954.tb01476.x.

Griffiths, I. 1954b. On the nature of the fronto-parietal in Amphibia, Salientia. emphProc Zool Soc Lond 123 (4):781–792. doi: 10.1111/j.1096-3642.1954.tb00204.x.

Grifone, R., T. Jarry, M. Dandonneau, J. Grenier, D. Duprez, and R. G. Kelly. 2008. Properties of branchiomeric and somite-derived muscle development in Tbx1 mutant embryos. *Dev Dynam* 237 (10):3071–3078. doi: 10.1002/dvdy.21718.

Grifone, R., and R. G. Kelly. 2007. Heartening news for head muscle development. *Trends Genet* 23 (8):365–369. doi: 10.1016/j.tig.2007.05.002.

Gross, J. B., and J. Hanken 2004. Use of fluorescent dextran conjugates as a long-term marker of osteogenic neural crest in frogs. *Dev Dynam* 230:100–106. doi: 10.1002/dvdy.20036.

Gross, J. B., and J. Hanken. 2005. Cranial neural crest contributes to the bony skull vault in adult *Xenopus laevis*: insights from cell labeling studies. *J Exp Zool B (Mol Dev Evol)* 304 (2):169–176. doi: 10.1002/jez.b.21028.

Gross, J. B., and J. Hanken. 2008. Review of fate-mapping studies of osteogenic cranial neural crest in vertebrates. *Dev Biol* 317 (2):389–400. doi: 10.1016/j.ydbio.2008.02.046.

Gross, M. K., L. Moran-Rivard, T. Velasquez, M. N. Nakatsu, K. Jagla, and M. Goulding. 2000. Lbx1 is required for muscle precursor migration along a lateral pathway into the limb. *Development* 127 (2):413–424.

Hacker, A., and S. Guthrie. 1998. A distinct developmental programme for the cranial paraxial mesoderm in the chick embryo. *Development* 125 (17):3461–3472.

Hall, B. K. 1994. "Introduction." In *Homology: the hierarchichal basis of comparative biology*, edited by B. K. Hall. San Diego, CA: Academic Press.

Hall, B. K. 1995. Homology and embryonic development. *Evol Biol* 28:1–37. doi: 10.1007/978-1-4615-1847-1_1.

Hall, B. K. 1999. *Evolutionary Developmental Biology*. 2nd ed. Kulwer Academic Publishers: Dordrecht, Netherlands.

Hall, B. K. 2003. Descent with modification: the unity underlying homology and homoplasy as seen through an analysis of development and evolution. *Biol Rev Camb Philos* 78 (3):409–433. doi: 10.1017/S1464793102006097.

Hanken, J., and B. K. Hall (Eds.). 1993. *The Skull*. 3 vols. Chicago: The University of Chicago Press.

Hanken, J., and J. B. Gross. 2005. Evolution of cranial development and the role of neural crest: insights from amphibians. *J Anat* 207 (5):437–446. doi: 10.1111/j.1469-7580.2005.00481.x.

Harel, I., Y. Maezawa, R. Avraham, A. Rinon, H.-Y. Ma, J. W. Cross, N. Leviatan, J. Hegesh, A. Roy, J. Jacob-Hirsch, G. Rechavi, J. Carvajal, S. Tole, C. Kioussi, S. Quaggin, and E. Tzahor. 2012. Pharyngeal mesoderm regulatory network controls cardiac and head muscle morphogenesis. *Proc Natl Acad Sci USA* 109 (46):18839–18844. doi: 10.1073/pnas.1208690109.

Harel, I., E. Nathan, L. Tirosh-Finkel, H. Zigdon, N. GuimarÃčes-Camboa, S. M. Evans, and E. Tzahor. 2009. Distinct origins and genetic programs of head muscle satellite cells. *Dev Cell* 16 (6):822–832. doi: 10.1016/j.devcel.2009.05.007.

Havstad, J. C., L. C. S. Assis, and O. Rieppel. 2015. The semaphorontic view of homology. *J Exp Zool B (Mol Dev Evol)* 324 (7):578–587. doi: 10.1002/jez.b.22634.

Heffner, C. S., C. Herbert Pratt, R. P. Babiuk, Y. Sharma, S. F. Rockwood, L. R. Donahue, J. T. Eppig, and S. A. Murray. 2012. Supporting conditional mouse mutagenesis with a comprehensive cre characterization resource. *Nat Commun* 3:1218–1218. doi:

10.1038/ncomms2186.

Hennig, W. 1966. *Phylogenetic systematics*. Urbana, IL: University of Illinois Press.

Henrique, D., J. Adam, A. Myat, A. Chitnis, J. Lewis, and D. Ish-Horowicz. 1995. Expression of a *Delta* homologue in prospective neurons in the chick. *Nature* 375 (6534):787–790. doi: 10.1038/375787a0.

Henry, J., and M. Elkins. 2001. Cornea-lens transdifferentiation in the anuran, *Xenopus tropicalis*. Dev Genes Evol 211 (8):377–387. doi: 10.1007/s004270100163.

Hirasawa, T., S. Fujimoto, and S. Kuratani. In press. Expansion of the neck reconstituted the shoulder-diaphragm in amniote evolution. *Dev Growth Differ* doi: 10.1111/dgd.12243.

Horigome, N., M. Myojin, T. Ueki, S. Hirano, S. Aizawa, and S. Kuratani. 1999. Development of cephalic neural crest cells in embryos of *Lampetra japonica*, with special reference to the evolution of the jaw. *Dev Biol* 207 (2):287–308. doi: 10.1006/dbio.1998.9175.

Horstadius, S., Sellman, S. 1946. Experimentelle Untersuchungen uber die Determination des knorpeligen Kopfskelettes bei Urodelen. *Nov Act Reg Soc Scient Ups Ser IV* 13: 1–170.

Hosokawa, R., M. Urata, J. Han, A. Zehnaly, P. Bringas, K. Nonaka, and Y. Chai. 2007. TGF-β mediated Msx2 expression controls occipital somites-derived caudal region of skull development. *Dev Biol* 310 (1):140–153. doi: 10.1016/j.ydbio.2007.07.038.

Howes, G. B., and H. H. Swinnerton. 1901. On the development of the skeleton of the Tuatara, *Sphenodon punctatus*: with remarks on the egg, on the hatching, and on the hatched young. *Trans Zool Soc London* 16 (1):1–86. doi: 10.1111/j.1096-3642.1901.tb00026.x.

Huang, R., B. Christ, and K. Patel. 2006. Regulation of scapula development. *Anat Embryol* 211 Suppl 1:65–71. doi: 10.1007/s00429-006-0126-9.

Huang, R., Q. Zhi, C. P. Ordahl, and B. Christ. 1997. The fate of the first avian somite. *Anat Embryol* 195 (5):435–449.

Huang, R., Q. Zhi, K. Patel, J. Wilting, and B. Christ. 2000a. Dual origin and segmental organisation of the avian scapula. *Development* 127 (17):3789–3794.

Huang, R. J., Q. Zhi, K. Patel, J. Wilting, and B. Christ. 2000b. Contribution of single

somites to the skeleton and muscles of the occipital and cervical regions in avian embryos. *Anat Embryol* 202 (5):375–383. doi: 10.1007/s004290000131.

Hutson, M. R., and M. L. Kirby. 2007. Model systems for the study of heart development and disease. Cardiac neural crest and conotruncal malformations. *Semin Cell Dev Biol* 18 (1):101–110. doi: 10.1016/j.semcdb.2006.12.004.

Huxley, T. H. 1864. *Lectures on the elements of comparative anatomy: on the classification of animals and on the vertebrate skull*. London: John Churchill and Sons.

Ishibashi, S., N. R. Love, and E. Amaya. 2012. A simple method of transgenesis using I-*Sce*I meganuclease in *Xenopus*. *Methods Mol Biol* 917:205–218. doi: 10.1007/978-1-61779-992-1_12.

Jacobson, A., and S. Meier. 1984. Morphogenesis of the head of a newt: mesodermal segments, neuromeres, and distribution of neural crest. *Dev Biol* 106 (1):181–193.

Janvier, P. 1996. Early vertebrates. *Oxford Monographs on Geology and Geophysics* 33:1–393.

Jarvik, E. 1963. The composition of the intermandibular division of the head in fish and tetrapods and the diphyletic origin of the tetrapod tongue. *Kung Svensk Vetens Handl* 4(9): 1–74.

Jarvik, E. 1967. The homologies of the frontal and parietal bones in fishes and tetrapods. *Colloq Int Cent Nat Rech Scient* 163:181–213.

Jenkins, F. A. J., Weijs, W. A. 1979. The functional anatomy of the shoulder in the Virginia opossum (*Didelphis virginiana*). *J Zool London* 188:379–410. doi: 10.1111/j.1469-7998.1979.tb03423.x.

Jenkins, F. A., D. M. Walsh, and R. L. Carroll. 2007. Anatomy of *Eocaecilia micropodia*, a limbed caecilian of the early Jurassic. *Bull Mus Comp Zool* 158 (6):285–365. doi: 10.3099/0027-4100(2007)158[285:AOEMAL]2.0.CO;2.

Jiang, X., S. Iseki, R. E. Maxson, H. M. Sucov, and G. M. Morriss-Kay. 2002. Tissue origins and interactions in the mammalian skull vault. *Dev Biol* 241 (1):106–116. doi:

10.1006/dbio.2001.0487.

Jouve, C., T. Iimura, and O. Pourquie. 2002. Onset of the segmentation clock in the chick embryo: evidence for oscillations in the somite precursors in the primitive streak. *Development* 129 (5):1107–1117.

Kardong, K. V. 2002. *Vertebrates: comparative anatomy, function, evolution*. 3rd edn. ed. Boston: McGraw Hill.

Kague, E., M. Gallagher, S. Burke, and M. Parsons. 2012. Skeletogenic fate of zebrafish cranial and trunk neural crest. *PLoS ONE* 7 (11):e47394. doi: 10.1371/journal.pone.0047394.

Kant, R., and R. S. Goldstein. 1999. Plasticity of axial identity among somites: cranial somites can generate vertebrae without expressing Hox genes appropriate to the trunk. *Dev Biol* 216 (2):507–520.

Kassar-Duchossoy, L., B. Gayraud-Morel, D. GomÃĺs, D. Rocancourt, M. Buckingham, V. Shinin, and S. Tajbakhsh. 2004. Mrf4 determines skeletal muscle identity in Myf5:Myod double-mutant mice. *Nature* 431 (7007):466–471. doi: 10.1038/nature02876.

Keegan, B. R., J. L. Feldman, G. Begemann, P. W. Ingham, and D. Yelon. 2005. Retinoic acid signaling restricts the cardiac progenitor pool. *Science* 307 (5707):247–249. doi: 10.1126/science.1101573.

Kelly, R. G. 2010. Core issues in craniofacial myogenesis. *Exp Cell Res* 316 (18):3034–3041. doi: 10.1016/j.yexcr.2010.04.029.

Kelly, R. G., L. A. Jerome-Majewska, and V. E. Papaioannou. 2004. The del22q11.2 candidate gene *Tbx1* regulates branchiomeric myogenesis. *Hum Mol Genet* 13 (22):2829–2840. doi: 10.1093/hmg/ddh304.

Kerney, R. R., A. L. Brittain, B. K. Hall, and D. R. Buchholz. 2012. Cartilage on the move: cartilage lineage tracing during tadpole metamorphosis. *Dev Growth Differ* 54 (8):739–752. doi: 10.1111/dgd.12002.

Kimmel, C. B., C. T. Miller, and R. J. Keynes. 2001. Neural crest patterning and the evolution of the jaw. *J Anat* 199 (Pt 1–2):105–120. doi: 10.1046/j.1469-7580.2001.19910105.x.

Kmita, M., and D. Duboule. 2003. Organizing axes in time and space; 25 years of colinear tinkering. *Science* 301 (5631):331–333. doi: 10.1126/science.1085753.

Kleinteich, T., and A. Haas. 2007. Cranial musculature in the larva of the caecilian, *Ichthyophis kohtaoensis* (Lissamphibia: Gymnophiona). *J Morphol* 268 (1):74–88. doi: 10.1002/jmor.10503.

Klymkowsky, M., and J. Hanken. 1991. Whole-mount staining of *Xenopus* and other vertebrates. *Methods in Cell Biol* 36:419–441. doi: 10.1016/S0091-679X(08)60290-3.

Knight, R. D., K. Mebus, and H. H. Roehl. 2008. Mandibular arch muscle identity is regulated by a conserved molecular process during vertebrate development. *J Exp Zool B (Mol Dev Evol)* 310B (4):355–369. doi: 10.1002/jez.b.21215.

Knight, R. D., and T. F. Schilling. 2006. Cranial neural crest and development of the head skeleton. *Adv Exp Med Biol* 589:120–133. doi: 10.1007/978-0-387-46954-6_7.

K öntges, G., and A. Lumsden. 1996. Rhombencephalic neural crest segmentation is preserved throughout craniofacial ontogeny. *Development* 122 (10):3229–3242.

Koyabu, D., W. Maier, and M. R. Sánchez-Villagra. 2012. Paleontological and developmental evidence resolve the homology and dual embryonic origin of a mammalian skull bone, the interparietal. *Proc Natl Acad Sci USA* 109 (35):14075–14080. doi: 10.1073/pnas.1208693109.

Kuhlbrodt, K., B. Herbarth, E. Sock, I. Hermans-Borgmeyer, and M. Wegner. 1998. Sox10, a novel transcriptional modulator in glial cells. *J Neurosci* 18 (1):237–250.

Kuijper, S., A. Beverdam, C. Kroon, A. Brouwer, S. Candille, G. Barsh, and F. Meijlink. 2005. Genetics of shoulder girdle formation: roles of Tbx15 and aristaless-like genes. *Development* 132 (7):1601–1610. doi: 10.1242/dev.01735.

Kuratani, S. 1997. Spatial distribution of postotic crest cells defines the head/trunk interface of the vertebrate body: embryological interpretation of peripheral nerve morphology and evolution of the vertebrate head. *Anat Embryol* 195 (1):1–13.

Kuratani, S. 2008a. Evolutionary developmental studies of cyclostomes and the origin of the vertebrate neck. *Dev Growth Differ* 50:S189–S194. doi: 10.1111/j.1440-169X.2008.00985.x.

Kuratani, S. 2008b. Evolutionary developmental studies of cyclostomes and the ori-

gin of the vertebrate neck. *Dev Growth Differ* 50 Suppl 1:S189–94. doi: 10.1111/j.1440-169X.2008.00985.x.

Kuratani, S. C., and M. L. Kirby. 1991. Initial migration and distribution of the cardiac neural crest in the avian embryo: an introduction to the concept of the circumpharyngeal crest. *Am J Anat* 191 (3):215–227. doi: 10.1002/aja.1001910302.

Kusakabe, R., S. Kuraku, and S. Kuratani. 2011. Expression and interaction of muscle-related genes in the lamprey imply the evolutionary scenario for vertebrate skeletal muscle, in association with the acquisition of the neck and fins. *Dev Biol* 350 (1):217–227. doi: 10.1016/j.ydbio.2010.10.029.

Kuratani, S., Y. Murakami, Y. Nobusada, R. Kusakabe, and S. Hirano. 2004. Developmental fate of the mandibular mesoderm in the lamprey, *Lethenteron japonicum*: comparative morphology and development of the gnathostome jaw with special reference to the nature of the trabecula cranii. *J Exp Zool B (Mol Dev Evol)* 302B (5):458–468. doi: 10.1002/jez.b.21011.

Lakso, M. S., B: Mosinger, B; Lee, EJ; Manning, RW; Yu, SH; Mulder, KL; Westphal, H. 1992. Targeted oncogene activation by site-specific recombination in transgenic mice. *Proc Natl Acad Sci USA* 89 (14):6232–6.

Langille, R., and B. Hall. 1987. Development of the head skeleton of the Japanese medaka, *Oryzias latipes* (Teleostei). *J Morphol* 193 (2):135–158. doi: 10.1002/jmor.1051930203.

Laubichler, M. D. 2000. Homology in development and development of the homology concept. *Am Zool* 50 (5):777–788.

Laubichler, M. D. 2013. "Homology as a bridge between evolutionary morphology, developmental evolution, and phylogenetic systematics." In *The evolution of phylogenetic systematics*. Berkeley, CA: University of California Press.

Lauder, G. V. 1982. Patterns of evolution in the feeding mechanism of actinopterygian fishes. *Am Zool* 22 (2):275–285. doi: http://dx.doi.org/10.1093/icb/22.2.275.

Laue, K., M. J änicke, N. Plaster, C. Sonntag, and M. Hammerschmidt. 2008. Restriction of retinoic acid activity by Cyp26b1 is required for proper timing and patterning of osteogene-

sis during zebrafish development. *Development* 135 (22):3775–3787. doi: 10.1242/dev.021238.

Le Lièvre, C. S. 1978. Participation of neural crest-derived cells in the genesis of the skull in birds. *J Embryol Exp Morphol* 47:17–37.

Le Lièvre, C. S., and N. M. Le Douarin. 1975. Mesenchymal derivatives of the neural crest: analysis of chimaeric quail and chick embryos. *J Embryol Exp Morphol* 34 (1):125–154.

Lebedkina, N. S. 1979. *Evolution of the amphibian skull*. Moscow: Nauka (in Russian; translated in 2004, Sofia: Pensoft).

Lee, Y.-H., and J.-P. Saint-Jeannet. 2011. Cardiac neural crest is dispensable for outflow tract septation in *Xenopus*. *Development* 138 (10):2025–2034. doi: 10.1242/dev.061614.

Lescroart, F., W. Hamou, A. Francou, M. Théveniau-Ruissy, R. G. Kelly, and M. Buckingham. 2015. Clonal analysis reveals a common origin between nonsomite-derived neck muscles and heart myocardium. *Proc Natl Acad Sci USA* 112 (5):1446–1451. doi: 10.1073/pnas.1424538112.

Lescroart, F., R. G. Kelly, J.-F. Le Garrec, J.-F. Nicolas, S. M. Meilhac, and M. Buckingham. 2010. Clonal analysis reveals common lineage relationships between head muscles and second heart field derivatives in the mouse embryo. *Development* 137 (19):3269–3279. doi: 10.1242/dev.050674.

Livet, J., T. A. Weissman, H. Kang, R. W. Draft, J. Lu, R. A. Bennis, J. R. Sanes, and J. W. Lichtman. 2007. Transgenic strategies for combinatorial expression of fluorescent proteins in the nervous system. *Nature* 450 (7166):56–62. doi: 10.1038/nature06293.

Lohnes, D., M. Mark, C. Mendelsohn, P. DollÃl, A. Dierich, P. Gorry, A. Gansmuller, and P. Chambon. 1994. Function of the retinoic acid receptors (RARs) during development. (I) Craniofacial and skeletal abnormalities in RAR double mutants. *Development* 120 (10):2723–2748.

Love, N. R., R. Thuret, Y. Chen, S. Ishibashi, N. Sabherwal, R. Paredes, J. Alves-Silva, K. Dorey, A. M. Noble, M. J. Guille, Y. Sasai, N. Papalopulu, and E. Amaya. 2011. pTransgenesis: a cross-species, modular transgenesis resource. *Development* 138 (24):5451–5458. doi: 10.1242/dev.066498.

Lours-Calet, C., L. E. Alvares, A. S. El-Hanfy, S. Gandesha, E. H. Walters, D. R. Sobreira, K. R. Wotton, E. C. Jorge, J. A. Lawson, A. K. Lewis, M. Tada, C. Sharpe, G. Kardon, and S. Dietrich. 2014. Evolutionarily conserved morphogenetic movements at the vertebrate head-trunk interface coordinate the transport and assembly of hypopharyngeal structures. *Dev Biol* 390 (2):231–246. doi: 10.1016/j.ydbio.2014.03.003.

Lu, J., R. Bassel-Duby, A. Hawkins, P. Chang, R. Valdez, H. Wu, L. Gan, J. Shelton, J. Richardson, and E. Olson. 2002. Control of facial muscle development by MyoR and capsulin. *Science* 298 (5602):2378–2381. doi: 10.1126/science.1078273.

Lubosch, W. 1938. "Muskeln des Kopfes: Viscerale Muskulatur." In *Handbuch der vergleichenden anatomie der wirbeltiere*, edited by L. Bolk, E. Göppert, E. Kallius and W. Lubosch, 1011–1105. Berlin: Urban Schwarzenberg.

Lyson, T. R., B.-A. S. Bhullar, G. S. Bever, W. G. Joyce, K. de Queiroz, A. Abzhanov, and J. A. Gauthier. 2013. Homology of the enigmatic nuchal bone reveals novel reorganization of the shoulder girdle in the evolution of the turtle shell. *Evol Dev* 15 (5):317–325. doi: 10.1111/ede.12041.

Mallatt, J. 1996. Ventilation and the origin of jawed vertebrates: a new mouth. *Zool J Linn Soc* 117 (4):329–404. doi: 10.1111/j.1096-3642.1996.tb01658.x.

Marcucio, R. S., and D. M. Noden. 1999. Myotube heterogeneity in developing chick craniofacial skeletal muscles. *Dev Dynam* 214 (3):178–194.
doi: 10.1002/(SICI)1097-0177(199903)214:3lt;178::AID-AJA2gt;3.0.CO;2-4.

Martindale, M. Q., S. Meier, and A. G. Jacobson. 1987. Mesodermal metamerism in the teleost, *Oryzias latipes* (the Medaka). *J Morphol* 193 (3):241–252.

Matsuoka, T., P. E. Ahlberg, N. Kessaris, P. Iannarelli, U. Dennehy, W. D. Richardson, A. P. Mcmahon, and G. Koentges. 2005. Neural crest origins of the neck and shoulder. *Nature* 436 (7049):347–355. doi: 10.1038/nature03837.

Matthaei, K. I. 2007. Genetically manipulated mice: a powerful tool with unsuspected caveats. *J Physiol* 582 (Pt 2):481–488. doi: 10.1113/jphysiol.2007.134908.

McBratney-Owen, B., S. Iseki, S. D. Bamforth, B. R. Olsen, and G. M. Morriss-Kay. 2008.

Development and tissue origins of the mammalian cranial base. *Dev Biol* 322 (1):121–132. doi: 10.1016/j.ydbio.2008.07.016.

McCauley, D. W., and M. Bronner-Fraser. 2003. Neural crest contributions to the lamprey head. *Development* 130 (11):2317–2327. doi: 10.1242/dev.00451.

McCauley, D. W., and M. Bronner-Fraser. 2006. Importance of SoxE in neural crest development and the evolution of the pharynx. *Nature* 441 (7094):750–752. doi: 10.1038/nature04691.

McGonnell, I. M. 2001. The evolution of the pectoral girdle. *J Anat* 199 (Pt 1-2):189–194. doi: 10.1046/j.1469-7580.2001.19910189.x.

Meier, S. 1979. Development of the chick embryo mesoblast: formation of the embryonic axis and establishment of the metameric pattern. *Dev Biol* 73 (1):25–45.

Meier, S., and D. Packard. 1984. Morphogenesis of the cranial segments and distribution of neural crest in the embryos of the snapping turtle, *Chelydra serpentina*. *Dev Biol* 102 (2):309–323.

Meier, S., and P. P. L. Tam. 1982. Metameric pattern development in the embryonic axis of the mouse. *Differentiation* 21 (2):95–108.

Miller, C. T., L. Maves, and C. B. Kimmel. 2004. *moz* regulates Hox expression and pharyngeal segmental identity in zebrafish. *Development* 131 (10):2443–2461. doi: 10.1242/dev.01134.

Millot, J., and J. Anthony. 1958. *Anatomie de Latimeria chalumnae. Vol I. Squellete, muscles et formation de soutien*. Paris: Centre Nationale de la Recherche Scientifique.

Milner, A. R. 1988. "The relationships and origins of living amphibians." In *The phylogeny and classification of tetrapods*, edited by M. J. Benton, 59–102. Oxford: Clarendon Press.

Minsuk, S. B., and R. E. Keller. 1996. Dorsal mesoderm has a dual origin and forms by a novel mechanism in *Hymenochirus*, a relative of *Xenopus*. *Dev Biol* 174 (1):92–103. doi: 10.1006/dbio.1996.0054.

Modesto, S. R., and H. D. Sues. 2004. The skull of the Early Triassic archosauromorph reptile *Prolacerta broomi* and its phylogenetic significance. *Zool J Linn Soc* 140 (3):335–351.

doi: 10.1111/j.1096-3642.2003.00102.x.

Mongera, A., and C. NÃijsslein-Volhard. 2013. Scales of fish arise from mesoderm. *Curr Biol* 23 (9):R338–9. doi: 10.1016/j.cub.2013.02.056.

Mongera, A., A. P. Singh, M. P. Levesque, Y.-Y. Chen, P. Konstantinidis, and C. NÃijsslein-Volhard. 2013. Genetic lineage labeling in zebrafish uncovers novel neural crest contributions to the head, including gill pillar cells. *Development* 140 (4):916–925. doi: 10.1242/dev.091066.

Mootoosamy, R. C., and S. Dietrich. 2002. Distinct regulatory cascades for head and trunk myogenesis. *Development* 129 (3):573–583.

Morriss-Kay, G. M. 2001. Derivation of the mammalian skull vault. *J Anat* 199 (Pt 1–2):143–151. doi: 10.1046/j.1469-7580.2001.19910143.x.

Nathan, E., A. Monovich, L. Tirosh-Finkel, Z. Harrelson, T. Rousso, A. Rinon, I. Harel, S. M. Evans, and E. Tzahor. 2008. The contribution of Islet1-expressing splanchnic mesoderm cells to distinct branchiomeric muscles reveals significant heterogeneity in head muscle development. *Development* 135 (4):647–657. doi: 10.1242/dev.007989.

Neal, H. 1918. Neuromeres and metameres. *J Morphol* 31 (2):293–315.

Niederreither, K., and P. DollÃĺ. 2008. Retinoic acid in development: towards an integrated view. *Nat Rev Genet* 9 (7):541–553. doi: 10.1038/nrg2340.

Noden, D. M. 1978. The control of the avian cephalic neural crest cytodifferentiation. I. Skeletal and connective tissues. *Dev Biol* 67:296–312. doi: 10.1016/0012-1606(78)90201-4.

Noden, D. M. 1982. "Patterns and organization of craniofacial skeletogenic and myogenic mesenchyme: a perspective." In *Factors and mechanisms influencing bone growth*, edited by A. Dixon and B. Sarnat, 167–203. New York: Alan R. Liss, Inc.

Noden, D. M. 1983a. The embryonic origins of avian cephalic and cervical muscles and associated connective tissues. *Am J Anat* 168 (3):257–276. doi: 10.1002/aja.1001680302.

Noden, D. M. 1983b. The role of the neural crest in patterning of avian cranial skeletal, connective, and muscle tissues. *Dev Biol* 96 (1):144–165.

Noden, D. M. 1986. Origins and Patterning of Craniofacial Mesenchymal Tissues. J Cran-

iofac Genet Dev Biol Suppl 2:15–31.

Noden, D. M. 1988. Interactions and fates of avian craniofacial mesenchyme. *Development* 103 Suppl:121–140.

Noden, D. M., and P. Francis-West. 2006. The differentiation and morphogenesis of craniofacial muscles. *Dev Dynam* 235 (5):1194–1218. doi: 10.1002/dvdy.20697.

Noden, D. M., R. Marcucio, A. G. Borycki, and C. P. Emerson. 1999. Differentiation of avian craniofacial muscles: I. Patterns of early regulatory gene expression and myosin heavy chain synthesis. *Dev Dynam* 216 (2):96–112. doi: 10.1002/(SICI)1097-0177(199910)216:2<96::AID-DVDY2>3.0.CO;2-6.

Noden, D. M., and R. A. Schneider. 2006. Neural crest cells and the community of plan for craniofacial development: historical debates and current perspectives. *Adv Exp Med Biol* 589:1–23. doi: 10.1007/978-0-387-46954-6_1.

Noden, D. M., and P. A. Trainor. 2005. Relations and interactions between cranial mesoderm and neural crest populations. *J Anat* 207 (5):575–601. doi: 10.1111/j.1469-7580.2005.00473.x.

Northcutt, R. G. 1990. Ontogeny and phylogeny: a re-evaluation of conceptual relationships and some applications. *Brain Behav Evolut* 36 (2–3):116–140. doi: 10.1159/000115302.

Northcutt, R. G. 2005. The new head hypothesis revisited. *J Exp Zool B (Mol Dev Evol)* 304 (4):274–297. doi: 10.1002/jez.b.21063.

Nye, H. L. D., J. A. Cameron, E. A. G. Chernoff, and D. L. Stocum. 2003. Extending the table of stages of normal development of the axolotl: limb development. *Dev Dynam* 226 (3):555–560. doi: 10.1002/dvdy.10237.

O'Rahilly, R., and F. Müller. 1984. The early development of the hypoglossal nerve and occipital somites in staged human embryos. *Am J Anat* 169 (3):237–257.

Olsson, L., R. Ericsson, and R. Cerny. 2005. Vertebrate head development: segmentation, novelties, and homology. *Theor Biosci* 124 (2):145–163. doi: 10.1016/j.thbio.2005.06.001.

Olsson, L., P. Falck, K. Lopez, J. Cobb, and J. Hanken. 2001. Cranial neural crest cells contribute to connective tissue in cranial muscles in the anuran amphibian, Bombina orien-

talis. *Dev Biol* 237 (2):354–367. doi: 10.1006/dbio.2001.0377.

Olsson, L., and J. Hanken. 1996. Cranial neural-crest migration and chondrogenic fate in the oriental fire-bellied toad *Bombina orientalis*: defining the ancestral pattern of head development in anuran amphibians. *J Morphol* 229 (1):105–120. doi: 10.1002/(SICI)1097-4687(199607)229:1<105::AID-JMOR7>3.0.CO;2-2.

Onai, T., T. Aramaki, H. Inomata, T. Hirai, and S. Kuratani. 2015. Ancestral mesodermal reorganization and evolution of the vertebrate head. *Zoological Letters* 1:29. doi: 10.1186/s40851-015-0030-3.

Ota, K. G., S. Kuraku, and S. Kuratani. 2007. Hagfish embryology with reference to the evolution of the neural crest. *Nature* 446 (7136):672–675. doi: 10.1038/nature05633.

Owen, R. 1843. Lectures on the comparative anatomy and physiology of the invertebrate animals. London: Longman Brown Green Longmans.

Owen, R. 1866. *On the Anatomy of Vertebrates*. Vol I. Fishes and Reptiles. London: Longmans, Green, and Co.

Panganiban, G., S. M. Irvine, C. Lowe, H. Roehl, L. S. Corley, B. Sherbon, J. K. Grenier, J. F. Fallon, J. Kimble, M. Walker, G. A. Wray, B. J. Swalla, M. Q. Martindale, and S. B. Carroll. 1997. The origin and evolution of animal appendages. *Proc Natl Acad Sci USA* 94 (10):5162–5166. doi: 10.1073/pnas.94.10.5162.

Parker, W. K., and G. T. Bettany. 1877. *The morphology of the skull*. London, UK: Macmillan and Co.

Parrington, F. 1937. A note on the supratemporal and tabular bones in reptiles. *J Nat Hist* 20 (115):69–76. doi: 10.1080/00222933708655315.

Patterson, C. 1982. "Morphological characters and homology." In *Problems of phylogenetic reconstruction*, edited by K. A. Joysey and A. E. Friday, 21–74. London and New York: Academic Press.

Pellegrini, M., S. Pantano, M. P. Fumi, F. Lucchini, and A. Forabosco. 2001. Agenesis of the scapula in Emx2 homozygous mutants. *Dev Biol* 232 (1):149–156. doi: 10.1006/dbio.2001.0159.

Perotti, M. G. 2001. Skeletal development of *Leptodactylus chaquensis* (Anura: Leptodactylidae). *Herpetologica* 57 (3):318–335.

Piatt, J. 1938. Morphogenesis of the cranial muscles of *Amblystoma punctatum*. *J Morphol* 63 (3):531–587.

Piekarski, N. 2009. "A long-term fate map of the anterior somites in the Mexican axolotl (*Ambystoma mexicanum*)." PhD Dissertation, Friedrich Schiller University of Jena.

Piekarski, N., J. B. Gross, and J. Hanken. 2014. Evolutionary innovation and conservation in the embryonic derivation of the vertebrate skull. *Nat Commun* 5:5661. doi: 10.1038/ncomms6661.

Piekarski, N., and L. Olsson. 2011. A somitic contribution to the pectoral girdle in the axolotl revealed by long-term fate mapping. *Evol Dev* 13 (1):47–57. doi: 10.1111/j.1525-142X.2010.00455.x.

Piekarski, N., and L. Olsson. 2007. Muscular derivatives of the cranialmost somites revealed by long-term fate mapping in the Mexican axolotl (*Ambystoma mexicanum*). *Evol Dev* 9 (6):566–578. doi: 10.1111/j.1525-142X.2007.00197.x.

Piekarski, N., and L. Olsson. 2013. Resegmentation in the Mexican axolotl, *Ambystoma mexicanum*. *J Morphol* 275 (2):141–152. doi: 10.1002/jmor.20204.

Platt, J. B. 1893. Ectodermic origin of the cartilages of the head. *Anat Anz* 8:506–509.

Prols, F., F. Ehehalt, M. Rodriguez-Niedenfuhr, L. He, R. Huang, and B. Christ. 2004. The role of Emx2 during scapula formation. *Dev Biol* 275 (2):315–324. doi: 10.1016/j.ydbio.2004.08.003.

Pu, Q., K. Patel, and R. Huang. 2015. The lateral plate mesoderm: a novel source of skeletal muscle. *Results Probl Cell Differ* 56:143–163. doi: 10.1007/978-3-662-44608-9_7.

Quarto, N., D. C. Wan, M. D. Kwan, N. J. Panetta, S. Li, and M. T. Longaker. 2009. Origin matters: differences in embryonic tissue origin and Wnt signaling determine the osteogenic potential and healing capacity of frontal and parietal calvarial bones. *J Bone Miner Res* 25 (7):1680–1694. doi: 10.1359/jbmr.091116.

Reinbach, W. 1939. Untersuchungen über die entwicklung des kopfskeletts von *Calyptocephalus gayi* (mit einem anhang über das os supratemporale der anuren amphibien). *Zeit*

Naturwiss (Jena) 72:211–362.

Reisz, R. R. 1977. Petrolacosaurus, oldest known diapsid reptile. *Science* 196 (4294):1091–1093. doi: 10.1126/science.196.4294.1091.

Remane, A. 1952. *Die grundlagen des natürlichen systems, der vergleichenden anatomie und der phylogenetik*. Leipzig: Akademische Verlagsgesellschaft, Geest Portig K.-G.

Rieppel, O. 1992. The skull in a hatchling of *Sphenodon punctatus*. *J Herpetol* 26 (1):80–84. doi: 10.2307/1565028.

Robinson, P. L. 1973. A problematic reptile from the British Upper Trias. *J Geol Soc* 129:457–479. doi: 10.1144/gsjgs.129.5.0457.

Roĉek, Z. 1988. Origin and evolution of the frontoparietal complex in anurans. *Amp-Rept* 9 (4):385–403. doi: 10.1163/156853888X00062.

Roĉek, Z., and J. C. Rage. 2000. "Anatomical transformations in the transitions from temnospondyl to proanuran stages." In *Amphibian Biology*, edited by H. Heatwole and M. Davies, 1274–1282. Chipping Norton: Surrey Beatty Sons.

Romer, A. S., Parsons, T. S. 1949. *The vertebrate body*. Fort Worth: Saunders College Publishing.

Rudel, D., and R. J. Sommer. 2003. The evolution of developmental mechanisms. *Dev Biol* 264 (1):15–37.

Sadaghiani, B., and C. H. Thiébaud. 1987. Neural crest development in the *Xenopus laevis* embryo, studied by interspecific transplantation and scanning electron microscopy. *Dev Biol* 124 (1):91–110. doi: 10.1016/0012-1606(87)90463-5.

Sánchez-Villagra, M. R., and W. Maier. 2006. Homologies of the mammalian shoulder girdle: a response to Matsuoka et al. (2005). *Evol Dev* 8 (2):113–115. doi: 10.1111/j.1525-142X.2006.00081.x.

Sambasivan, R., B. Gayraud-Morel, G. Dumas, C. Cimper, S. Paisant, R. G. Kelly, R. Kelly, and S. Tajbakhsh. 2009. Distinct regulatory cascades govern extraocular and pharyngeal arch muscle progenitor cell fates. *Dev Cell* 16 (6):810–821. doi: 10.1016/j.devcel.2009.05.008.

Schilling, T. F., and C. B. Kimmel. 1994. Segment and cell type lineage restrictions during pharyngeal arch development in the zebrafish embryo. *Development* 120 (3):483–494.

Schmidt, J., M. Schuff, and L. Olsson. 2011. A role for FoxN3 in the development of cranial cartilages and muscles in *Xenopus laevis* (Amphibia: Anura: Pipidae) with special emphasis on the novel rostral cartilages. *J Anat* 218 (2):226–242. doi: 10.1111/j.1469-7580.2010.01315.x.

Schmidt-Supprian, M., and K. Rajewsky. 2007. Vagaries of conditional gene targeting. *Nat Immunol* 8 (7):665–668. doi: 10.1038/ni0707-665.

Schneider, R. A. 1999. Neural crest can form cartilages normally derived from mesoderm during development of the avian head skeleton. *Dev Biol* 208 (2):441–455. doi: 10.1006/dbio.1999.9213.

Schneider, R. A., and J. A. Helms. 2003. The cellular and molecular origins of beak morphology. *Science* 299 (5606):565–568. doi: 10.1126/science.1077827.

Schoch, R. R. 2006. Skull ontogeny: developmental patterns of fishes conserved across major tetrapod clades. *Evol Dev* 8 (6):524–536. doi: 10.1111/j.1525-142X.2006.00125.x.

Schoch, R. R. 2014. Amphibian skull evolution: the developmental and functional context of simplification, bone loss and heterotopy. *J Exp Zool B (Mol Dev Evol)* 322 (8):619–630. doi: 10.1002/.22599.

Schoch, R. R., and A. R. Milner. 2004. "Structure and implications of theories on the origin of lissamphibians." In *Recent advances in the origin and early radiations of vertebrates*, edited by G. Arratia, M. V. H. Wilson and R. Cloutier, 345–377. Munich: Verlag Dr. Friedrich Pfeil.

Schoch, R. R., and F. Witzmann. 2011. BystrowâĂŹs Paradox–gills, fossils, and the fish-to-tetrapod transition. *Acta Zool* 92 (3):251–265. doi: 10.1111/j.1463-6395.2010.00456.x.

Sedra, S. N. 1949. On the homology of certain elements in the skull of *Bufo regularis* Reuss (Salientia). *Proc Zool Soc Lond* 119 (3):633–641. doi: 10.1111/j.1096-3642.1949.tb00893.x.

Sefton, E. M., N. Piekarski, and J. Hanken 2015. Dual embryonic origin and patterning of the pharyngeal skeleton in the axolotl (*Ambystoma mexicanum*). *Evol Dev* 17 (3):175–184.

doi: 10.1111/ede.12124.

Sharpe, J. 2002. Optical projection tomography as a tool for 3D microscopy and gene expression studies. *Science* 296 (5567):541–545. doi: 10.1126/science.1068206.

Shearman, R. M. 2005. Growth of the pectoral girdle of the Leopard frog, *Rana pipiens* (Anura: Ranidae). *J Morphol* 264 (1):94-104. doi: 10.1002/jmor.10322.

Shearman, R. M. 2008. Chondrogenesis and ossification of the lissamphibian pectoral girdle. *J Morphol* 269 (4):479-95. doi: 10.1002/jmor.10597.

Shih, H. P., M. K. Gross, and C. Kioussi. 2007. Cranial muscle defects of Pitx2 mutants result from specification defects in the first branchial arch. *Proc Natl Acad Sci USA* 104 (14):5907–5912. doi: 10.1073/pnas.0701122104.

Shih, H. P., M. K. Gross, and C. Kioussi. 2007b. Expression pattern of the homeodomain transcription factor Pitx2 during muscle development. *Gene Expr Patterns* 7 (4):441–451. doi: 10.1016/j.modgep.2006.11.004.

Shubin, N., E. B. Daeschler, and F. A. Jenkins. 2015. "Origin of the tetrapod neck and shoulder." In *Great transformations in vertebrate evolution*, edited by K. P. Dial, N. Shubin and E. L. Brainerd, 70–84. Chicago: University of Chicago Press.

Shubin, N., C. Tabin, and S. Carroll. 1997. Fossils, genes and the evolution of animal limbs. *Nature* 388 (6643):639–648. doi: 10.1038/41710.

Smirnov, S. V. 1995. Extra bones in the Pelobates skull as evidence of the paedomorphic origin in the anurans. *Zhur Obs Biol* 56 (3):317–328.

Smirnov, S. V., A. B. Vassilieva, and K. M. Merkulova. 2008. Role of heterochronies in the morphogenesis of amphibian skull bones: an experimental study. *Dokl Biol Sci* 418:64–66. doi: 10.1134/S0012496608010225.

Smith, G. 1904. The middle ear and columella of birds. *Q J Microsc Sci* 48:11–17.

Smith, J. C., B. M. Price, J. B. Green, D. Weigel, and B. G. Herrmann. 1991. Expression of a *Xenopus* homolog of Brachyury (T) is an immediate-early response to mesoderm induction. *Cell* 67 (1):79–87.

Sobkow, L., H.-H. Epperlein, S. Herklotz, W. L. Straube, and E. M. Tanaka. 2006. A germline GFP transgenic axolotl and its use to track cell fate: dual origin of the fin mesenchyme during development and the fate of blood cells during regeneration. *Dev Biol* 290 (2):386–397. doi: 10.1016/j.ydbio.2005.11.037.

Spemann, H. 1915. "Zur geschichte und kritik des begriffs der homologie." In *Allgemeine Biologie*, edited by C. Chun and W. Johannsen. Leipzig: B. G. Teubner.

Stolfi, A., T. B. Gainous, J. J. Young, A. Mori, M. Levine, and L. Christiaen. 2010. Early chordate origins of the vertebrate second heart field. *Science* 329 (5991):565–568. doi: 10.1126/science.1190181.

Stone, L. 1926. Further experiments on the extirpation and transplantation of mesectoderm in *Amblystoma punctatum*. *J Exp Zool* 44 (1):95–131. doi: 10.1002/jez.1400440104.

Stone, L. S. 1929. Experiments showing the role of migrating neural crest (mesectoderm) in the formation of head skeleton and loose connective tissue in *Rana palustris*. *Roux Arch Dev Biol* 118:40–77. doi: 10.1007/BF02108871.

Stone, L. S. 1932. Transplantation of hyobranchial mesentoderm, including the right lateral anlage of the second basibranchium, in *Amblystoma punctatum*. *J Exp Zool* 62 (1):109–123. doi: 10.1002/jez.1400620105.

Striedter, G. F., and R. G. Northcutt. 1991. Biological hierarchies and the concept of homology. *Brain Behav Evolut* 28 (4–5):177–189. doi: 10.1159/000114387.

Summerbell, D., P. R. Ashby, O. Coutelle, D. Cox, S. Yee, and P. W. Rigby. 2000. The expression of Myf5 in the developing mouse embryo is controlled by discrete and dispersed enhancers specific for particular populations of skeletal muscle precursors. *Development* 127 (17):3745–3757.

Tada, M. N., and S. Kuratani. 2015. Evolutionary and developmental understanding of the spinal accessory nerve. *Zool Lett* 1 (4):10.1186. doi: 10.1186/s40851-014-0006-8.

Tan, S. S., and G. M. Morriss-Kay. 1986. Analysis of cranial neural crest cell migration and early fates in postimplantation rat chimaeras. *J Embryol Exp Morphol* 98:21–58.

Tajbakhsh, S., D. Rocancourt, G. Cossu, and M. Buckingham. 1997. Redefining the genetic hierarchies controlling skeletal myogenesis: Pax-3 and Myf-5 act upstream of MyoD. *Cell* 89 (1):127–138.

Theis, S., K. Patel, P. Valasek, A. Otto, Q. Pu, I. Harel, E. Tzahor, S. Tajbakhsh, B. Christ, and R. Huang. 2010. The occipital lateral plate mesoderm is a novel source for vertebrate neck musculature. *Development* 137 (17):2961–2971. doi: 10.1242/dev.049726.

Thermes, V., C. Grabher, F. Ristoratore, F. Bourrat, A. Choulika, J. Wittbrodt, and J. S. Joly. 2002. I-SceI meganuclease mediates highly efficient transgenesis in fish. *Mech Dev* 118 (1-2):91–98. doi: 10.1016/S0925-4773(02)00218-6.

Thompson, H., A. Ohazama, P. T. Sharpe, and A. S. Tucker. 2012. The origin of the stapes and relationship to the otic capsule and oval window. *Dev Dynam* 241 (9):1396–1404. doi: 10.1002/dvdy.23831.

Thyng, F. W. 1906. The squamosal bone in tetrapodous vertebrata. *Proc Boston Soc Natur Hist* 32 (11):387–425.

Timmons, P. M., J. Wallin, P. W. Rigby, and R. Balling. 1994. Expression and function of Pax 1 during development of the pectoral girdle. *Development* 120 (10):2773–2785.

Tirosh-Finkel, L., H. Elhanany, A. Rinon, and E. Tzahor. 2006. Mesoderm progenitor cells of common origin contribute to the head musculature and the cardiac outflow tract. *Development* 133 (10):1943–1953. doi: 10.1242/dev.02365.

Toerien, M. J. 1963. Experimental studies on the origin of the cartilage of the auditory capsule and columella in Ambystoma. *J Embryol Exp Morphol* 11:459–473.

Tokita, M., and R. A. Schneider. 2009. Developmental origins of species-specific muscle pattern. *Dev Biol* 331 (2):311–325. doi: 10.1016/j.ydbio.2009.05.548.

Trainor, P., and R. Krumlauf. 2000. Plasticity in mouse neural crest cells reveals a new patterning role for cranial mesoderm. *Nat Cell Biol* 2 (2):96–102. doi: 10.1038/35000051.

Trainor, P. A., S. S. Tan, and P. P. Tam. 1994. Cranial paraxial mesoderm: regionalisation of cell fate and impact on craniofacial development in mouse embryos. *Development* 120

(9):2397–2408.

Trinajstic, K., S. Sanchez, V. Dupret, P. Tafforeau, J. Long, G. Young, T. Senden, C. Boisvert, N. Power, and P. E. Ahlberg. 2013. Fossil musculature of the most primitive jawed vertebrates. *Science* 341 (6142):160–164. doi: 10.1126/science.1237275.

True, J. R., and E. S. Haag. 2001. Developmental system drift and flexibility in evolutionary trajectories. *Evol Dev* 3 (2):109–119. doi: 10.1046/j.1525-142x.2001.003002109.x.

Trueb, L. 1970. Evolutionary relationships of casque-headed tree frogs with co-ossified skulls (family Hylidae). *Univ Kans Publ* 18:547–716.

Trueb, L., and J. Hanken. 1992. Skeletal development in *Xenopus laevis* (Anura: Pipidae). *J Morphol* 214 (1):1-41. doi: 10.1002/jmor.1052140102.

Tsuihiji, T., M. Kearney, and O. Rieppel. 2006. First report of a pectoral girdle muscle in snakes, with comments on the snake cervico-dorsal boundary. *Copeia* 2006 (2):206–215.

Tschopp, P., E. Sherratt, T. J. Sanger, A. C. Groner, A. C. Aspiras, J. K. Hu, O. Pourquié, J. Gros, and C. J. Tabin. 2014. A relative shift in cloacal location repositions external genitalia in amniote evolution. *Nature* 516 (7531):391–394. doi: 10.1038/nature13819.

Tzahor, E. 2009. Heart and craniofacial muscle development: a new developmental theme of distinct myogenic fields. *Dev Biol* 327 (2):273–279. doi: 10.1016/j.ydbio.2008.12.035.

Tzahor, E., H. Kempf, R. C. Mootoosamy, A. C. Poon, A. Abzhanov, C. J. Tabin, S. Dietrich, and A. B. Lassar. 2003. Antagonists of Wnt and BMP signaling promote the formation of vertebrate head muscle. *Genes Dev* 17 (24):3087–3099. doi: 10.1101/gad.1154103.

Ueno, S., G. Weidinger, and T. Osugi. 2007. Biphasic role for Wnt/β-catenin signaling in cardiac specification in zebrafish and embryonic stem cells. *Proc Natl Acad Sci USA* 104 (23):9685–9690. doi: 10.1073/pnas.0702859104.

Valasek, P., S. Theis, E. Krejci, M. Grim, F. Maina, Y. Shwartz, A. Otto, R. Huang, and K. Patel. 2010. Somitic origin of the medial border of the mammalian scapula and its homology to the avian scapula blade. *J Anat* 216 (4):482–488. doi: 10.1111/j.1469-7580.2009.01200.x.

Van Valen, L. M. 1982. Homology and causes. *J Morphol* 173 (3):305–312. doi: 10.1002/jmor.1051730307.

Vetter, B. 1874. Untersuchungen zur vergleichenden anatomie der kiemen-und kiefermusculatur der fische. *Jena Z Naturwiss* 8:405–458.

Viczian, A. S., A. G. Bang, W. A. Harris, and M. E. Zuber. 2006. Expression of *Xenopus laevis* Lhx2 during eye development and evidence for divergent expression among vertebrates. *Dev Dynam* 235 (4):1133–1141. doi: 10.1002/dvdy.20708.

von Baer, K. E. 1828. *ÃIJber entwickelungsgeschichte der thiere: beobachtung und reflexion*. KÃűnigsberg: BontrÃďger.

von Scheven, G., L. Alvares, R. Mootoosamy, and S. Dietrich. 2006. Neural tube derived signals and Fgf8 act antagonistically to specify eye versus mandibular arch muscles. *Development* 133 (14):2731–2745. doi: 10.1242/dev.02426.

Wagner, G. P. 2007. The developmental genetics of homology. *Nat Rev Genet* 8 (6):473–479. doi: 10.1038/nrg2099.

Wagner, G. P. 2014. *Homology, genes and evolutionary innovation*. Princeton: Princeton University Press.

Wagner, G. P., and M. D. Laubichler. 2000. Character edentification in evolutionary biology: the role of the organism. *Theor Biosci* 119 (1):20–40. doi: 10.1007/s12064-000-0003-7.

Wake, D. B. 1994. Comparative terminology. *Science* 265 (5169):268–269. doi: 10.1126/science.265.5169.268.

Wake, D. B. 1999. "Homoplasy, homology and the problem of 'sameness' in biology." In *Homology*, edited by G. R. Bock and G. Cardew, Novartis Foundation Symposium 222, 24–33. Chichester: John Wiley Sons.

Wiens, J. J. 1989. Ontogeny of the skeleton of *Spea bombifrons* (Anura: Pelobatidae). *J Morphol* 202:29–51. doi: 10.1002/jmor.1052020104.

Wild, E. R. 1997. Description of the adult skeleton and developmental osteology of the hyperossified horned frog, *Ceratophrys cornuta* (Anura:Leptodactylidae). *J Morphol* 232 (2):169–206. doi: 10.1002/(SICI)1097-4687(199705)232:2lt;169::AID-JMOR4gt;3.0.CO;2-5.

Wild, E. R. 1999. Description of the chondrocranium and osteogenesis of the Chacoan burrowing frog, *Chacophrys pierotti* (Anura: Leptodactylidae). *J Morphol* 242 (3):229–246. doi: 10.1002/(SICI)1097-4687(199912)242:3lt;229::AID-JMOR3gt;3.0.CO;2-N.

Wilkinson, M., and R. A. Nussbaum. 1997. Comparative morphology and evolution of the lungless caecilian *Atretochoana eiselti* (Taylor) (Amphibia: Gymnophiona: Typhlonectidae). *Biol J Linn Soc* 62 (1):39–109. doi: 10.1006/bijl.1997.0143.

Wilson, E. B. 1894. The embryological criterion of homology. *Biol Lectures Marine Biol Lab Woods Hole* 6th Lecture:101–124.

Wolff, G. 1895. Entwicklungsphysiologische Studien. I. Die regeneration der Urodelenlinse. *Roux Arch Dev Biol* 1:380–390.

Yoshida, T., P. Vivatbutsiri, G. Morriss-Kay, Y. Saga, and S. Iseki. 2008. Cell lineage in mammalian craniofacial mesenchyme. *Mech Dev* 125 (9–10):797–808. doi: 10.1016/j.mod.2008.06.007.

Zacharias, A. L., M. Lewandoski, M. A. Rudnicki, and P. J. Gage. 2011. Pitx2 is an upstream activator of extraocular myogenesis and survival. *Dev Biol* 349 (2):395–405. doi: 10.1016/j.ydbio.2010.10.028.

Ziermann, J. M., and R. Diogo. 2013. Cranial muscle development in the model organism *Ambystoma mexicanum*: implications for tetrapod and vertebrate comparative and evolutionary morphology and notes on ontogeny and phylogeny. *Anat Rec* 296 (7):1031–1048. doi: 10.1002/ar.22713.